MEIOTIC CROSSOVER PATTERNING IN *DROSOPHILA MELANOGASTER*

Michaelyn Ann Hartmann

A dissertation submitted to the faculty at the University of North Carolina at Chapel Hill in partial fulfillment of the requirements for the degree of Doctor of Philosophy in the Curriculum in Genetics and Molecular Biology in the School of Medicine.

Chapel Hill
2019

Approved by:

Jeff Sekelsky

Robert Duronio

Jill Dowen

Daniel McKay

Dale Ramsden

ABSTRACT

Michaelyn Ann Hartmann: Meiotic Crossover Patterning in *Drosophila melanogaster*
(Under the direction of Jeff Sekelsky)

Meiosis is an essential process to halve an organism's genome in preparation for transmission to the next generation. Recombination between homologous chromosomes is necessary for the proper segregation of chromosomes, and allows the generation of genetic diversity. Mistakes in meiosis can lead to aneuploidy, therefore, to minimize mistakes, recombination is a highly regulated process. Crossovers are patterned along a chromosome, and this patterning is dictated by three phenomena known as interference, assurance, and the centromere effect. Interference assures that a crossover does not occur too close to another crossover, assurance maintains that each chromosome gets at least one crossover, and the centromere effect suppresses crossovers that occur too close to the centromere. The work detailed in this dissertation first focuses on the proteins involved in crossover formation and then investigates the regulation of the suppression of centromere-proximal crossovers. I have gained insight into a potential endonuclease, Ankle1, as well as further elucidated the role of the mei-MCM complex in creating meiotic crossovers. In addition, I discovered that centromere-proximal crossover suppression is regulated both by the highly-repetitive heterochromatin adjacent to the centromere, as well as the protein-mediated centromere effect, which extends into the euchromatin and dissipates with distance from the centromere. Overall these findings have provided insight into the mechanisms of crossover formation and patterning and provided the foundation for future studies of meiotic crossover control.

To my mom, for your constant love and support.

You are the strongest, most amazing woman I

know and you will always be my role model.

I wouldn't be where I am without you.

ACKNOWLEDGEMENTS

I would first like to thank my advisor, Jeff Sekelsky. Thank you for always being there and striving to be the best mentor. You have been a wonderful teaching role model and you have definitely inspired me to be be a great teacher and mentor. Thank you for allowing me to explore my interests throughout graduate school, it made graduate school enjoyable and allowed me to reach my goals and obtain my dream job. I am truly grateful to have been a member of the Sekelsky lab.

Thank you also to my committee, Bob Duronio, Dan McKay, Jill Dowen, and Dale Ramsden, for your scientific guidance and support.

I want to thank the extraordinary people I have had the pleasure of working with in the Sekelsky Lab: Nicole Crown, Noelle Romero, Danielle Rognstad, Stephanie Bellendir, Simon Brady, Julie Korda Holsclaw, Greg Zapotoczny, Juan Carvajal Garcia, Leeza Santiago Millan, Carolyn Turcotte, Alex Stutzman, and Evan Dewey. I especially want to thank Susan Cheek for helping me stay sane and maintaining a great lab environment. I want to thank my two outstanding undergraduates that I was lucky enough to mentor: Caitlin Moffatt and Leela Wissmann. I also want to specially thank one of my very best friends and labmate, Talia Hatkevich. Talia has helped me grow and find myself throughout graduate school and I will always be grateful for our friendship. Working with all of these amazing people helped brighten every day and I will always be thankful for all of your love and support.

I especially want to thank my family. I am so thankful to my mom for all that she does

for me. I have always appreciated the supportive texts and calls from all of my family members, it helped me feel close to family even being so far away. I am very happy that I adopted the best cat in the entire world, Louie, who always keeps me company at home and unconditionally loves me. I also appreciate Nichole Adiletta and am so thankful that we have been able to keep up our long-distance friendship over the years. I am so lucky to have met Tim Ross-Elliott during graduate school (thanks to Talia) and can't wait to continue our journey together in Boston.

TABLE OF CONTENTS

LIST OF FIGURES

LIST OF TABLES

LIST OF ABBREVIATIONS

AICc	Corrected Akaike Information Criterion
BF	Beam-Film
bp	Basepair
Cis	Cisplatin
CE	Measure of the centromere effect
cM	Centimorgan
CO	Crossover
CoC	Coefficient of Coincidence
dHJ	Double Holliday junction
DSB	Double strand break
FISH	Fluorescence in-situ hybridization
HJ	Holliday Junction
HR	Highly-repetitive
Indel	Insertion/deletion
IF	Immuno-fluorescence
IR	Ionizing radiation
LR	Less-repetitive
Mb	Megabase

MI	Meiosis I
MLR	Mei-9 Interaction-like Domain
MMS	Methyl Methanesulfonate
NCO	Noncrossover
NDJ	Nondisjunction
PBS	Phosphate Buffered Saline
RT	Room Temperature
SC	Synaptonemal Complex
SSC	Saline Sodium Citrate
SNP	Single Nucleotide Polymorphism
TE	Transposable Element

CHAPTER 1: INTRODUCTION

Meiosis is the fundamental process of sexual reproduction. To maintain a population by sexual reproduction, organisms must pass on only half of their genetic material through their gametes so that two gametes can unite to recreate the diploid organism. In many organisms, exchange between homologous chromosomes is necessary for the physical connection and proper segregation of chromosomes at meiosis I (MI). This exchange requires breaks in the DNA and crossovers between homologous chromosomes. Breaking and rearranging DNA is a precarious process; therefore, meiotic recombination must be an exceptionally coordinated system.

The scientific community often describes crossover formation as having two purposes. The first is the proper segregation of chromosomes, as already stated. The second purpose of crossovers is to generate genetic diversity by generating new combinations of alleles in a genome. However, this second purpose of crossovers stirs up an interesting debate. Is genetic diversity a reason *why* crossovers occur, or is it simply a *result* of crossovers? At this point, it is impossible to answer this question but it is an important example to remind us to always keep different perspectives in mind.

When mistakes do happen in meiosis, missegregation of chromosomes can lead to nondisjunction. The presence of an abnormal number of chromosomes is called aneuploidy, and this is the most common chromosome anomaly in humans and is the leading cause of miscarriages (Hassold and Hunt 2001). Only a few trisomy instances are viable, which include Patau syndrome (trisomy 13), Edwards syndrome (trisomy 18), and Down syndrome

(trisomy 21). Aneuploidy often arises from mistakes that occur in chromosome segregation in maternal MI, usually due to recombination errors. Specifically, MI nondisjunction events occur primarily in chromosomes that do not experience a crossover. Alternatively, apparent MII nondisjunction events occur primarily in chromosomes that experience a crossover proximal to the centromere (Koehler *et al.* 1996a).

Precursors to crossovers are double strand breaks (DSBs), which can be repaired as crossovers (COs), where exchange of genetic information occurs between chromosomes, or noncrossover gene conversions (NCOs), where smaller sequences are replaced by the homologous chromosome's sequence. DSBs are created by the evolutionarily conserved protein Spo11 (MEI-W68 in *Drosophila*) (Keeney *et al.* 1997; McKim and Hayashi-Hagihara 1998). A mechanism to explain how COs and NCOs are produced was first proposed by Robin Holliday (Holliday 1964). In Holliday's model, strands from homologous chromosomes swap pairing partners; this intermediate is termed a Holliday Junction (HJ) and is cleaved by resolvases. COs and NCOs could both be produced from this intermediate depending on which strand was nicked. This model has been subsequently revised throughout the years. Szostak *et al.* proposed that the process begins with a DSB on one chromatid, instead of nicks on homologous chromosomes as proposed to by Holliday (Szostak *et al.* 1983). Additionally, it was proposed that the intermediate was formed from two Holliday junctions instead of one, which is termed the double Holliday junction (dHJ). Allers and Lichten (2001) discovered that NCOs arose before COs and proposed an alternate model where NCOs arose from an earlier intermediate, a D-loop, and COs were preferentially formed from the dHJ.

DSB repair is a highly regulated process and DSBs that are destined to become COs are not selected at random. The majority of COs occur in the middle of a chromosome arm, and it is ensured that COs are distributed among all of the chromosomes. The DSBs that

are not selected to become COs become NCOs. DSBs are likely randomly distributed throughout the genome, including centromere-proximal regions, as evidenced by NCO distribution not being significantly different from a random distribution in whole-genome studies of CO and NCO events (Miller *et al.* 2016). The DSB fate choice of becoming a CO or NCO is a critically regulated process and is arguably one of the most important aspects of meiosis. Throughout this work, I discuss meiotic DSB repair and the mechanisms of DSB fate.

Meiotic crossover patterning phenomena

DSB fate is thought to be regulated by a few crossover patterning phenomena. First, assurance or the obligatory crossover ensures that there is at least one crossover per chromosome (or chromosome arm) (Wang *et al.* 2015). In most organisms, the frequency of chromosomes without a crossover is less than 1%, although there are a few exceptions (Charles 1938; Zhang *et al.* 2014). Additionally, studies have shown that chromosomes from oocytes that experienced nondisjunction more frequently include chromosomes without a crossover (Koehler *et al.* 1996a; Hatkevich *et al.* 2017). These results together support the idea that chromosomes must experience at least one crossover to have proper segregation in MI. Assurance is not achieved simply by having a large amount of DSBs along a chromosome arm, therefore increasing the chance that one will become a crossover. In many cases, there are few DSBs and crossover designation is an important process to ensure the obligatory crossover. Conversely, some organisms have many DSBs but very few COs and assurance ensures that these limited crossovers reach each chromosome.

In addition to assurance, interference is the process by which crossovers do not occur too close to each other along a chromosome arm. Interference was first discovered in *Drosophila* by Sturtevant recognizing that when a crossover occurred between two markers, it was less likely that a crossover occurred in an adjacent interval (Sturtevant 1913a).

Interference is classically measured by the Coefficient of Coincidence (CoC) (Charles 1938). To calculate CoC, crossovers are scored within two adjacent intervals. Both single crossovers (a crossover within just one of the intervals) and double crossovers (crossovers in both of the intervals) are scored. Then the observed frequency of double COs is compared with the frequency of double COs predicted if crossovers occurred independently, which is calculated from the number of single crossovers. Then CoC is calculated as the ratio of these two numbers. A CoC that equals 1 means there is no interference. A CoC < 1 indicates interference because the observed frequency of double COs was less than that predicted by occurrence of independent crossovers. Interference and assurance are interesting phenomena because they suggest some sort of communication between chromosomes and along a chromosome arm. The mechanisms of these phenomena are still largely unknown and a large area of interest.

The last crossover patterning phenomenon is known as the centromere effect, which was also discovered in *Drosophila* by Beadle (Beadle 1932). Beadle noticed that there were fewer crossovers between markers that were proximal to the “spindle-fibre” and so he therefore termed this the “spindle-fibre effect,” which is now referred to as the centromere effect. The centromere effect is seen in many organisms, but the mechanism of this suppression of crossovers is still completely unknown. Hatkevich *et al.* (2017) developed a measure of the centromere effect (*CE*), where *CE* = 1 – (observed/expected). Observed is the number of crossovers in a centromere-proximal interval and expected is the number of crossovers expected in this interval if there was a random distribution of crossovers. Therefore, the closer to 1, the stronger the centromere effect. Assurance, interference, and the centromere effect have unknown mechanisms, but insight into crossover patterning also comes from modeling of crossover distributions.

Crossover distribution modeling

Even though these crossover patterning mechanisms are not understood, we can use mathematical formulas to create models of crossover distribution. One such model that has been developed is the Beam-Film (BF) Model (Zhang *et al.* 2014). The Beam-Film model has parameters that are categorized as precursor parameters (number of precursors, precursor distribution among and along chromosomes, precursor density), and patterning parameters (designation driving force, interference, and end effects of interference). The resulting CO distribution results from interaction of designation driving force and interference. The idea is that there is stress along the entire chromosome and that stress will be relieved by designating a CO, and that relief of stress emanates out from the CO, dissipating with distance until a high amount of stress can again create a CO (Zhang *et al.* 2014; and reviewed in Wang *et al.* 2015). The parameter for "end effects of interference" represents the centromere effect, in which case this parameter can be set so that it behaves as if a crossover already occurred at that end and an interference signal will spread from that end. The BF model was able to accurately describe CO data sets from yeast, tomato, *Drosophila*, and grasshopper. Interestingly, the BF model suggests that the obligatory crossover is not a mechanism on its own, yet it is a result of the other crossover patterning parameters explained by the BF model. This is an interesting insight provided by the BF model and shows the value of modeling CO distribution.

The BF model helps explain the model of CO distribution; however, it does not directly address any of the mechanisms. Kleckner and colleagues have hypothesized that the mechanical stress involved in CO designation and interference is the stress caused by constraining the chromatin and that this relieved when a CO is formed (Zhang *et al.* 2014; and reviewed in Wang *et al.* 2015). They hypothesize that the stress is then relieved by spreading through the axis of the chromosome. There are other hypotheses about CO

distribution such as the polymer-based model and the counting model. The polymer-based model is explained by King and Mortimer (1990) where they propose that early structures randomly attach to chromosomes and some begin to polymerize and expand, thus inhibiting nearby early structures from polymerizing and dislodging other structures in the region. King and Mortimer (1990) suggest that these structures form the recombination nodules observed in electron microscopy images. The counting model proposes that COs are designated every "N" precursors. However, this model does not account for the fact that in some instances, number and distribution of COs will remain the same even if the number of precursors change (reviewed in Wang *et al.* 2015).

Modeling of crossover distribution gives us insight into the quantitative aspects of crossover designation, but it only allows us to speculate on the mechanisms of crossover distribution. Many labs are still focused on understanding the mechanisms involved in crossover distribution, and this will probably be an area of study for many years to come.

Drosophila as a model for meiotic crossover control

Drosophila melanogaster is an excellent model for meiotic recombination. Many of the processes and proteins involved in meiotic recombination are evolutionarily conserved, making *Drosophila* studies applicable to many other organisms and processes. *Drosophila* males do not undergo meiotic recombination, making it possible to observe progeny that have meiotic events from only one parent. *Drosophila* can also tolerate DNA sequence polymorphisms without having an increase or decrease in recombination frequency (Hilliker *et al.* 1991). This allows fine mapping of recombination events between SNPs of isogenized strains of *Drosophila* (Comeron *et al.* 2012; Miller *et al.* 2016). It is also possible to recover aneuploid progeny in *Drosophila*, especially with the *X* chromosome, allowing robust nondisjunction studies. *Drosophila* have been used for genetic screens that discovered the very first meiotic mutants, as well as recent studies using new techniques to identify even

more mutants (Sandler *et al.* 1968; Baker and Carpenter 1972; Sekelsky *et al.* 1999; Fedorova *et al.* 2001; Page *et al.* 2007; Collins *et al.* 2012).

Drosophila is also a great visual model for meiotic recombination because the ovary is arranged in accordance with developmental time (Lake and Hawley 2012). The ovary consists of ovarioles, which contain strings of developing egg chambers. The anterior tip of each ovariole contains the germarium, where meiosis begins and meiotic recombination occurs. The germline stem cell is in the most anterior region of the germarium, and this cell divides to create a cystoblast that will divide incompletely four times, creating a 16 cell cyst. Some of the cells within the cyst will enter meiosis, designated by the formation of synaptonemal complex (SC) between homologous chromosomes. By the end of meiotic recombination and the posterior end of the germarium, only one cell is designated as the oocyte. Thus, the germarium provides a snapshot of meiotic recombination and is a useful tool to visualize meiotic cells and progress of meiotic recombination.

Two pathways to crossover formation

DSB repair involves a number of different proteins that have varying functions in different organisms. Studies in *Saccharomyces cerevisiae* show that Msh4 and Msh5 form a hetero-oligomeric structure that facilitates meiotic crossover formation (Pochart *et al.* 1997). All meiotic crossovers are dependent upon Msh4 and Msh5 in *Caenorhabditis elegans* (Zalevsky *et al.* 1999). In contrast, *Schizosaccharomyces pombe* lacks orthologs of Msh4 and Msh5 and all crossovers are dependent on the Mus81-Mms4 resolvase (Boddy *et al.* 2001; Villeneuve and Hillers 2001; Smith *et al.* 2003). In *S. cerevisiae, msh4 msh5* double mutants have a 50-70% reduction in crossovers, and *mus81 mms4* double mutants have a 30-50% reduction in crossovers (Ross-Macdonald and Roeder 1994; Hollingsworth *et al.* 1995; De Los Santos *et al.* 2001). In *S. cerevisiae* and *A. thaliana*, double mutants for Msh4/Msh5 and Mus81/Mms4 show a more severe decrease in crossovers than the single

mutants, suggesting that these two complexes work in different pathways (De Los Santos *et al.* 2003; Berchowitz *et al.* 2007). These two pathways of crossover formation have been termed Class I, which is dependent on Msh4 and Msh5, and Class II, which is dependent on Mus81-Mms4.

Additionally, it was observed that Class I crossovers exhibit interference, while Class II crossovers do not. This was first modeled using crossover data in *A. thaliana* that showed crossover distribution can be explained by having one set of crossovers that experience interference and the other set does not (Copenhaver *et al.* 2002). In accordance with this modeling, crossovers in budding yeast and *A. thaliana msh4* and *msh5* mutants do not exhibit interference (Novak *et al.* 2001; Argueso *et al.* 2004; Lu *et al.* 2008). Additionally, crossovers in budding yeast and *A. thaliana* lacking Mus81-Mms4 experience interference. These results suggest that the Class I pathway dependent on Msh4 and Msh5 produces crossovers that experience interference and the Class II pathway dependent on Mus81-Mms4 produces non-interfering crossovers.

Drosophila have lost Msh4 and Msh5, but are thought to have been functionally replaced by a pro-CO complex termed mei-MCM (Kohl *et al.* 2012). The mei-MCM complex consists of REC, MEI-217 and MEI-218. REC is the *Drosophila* ortholog of MCM8, and is an MCM protein based on its N-terminal MCM domain and C-terminal AAA+ ATPase domain. MEI-217 and MEI-218 together resemble one full MCM protein with MEI-217 carrying the MCM domain, and MEI-218 carrying the AAA+ ATPase domain. However, the ATPase domain in MEI-218 has differences in key conserved, catalytic residues. Crossovers in *Drosophila* are dependent on the mei-MCM complex and experience interference, suggesting that most or all crossovers are created through the Class I pathway. Figure 1.1 illustrates the two pathways and *Drosophila* proteins involved in these pathways.

Major insight into the meiotic recombination pathways was gained when timing of CO and NCO product formation was studied in budding yeast. Allers and Lichten (2001) found that NCOs arose before COs did, but also that they arose before joint molecules (which are generally accepted to be dHJs). This result did not support the current model of meiotic recombination pathways, but instead suggested a pathway where NCOs form from an earlier intermediate and COs are preferentially formed from dHJs later in meiosis. McVey *et al.* showed that in *Drosophila* Blm is the helicase that processes the earlier intermediate, a D-loop, via SDSA into a NCO in mitotic DSB repair. (McVey *et al.* 2004). Yildiz *et al.* determined that MEI-9–ERCC1 together with the scaffolding protein MUS312, is the major meiotic resolvase that forms crossovers in *Drosophila* (Yildiz *et al.* 2002, 2004). MEI-9-ERCC1 is the *Drosophila* ortholog of XPF-ERCC1 and MUS312 is the *Drosophila* ortholog of SLX4.

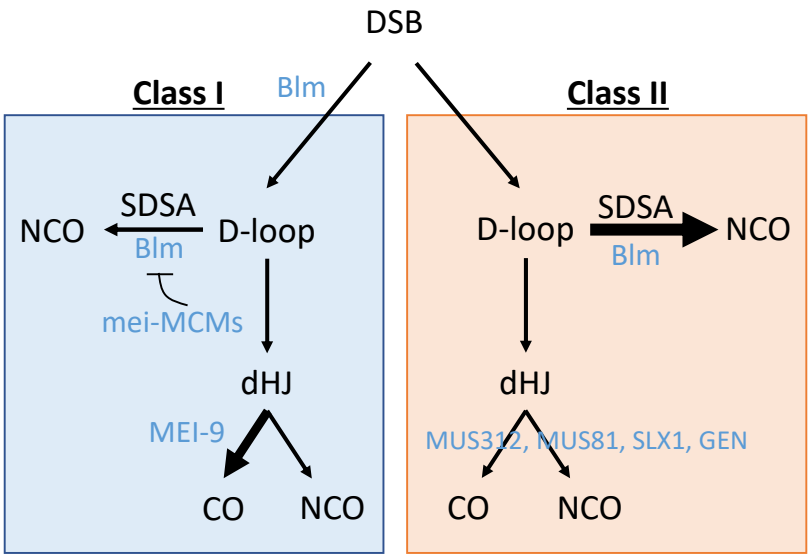

Figure 1.1. Two pathway DSB repair model. A DSB can repaired by Blm directing repair down the Class I pathway in which a D-loop is preferentially directed into becoming a dHJ by the mei-MCM complex, and dHJs are resolved by MEI-9 into COs. If Blm is absent, repair will be directed down the Class II pathway, where D-loops are preferentially migrated through SDSA to form NCOs and the remaining go through dHJs to be resolved in an unbiased manner as COs or NCOs by the endonucleases MUS81, SLX1, MUS312, and GEN.

In *S. cerevisiae,* Bloom syndrome helicase mutants, *sgs1,* reveal COs and NCOs that form at the same time (De Muyt *et al.* 2012). These COs and NCOs are both formed from dHJs, but the repair of these dHJs is not biased toward COs. In the absence of Sgs1, the resolvases Mus81-Mms4, Yen1, and Slx1-Slx4 resolve dHJs into COs and NCOs (De Muyt *et al.* 2012; Zakharyevich *et al.* 2012). This was shown through the fact that crossovers in *sgs1* mutants are resolved by these proteins. Mutants of *sgs1* in combination with mutants of these resolvases result in a buildup of intermediates and fewer COs and NCOs formed, which is worsened in *sgs1 mms4 yen1 slx1* quadruple mutants (De Muyt *et al.* 2012).

Studies in *Drosophila* have shown that *Blm* mutants in combination with mutations in either *mus81, mus312, or Gen* (the *Drosophila* Yen1 ortholog) are synthetically lethal (Andersen *et al.* 2011). Additionally, in *Blm* mutants, all crossovers are MEI-9 independent, which supports the idea that *Blm* mutants experience only Class II crossovers (Hatkevich *et al.* 2017). Hatkevich *et al.* also showed that *Blm* mutants lose all crossover patterning: assurance, interference, and the centromere effect, suggesting that these three crossover patterning phenomena are characteristic of Class I meiotic crossovers (Hatkevich *et al.* 2017). All of these results lead us to the model that Blm is responsible for directing DSBs down the Class I meiotic recombination pathway.

Centromere proximal crossover suppression in *Drosophila*

In meiosis, DSBs are mostly processed through the Class I pathway. It is important that crossovers are formed via the Class I pathway because proper crossover patterning is needed for the correct segregation of chromosomes in meiosis. Together, assurance, interference, and the centromere effect direct most crossovers to occur around the middle to distal region of a chromosome arm and to ensure that about one crossover occurs per arm. Crossovers are essential for the proper segregation of chromosomes as evidenced by the

fact that Meiosis I (MI) nondisjunction events more often contain chromosomes that are lacking a crossover (Koehler *et al.* 1996a). Additionally, proper crossover placement is essential, as evidenced by the fact that apparent Meiosis II (MII) nondisjunction events more often contain chromosomes that have centromere-proximal crossovers (Koehler *et al.* 1996b).

Crossovers are essential for the proper segregation of chromosomes in meiosis because of the way meiotic chromosomes are manipulated throughout meiosis. *Drosophila,* like some other organisms such as humans, mice and xenopus, are acentroliar; instead of the spindle organizing chromosomes in meiosis, the chromosomes arrange themselves into a mass called the karyosome before microtubules have a designated pole (Koehler *et al.* 1996b). Then microtubules will form together to create a bipolar spindle. In MI, homologous centromeres attach to microtubules from opposite poles, so when homologues are pulled apart, crossovers between them generate tension and ensure their proper orientation and separation to opposite poles (reviewed in Nambiar and Smith 2016). In MI, sister chromatid cohesion is placed along the chromosome arms keeping the bivalent together. At anaphase I, sister chromatid cohesion is released along the chromosome arms, but maintained in the peri-centromeric regions, which allows the reductional division in MI (reviewed in Hughes *et al.* 2018). Rec8 is the meiosis specific cohesin that is cleaved by separin on the arms in MI (Buonomo *et al.* 2000). It is still not known exactly how cohesin is maintained only in centromeric regions, but key players have been identified. The maintenance of centromere-proximal cohesion relies on the *Drosophila* MEI-S332, which is part of the Shugoshin family of proteins (Kerrebrock *et al.* 1995; Sekelsky and Hawley 1995). Phosphorylation of MEI-S332 by Aurora B kinase and the INCENP protein are needed for MEI-S332 localization at the centromere (Resnick *et al.* 2006). The peri-centromeric cohesion is then released in MII, allowing sister chromatids to separate to opposite poles.

MI nondisjunction events occur when homologous chromosomes do not segregate properly and go to the same pole in MI. Then in MII, the sisters segregate properly, so the resulting aneuploid gamete includes homologous chromosomes, identifiable by different centromeres as in Figure 1.2A. When MI proceeds normally and mistakes occur in MII, the two centromeres come from sisters, so they are the same, as shown in Figure 1.2B. As mentioned previously, apparent MII events from Trisomy 21 individuals more often have centromere-proximal crossover events (Koehler *et al.* 1996b). However, it was puzzling why these events appeared to be from MII nondisjunction when recombination occurs in MI.

Two hypotheses for how these events could have occurred were proposed by Lamb *et al.* (1996). The first explanation is termed “entanglement” where homologues are entangled by the centromere-proximal crossover and the bivalent remains together until separation at MII where sisters remain together and homologues separate to opposite poles as shown in Figure 1.2C. The second hypothesis is termed precocious separation of sister chromatids (PSSC). In this case, pericentromeric crossovers disrupt the cohesion of sisters and cause premature separation of the sisters at MI and then are susceptible to random segregation at MII, where both sisters could segregate to the same pole (Figure 1.2D). Therefore, these mistakes both occur at MI due to the peri-centromeric exchange, but are scored as MII events because they contain the same centromere.

What is important to note is that centromere-proximal crossovers are correlated with nondisjunction events. As discussed previously, it is thought that the centromere effect suppresses these centromere-proximal crossovers but the mechanism is unknown and largely unstudied. However, there are ideas about what could be suppressing centromere-proximal crossovers including heterochromatin and transposable elements.

Early studies of the centromere effect in *Drosophila* involved rearrangements of chromosomes and heterochromatin. Mather (1939) used chromosome rearrangements to

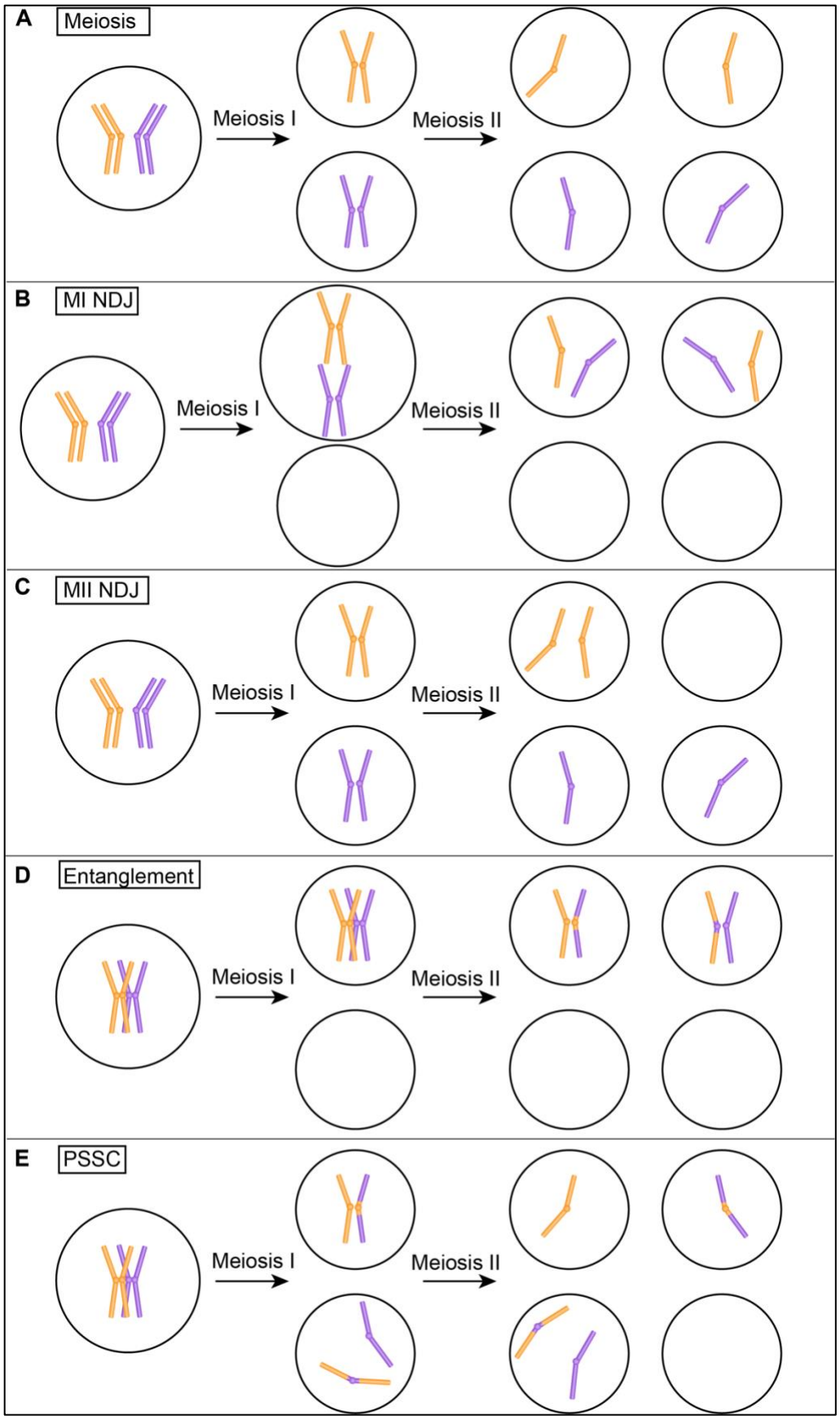
A
Meiosis
Meiosis I
Meiosis II
B
MI NDJ
Meiosis I
Meiosis II
C
MII NDJ
Meiosis I
Meiosis II
D
Entanglement
Meiosis I
Meiosis II
E
PSSC
Meiosis I
Meiosis II

Figure 1.2. Types of nondisjunction. (A) Schematic of chromosomes experiencing normal meiotic segregation. (B) In Meiosis I (MI) nondisjunction (NDJ), homologues missegregate and go to the same cell, and then sisters separate, resulting in gametes containing chromosomes with different centromeres (orange and purple). (C) in Meiosis II (MII) NDJ, homologues segregate properly in the first division, but then in one instance, sisters did not segregate properly in the second division (orange chromosomes), resulting in a gamete containing chromosomes with the same color centromere. (D) Entanglement begins with a peri-centromeric crossover causing both homologues to segregate to the same pole. Homologues remain together in a bivalent and separate in MII causing sisters to go to the same cell and resulting in gametes with the same centromeres, presenting as MII NDJ even though the mistake occurred in MI. (E) Precocious separation of sister chromatids (PSSC) occurs when peri-centromeric crossovers cause sister chromatid cohesion to be released early, resulting in random segregation of sisters into the same cell in MII (bottom).

show that when peri-centromeric heterochromatin is rearranged in a way that places euchromatin closer to the centromere, there is a greater decrease in crossovers in that euchromatin than a euchromatic region moved nearer to a large amount of heterochromatin (farther from the centromere than in the first case). Similarly, Yamamoto and Miklos (1978) showed that centromere-proximal suppression of crossovers moved farther into the euchromatin when sections of *X* chromosome heterochromatin were deleted. These studies suggest that the centromere effect depends on distance from the centromere and not necessarily the amount of heterochromatin. However, there are also studies that suggest heterochromatin directly plays a role in suppressing crossovers.

In cytological studies of DSBs, Mehrotra and McKim (2006) show that DSB markers do not colocalize with heterochromatin marker HP1. This result suggests that DSB machinery may not have access to the tightly packed chromatin, so crossovers are unable to form in this region. Nonetheless, the question still remains whether heterochromatin has the ability to decrease crossovers in adjacent euchromatic regions causing the suppression of crossovers we see in these regions.

Some heterochromatic regions contain transposable elements, which consist of middle-repetitive sequences. Transposable elements are abundant in the heterochromatin

that is adjacent to euchromatin, making these regions easier to assemble to the genome (Yamamoto *et al.* 1990; Carmena and González 1995). Transposable elements have been suggested to have an effect on crossover rate, by suppressing crossovers in peri-centromeric regions (Bartolome *et al.* 2001; Bartolome and Maside 2004; Kent *et al.* 2017). The interplay of transposable elements and gene density with crossover rate is a highly debated phenomenon (reviewed in Kent *et al.* 2017). It has been proposed that an increase in crossover rate in gene dense regions is favored due to the resulting increase in genetic diversity. Additionally, it is thought that crossing over is suppressed in regions that have a high density of transposable elements (TEs) to repress harmful recombination within repetitive elements. Recombination in repetitive regions can lead to insertions or deletions of repeats, or ectopic recombination events. Alternatively, it has been proposed that transposable elements themselves repress recombination. Miller *et al.* (2016) reported that crossovers can occur within TEs, but less frequently than would be expected if they were freely able to form within TEs. It has been suggested that active silencing of TEs could lead to the silencing or suppression of recombination around those regions (Kent *et al.* 2017). It is still unknown whether TEs or gene density directly or even indirectly affect recombination rates, but many studies have at least suggested a correlation between these factors.

Crossover patterning is such a complex and interesting field; however, it is very difficult to gain insight into the mechanisms controlling crossover designation. My thesis work has addressed crossover patterning by both examining proteins involved in crossover formation as well as the mechanisms governing centromere-proximal crossover suppression. I have gained important insights that have impacts in many research fields including endonucleases, meiotic recombination, and the centromere effect.

Scope of this work

De Muyt *et al.* saw that even in the quadruple *sgs1 mms4 yen1 slx1* mutant, there were still residual COs and NCOs, suggesting there were other resolvases yet to be identified that are able to resolve intermediates into COs and NCOs. MUS81 is an ERCC4 nuclease that has been shown to interact with SLX1 and MUS312 to resolve dHJs (Gaillard *et al.* 2003; Gaskell *et al.* 2007; Fekairi *et al.* 2009). MEI-9 is similar to MUS81 in that it is an ERCC4 nuclease and also interacts with MUS312. I hypothesized that there is another partner that interacts with MEI-9 and MUS312 to resolve HJs. This potential partner is Ankle1, which is similar to SLX1 because it contains a GIY-YIG nuclease domain. I examined Ankle1's potential role as an endonuclease in Chapter 2.

Interestingly, mutations in both *Blm* and the mei-MCM complex genetically interact: in *Blm rec* double mutants, crossovers are increased compared to *Blm* single mutants, suggesting that the mei-MCM complex may play a role in inhibiting crossovers in the Class II pathway. The role of the mei-MCM complex in the Class II pathway is investigated and described in Chapter 3. Little is known about how individual members of the mei-MCM complex contribute to crossovers, so I investigate this in the work described in Chapter 3.

I was particularly interested in the centromere effect and understanding how centromere-proximal crossovers were suppressed became the focus of my thesis work. Chapter 4 contains work that was published as a review paper on chromosome *4,* which delves into understanding why chromosome *4* does not experience crossing over. I hypothesize that chromosome *4* does not have crossovers because the entire chromosome is subject to the centromere effect. This is supported by the fact that *Blm* mutants do experience crossovers on chromosome *4.* Chapter 5 encompasses my experimental work on mapping centromere-proximal crossovers and discovering that these crossovers are suppressed by two mechanisms: the highly-repetitive heterochromatin completely

suppresses crossovers, and the centromere effect, which suppresses crossovers with a dissipating effect with distance from the centromere and encompasses the less-repetitive heterochromatin and proximal euchromatin. We also examine the effect of genomic sequence characteristics, such as transposable element density and gene density, on determining crossover rate.

CHAPTER 2: EXAMINATION OF ANKLE1 AS A POTENTIAL NUCLEASE

Preface

This chapter includes preliminary data on the examination of the potential nuclease Ankle1. This project encompassed my rotation and part of my first year of research in the Sekelsky Lab. I provide results suggesting that Ankle1 interacts with MUS312 and MEI-9; however, studies of an *Ankle1* deletion showed no meiotic defects or sensitivity to DNA-damaging agents. These results show support for a role of Ankle1 in creating mitotic crossovers in the absence of the *Fancm* helicase. I did not pursue this project as my dissertation research to instead focus on the centromere effect. Here, I detail the preliminary results I obtained on the potential nuclease Ankle1, and suggest possible future studies.

Introduction

Throughout DNA replication and recombination, DNA forms different branched structures, which need to be resolved for proper completion of DNA replication and maintenance of genome integrity. SLX4 is a scaffolding protein known to assemble with multiple structure-specific nucleases that will aid in the resolution of Y forks, 3' flaps, 5' flaps, replication forks, and Holliday Junctions (HJs) (Muñoz *et al.* 2009). SLX4 interacts with nucleases such as GEN1, XPF-ERCC1 and MUS81-EME1 in distinct complexes (Fekairi *et al.* 2009; Muñoz *et al.* 2009; Wyatt *et al.* 2013).

One of the complexes formed is the interaction of SLX4 with SLX1, and MUS81-EME1. This complex is utilized in HJ resolution in meiotic recombination as well as mitotic DSB repair pathways (Gaillard *et al.* 2003; Gaskell *et al.* 2007; Fekairi *et al.* 2009). Another

complex formed with SLX4 contains XPF-ERCC1, which is involved in resolving interstrand crosslinks as well as HJs (Fekairi *et al.* 2009). MUS312 and MEI-9–ERCC1 are the *Drosophila* homologs of this complex, which is involved in meiotic DSB repair and thought to be the major meiotic resolvase that generates crossovers (Radford *et al.* 2005, 2007). However, in the absence of MEI-9 or MUS312, there are still some residual crossovers (Radford *et al.* 2005; Andersen *et al.* 2009). Therefore, I hypothesize that there is another resolvase involved in creating meiotic crossovers.

MEI-9 and MUS81 are both nucleases that belong to the ERCC4 nuclease family, and both have binding partners containing inactive nuclease domains (Figure 2.1A). MUS81-EME1 pairs with SLX1-SLX4 to resolve junctions, so due to the similarities between MUS81 and MEI-9, I hypothesize there is another protein within the MUS312-MEI-9-ERCC1 resolvase complex similar to SLX1. SLX1 has a GIY nuclease domain (Coulon *et al.* 2004; Svendsen *et al.* 2009), so I set to identify another protein in *Drosophila* that contains a GIY nuclease domain that may form a similar complex with MUS312, MEI-9-ERCC1.

Besides Slx1, the mammalian genome includes only one other GIY-YIG nuclease domain containing protein, Ankle1 (Dunin-Horkawicz *et al.* 2006; Zlopasa *et al.* 2016). At the start of this study, not much was known about Ankle1. Brachner *et al.* showed that enriching Ankle1 induced DNA cleavage and the DNA damage response and that the GIY-YIG and LEM domains of this protein are required for that activity (Brachner *et al.* 2012). The *Caenorhabditis elegans* homolog was identified as LEM-3, and was isolated in a screen for mutants sensitive to ionizing radiation (IR) (Dittrich *et al.* 2012). Dittrich *et al.* also found that *lem-3* mutants were sensitive to other types of DNA-damaging agents suggesting a role for LEM-3/Ankle1 following DNA damage. We identified a candidate protein, CG8679 in *Drosophila melanogaster* that also contains a LEM domain and a GIY-YIG nuclease domain as well as the ankyrin repeat (ANK) domain found in *C. elegans* LEM-3 and mammalian

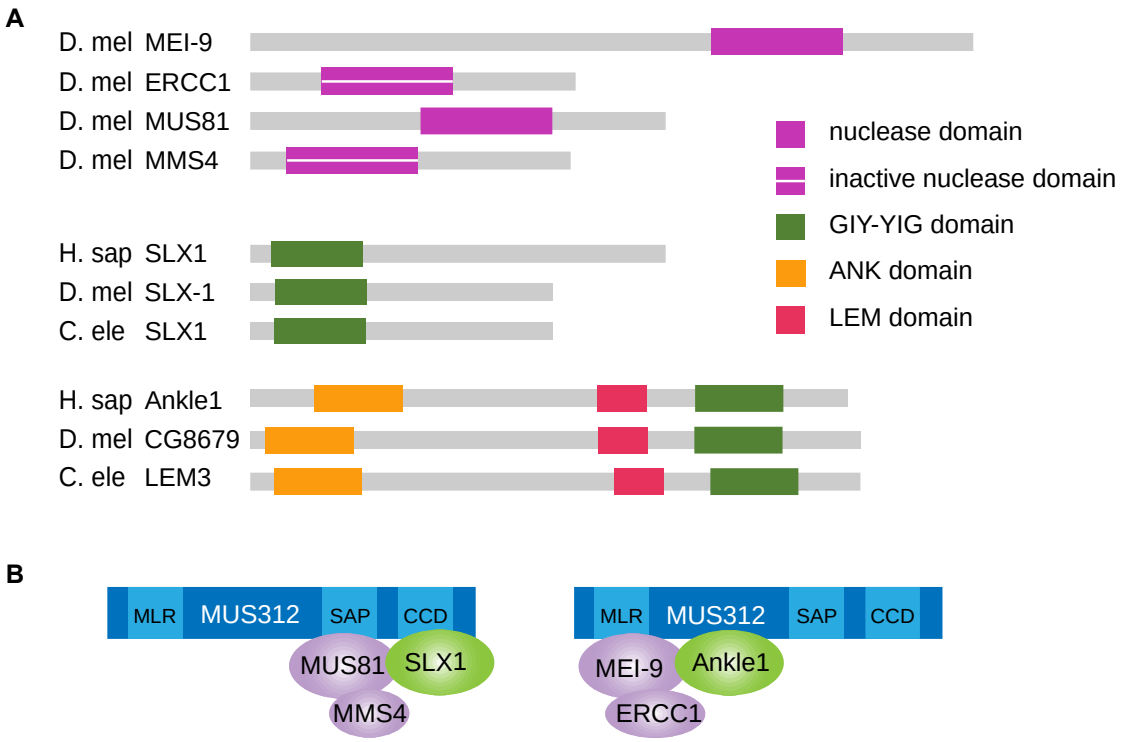

Figure 2.1. Nucleases and Ankle1 Model. (A) Schematic of domains within nucleases that assemble into complexes as shown in (B). Domains shown include the ERCC4 nuclease domain, predicted inactive nuclease domain, GIY-YIG domain, ANK domain, and LEM domain. (B) shows predicted nuclease complexes with the scaffolding protein, MUS312. We hypothesize that Ankle1 acts as part of the complex on the right as a nuclease with MEI-9 and ERCC1. Domains in MUS312 shown are the MUS312/MEI-9 interaction like domain (MLR), the SAF-A/B, Acinus, and PIAS (SAP) domain involved in substrate recognition, and the conserved C-terminal domain (CCD) involved in SLX1 interaction (Fekairi *et al.* 2009).

Ankle1 (Figure 2.1A) (Dunin-Horkawicz *et al.* 2006; Brachner *et al.* 2012). From now on, I refer to the candidate gene *CG8679* as *Ankle1* in *Drosophila.* SLX1 interacts with MUS312 near the C-terminal end (Fekairi *et al.* 2009; Svendsen *et al.* 2009; Castor *et al.* 2013), and MUS81-EME1 interacts with MUS312 through its SAP domain (Castor *et al.* 2013; Kim *et al.* 2013). Alternatively, MEI-9 interacts near the N-terminus of MUS312, in what Fekairi *et al.* have termed the MEI-9 interaction like domain (MLR) (Yildiz *et al.* 2002; Fekairi *et al.* 2009). I hypothesize that Ankle1 is part of a complex with MUS312 and MEI-9-ERCC1 and predict that Ankle1 will interact with MEI-9 and MUS312 near the MLR domain (Figure 2.1B). I

performed yeast two-hybrid studies to examine these interactions and to confirm other interactions within the MUS312 complexes. I created a deletion of *Ankle1* in *Drosophila* using the CRISPR/Cas9 system and characterized this mutant by measuring meiotic nondisjunction, sensitivity to DNA damaging agents, and mitotic recombination.

Materials and Methods

Yeast two-hybrid

Vectors were created using either pGBD-DEST (James et al. 1996) or pACT2.2gtwy (Addgene plasmid 11346 deposited by Guy Caldwell) using the Gateway Vector Conversion System (Life Technologies, Carlsbad, CA). Full-length and truncated versions of *mei-218*, full-length *Slx1*, and full-length *mei-9* were previously made (Radford et al. 2005; Andersen et al. 2009). *mus-81* and *Ankle1* were cloned into pGBD-DEST. *mus-81* and *mms-4* were cloned from other vectors and *Ankle1* was cloned from the BacPac genomic DNA clone library (ID BACR34H23). Constructs were transformed into *Saccharomyces cerevisiae* strain PJ69-4A (James et al. 1996). Co-transformants were obtained by selecting for growth on plates with Yeast Extract-Peptone-Dextrose (YPD) media containing supplements lacking tryptophan (-trp) and leucine (-leu) after growth for 3 days at 30°C. Single colonies were re-streaked onto fresh -trp -leu plates and grown for 3 days at 30°C. Colonies were then streaked onto triple dropout (-trp -leu -his) plates, grown for 3 days at 30°C and scored for interaction. It was verified that single transformants did not self activate and did not grow on double and triple dropout plates. For serial dilutions, yeast cultures were grown in -trp -leu dropout media to saturation, diluted 4 times by 10 fold and all five solutions were plated on -trp -leu and -trp -leu -his plates.

CRISPR/Cas9 Deletion of Ankle1

Ankle1^{dsRED} was created using the CRISPR/Cas9 technology (Gratz et al. 2013). Two gRNAs were cloned into the pCFD4 vector pCFD4-U6:1_U6:3tandemgRNAs (Addgene

plasmid #49411) that targeted two locations near the 5' and 3' ends of the *Ankle1* gene. Sequence of gRNAs were 5'- CCGTTTCGCATGCCGCACA-3' and 5'-CTCCGCCAGATAGATGTGCA-3'. *Ankle1* is 2,115 bps and the deletion is of 1,908 bps. A repair template vector was co-injected, which contains approximately 1kb of homologous sequence on either side of the two cuts and a dsRED in between, with the goal of making a deletion of *Ankle1* and inserting a copy of dsRED for easy screening of deletions. Injected flies were crossed to *Pin/CyO* and progeny were screened for red fluorescent eyes. Multiple dsRED flies were collected and stocks of *Ankle1*^{dsRED}*/ CyO* were created. Stocks were verified by PCR screening using one primer in the fly genome and one primer in dsRED to ensure that dsRED was inserted correctly and a partial deletion of *Ankle1* was created. All stocks that experienced proper placement of dsRED in the *Ankle1* deletion were kept and maintained at 25°C on standard cornmeal medium.

Sensitivity assays

Approximately 5-6 virgin females (heterozygous for mutation, with a balancer chromosome) and 3 males (heterozygous for mutation, with a balancer chromosome) were crossed and allowed to mate in a vial for 3 days. After 3 days, parents were flipped into another vial and allowed to lay for another 3 days. Those parents were emptied from vial and the following day, the larvae were exposed to the mutagenizing agent. Progeny were scored from first brood as the "untreated" group and the second brood was "treated." Number of mutant progeny were compared to heterozygous progeny (mutation/balancer chromosome). The *mei-9* mutants were scored differently because the *mei-9* mutation is on the X. Female *C(1)DX* flies (attached X) were crossed to *mei-9* mutant males. Therefore, any resulting male progeny were mutant and resulting females were *C(1)DX*, and expected progeny in a normal case would be 50% male and female. Mutagenizing agents included methyl methanesulfonate (MMS), ionizing radiation (IR) and cisplatin (cis) at designated

concentrations. MMS induces DNA alkylation and possibly double strand breaks, IR induces double strand breaks, and cisplatin induces inter-strand crosslinks (Radford 1985; Lundin *et al.* 2005; Sawant *et al.* 2017). Alleles used in this study were *Ankle1*^{dsRED}, *Df(2L)Exel6047* (deficiency chromosome with deletion of CG8679), *mei-9*^{a} (Yildiz *et al.* 2002), *Fancm*^{0693} (Kuo *et al.* 2014) , *Fancm*^{del} (Romero *et al.* 2016), *mus312*^{D1} , and *mus312*^{Z1973} (Andersen *et al.* 2011). Treated and untreated classes were compared using unpaired t-test in Prism 8.

Nondisjunction assay

Approximately 5-6 virgin females of desired genotype (WT or *Ankle1*^{dsRED}*/Df(2L)Exel6047*) were crossed to three *y cv v f / B*^{s} *Y y*$^{+}$ males in 10 vials. Parents were flipped to new vials after three days, then emptied after three more days. Progeny were scored for nondisjunction (NDJ). Parental genotypes were XX females (B^{+}), XY males (B^{-}), and exceptional progeny were XXY females (B^{-}), and XO males (B^{+}). Exceptional class numbers were multiplied by two to account for nonviable exceptional progeny (XXX, OY). WT nondisjunction data was obtained from Hartmann *et al.* (2019, *in preparation*). WT and *Ankle1* NDJ rates were compared using fisher's exact test.

Mitotic crossover assay

Mitotic crossovers were scored by crossing males of desired genotype with *st Sb/+* to females homozygous for *st Sb.* Mitotic crossovers were scored between *st* and *Sb*. *Fancm mus312* data is previously published (Kuo *et al.* 2014). Statistical analyses were performed using fisher's exact test.

Results

Nuclease Complex Interactions

I hypothesize that Ankle1 interacts in a complex with MUS312 and MEI-9-ERCC1, so I first set out to characterize these interactions as well as confirm other protein interactions

in complex with MUS312 using the yeast two-hybrid system. I confirmed interaction between MUS312 and MEI-9, MUS81 and MMS4, MUS81 and SLX1 (Figure 2.2). I was not able to recapitulate the interaction between MUS312 and MUS81, or MUS312 and SLX1. Interaction between MUS312 and SLX1 was previously shown with *Drosophila* proteins in yeast two-hybrid, and MUS312 and MUS81 have been shown to interact in human cells, but not with *Drosophila* proteins (Andersen *et al.* 2009; Wyatt *et al.* 2013). However, in using truncations of MUS312, I show that SLX1 and MUS81 interact near the C terminus, as expected from previous studies and the model shown in Figure 2.2B.

To test if Ankle1 is a component of the complex, we tested interactions between Ankle1 with MUS312 and MEI-9. Via the yeast two-hybrid system, there is an interaction between Ankle1 and MEI-9 and the N-terminus of MUS312. There is no interaction between Ankle1 and full length MUS312, but we do see the interaction in N-terminal truncations of MUS312. We hypothesized that Ankle1 interacts in a complex with MEI-9, and since MEI-9 is known to interact with MUS312 near the N-terminus, we expected Ankle1 to also interact near the N-terminus. Full length MUS312 did not produce interactions with SLX1, MUS81, or Ankle1, even though truncated forms were able to produce an interaction. I predict that the full-length MUS312 may not be expressed properly or fold in the correct configurations to produce these interactions in the yeast two-hybrid system.

The interactions of Ankle1 with MEI-9 and the N-terminus of MUS312 are suggestive of a complex where Ankle1 may act as a nuclease in concert with MEI-9 and MUS312. I sought to test the functions of Ankle1 *in vivo,* by creating a deletion of *Ankle1* in *Drosophila melanogaster.*

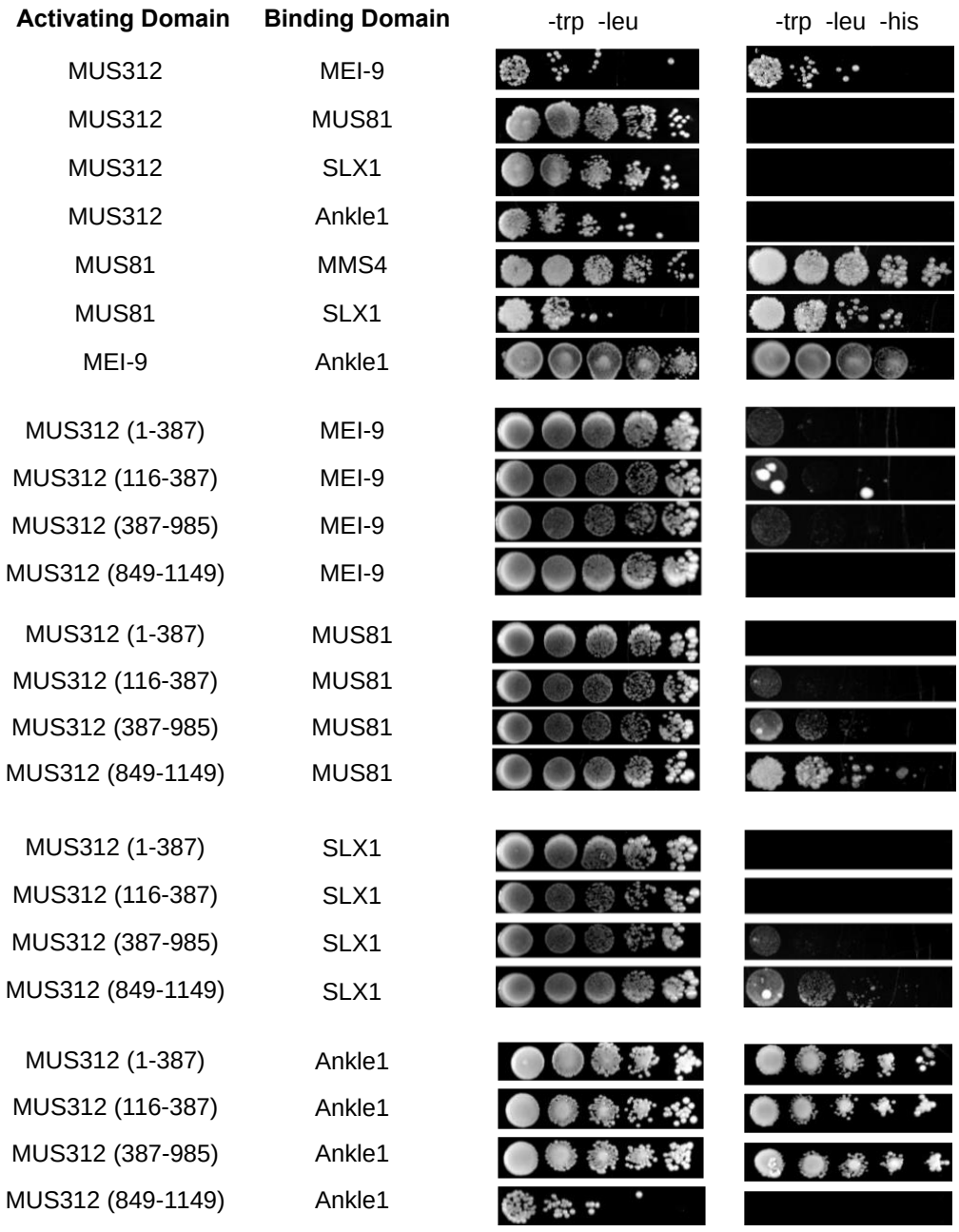

Figure 2.2. Yeast Two-Hybrid with proposed components of nuclease complexes. Genes of the proteins in the activating domain column were cloned into the pACT2.2gtwy vector to be expressed as a fusion protein with the Gal4 activating domain. Genes of the proteins in the binding domain column were cloned into the pGBD-DEST vector to be expressed as a fusion protein with the Gal4 binding domain. Serial dilutions are shown on -trp -leu plates and -trp -leu -his plates. Growth on triple dropout plates indicates interaction between the two proteins.

Ankle1 deletion and characterization

I created a CRISPR deletion of *Ankle1* with an insertion of dsRED as described in Materials and Methods. Since MEI-9 works with MUS312 to resolve HJs to create meiotic crossovers, I hypothesized that *Ankle1* may also play a role in resolution of meiotic crossovers. If *Ankle1* is required for meiotic crossovers, I hypothesize a decrease in crossovers in the mutant, and a subsequent increase in nondisjunction. I first screened for nondisjunction in *Ankle1* mutants, which shows no significant increase in nondisjunction as compared to wild-type (p=0.56) (Table 2.1). I therefore conclude that *Ankle1* either does not play a role in the meiotic function of this complex or its function is redundant.

	XX	XY	XXY	XO	
Genotype	**Females**	**Males**	**Females**	**Males**	**Total**
WT (*yw*)	1551	1481	0	1	**3033**
Ankle1	1107	766	2	0	**1875**

Table 2.1. Nondisjunction of Ankle1. Nondisjunction of *Ankle1^{dsRED}/ Df(2L)Exel6047* was scored (see materials and methods). Parental classes are XX females and XY males, exceptional classes are XXY females and XO males. WT data is from Hartmann *et al.* (2019, *in preparation*). WT is not significantly different from *Ankle1* using fisher's exact test (p=0.56).

Ankle1 sensitivity to DNA-damaging agents

Since LEM-3 has a role following DNA damage in *C. elegans*, I tested the response of *Ankle1* mutants in *Drosophila* to DNA-damaging agents including IR, MMS, and Cisplatin. Ionizing radiation is a DSB-inducing agent (Radford 1985). *Ankle1* mutants did not have decreased survival when exposed to two doses of IR (Figure 2.3 and Table 2.2) (1500 rads p=0.11, 2000 rads p=0.48). I used *mei-9* mutants as a positive control as they have been shown to be sensitive to IR (Baker *et al.* 1978) (Figure 2.3 and Table 2.2). *Ankle1* did show a slight, but not significant, decrease in viability with exposure to 1500 rads, but a similar decrease was not observed when exposed to 2000 rads, so I conclude that *Ankle1* mutants

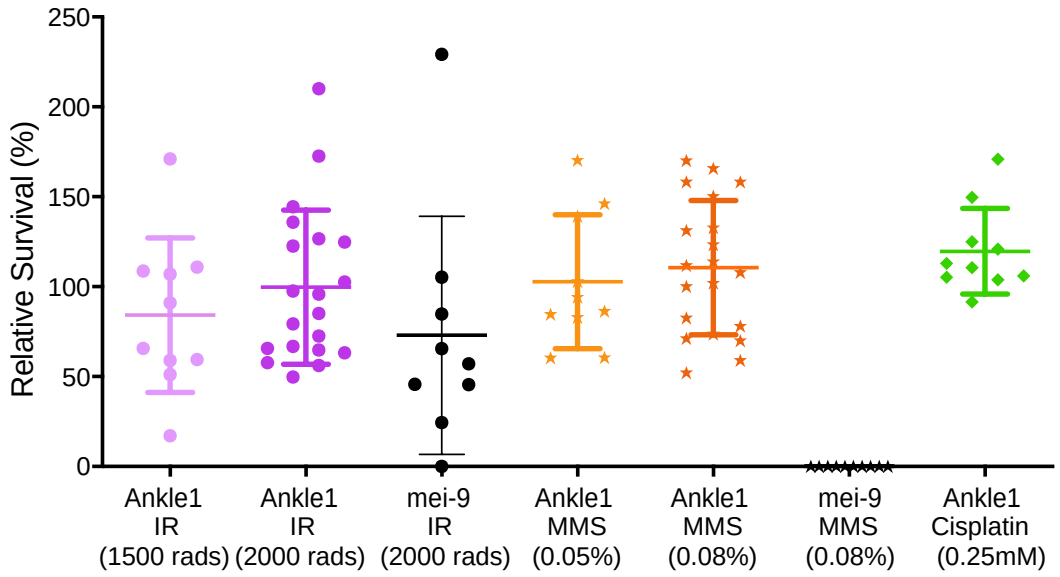

Figure 2.3 Sensitivity Assays of *Ankle1.* Flies heterozygous for *Ankle* or *mei-9* mutations were mated and scored for the ratio of heterozygous progeny to homozygous mutant progeny. That ratio was compared between treated and untreated broods. Numbers and significance values between treated and untreated are shown in Table 2.2. *Note: These experiments were not done at the same time.

are not sensitive to IR. Mutants sensitive methyl methanosulfate (MMS) have defects in homologous recombination (HR), so we tested if *Ankle1* mutants are sensitive to MMS (Lundin *et al.* 2005). *Ankle1* mutants are not sensitive to two different concentrations of MMS, whereas the positive control, *mei-9* is severely sensitive (Figure 2.3, Table 2.2) (*Ankle1* 0.05% MMS p=0.82, *Ankle1* 0.08% MMS p=0.58, *mei-9* 0.08% MMS p<0.0001). *Ankle1* is also not sensitive Cisplatin, which induces interstrand crosslinks (Sawant *et al.* 2017) (Figure 2.3, Table 2.2, p=0.07 *note, *Ankle1* experiences *increased* survival when exposed to Cisplatin, which may or may not be biologically relevant).

Mitotic role of Ankle1

Since *Ankle1* does not experience meiotic nondisjunction or sensitivity to DNA-damaging agents, I sought to determine if *Ankle1* has a role in mitotic recombination. It is thought that when helicases are absent, mitotic crossovers are more likely to occur because

Genotype	Treatment	Mutant Progeny	Heterozygous	Total	Biological Replicates	*p* Value
Ankle1	IR (1500 rads)	362	783	1145	10	0.11
	Untreated	521	760	1281	10	
Ankle1	IR (2000 rads)	228	475	703	20	0.48
	Untreated	840	1638	2478	20	
mei-9	IR (2000 rads)	74	81	155	10	0.16
	Untreated	571	499	1070	10	
Ankle1	MMS (0.05%)	304	559	863	10	0.82
	Untreated	347	642	989	10	
Ankle1	MMS (0.08%)	622	1074	1696	20	0.58
	Untreated	848	1631	2479	20	
mei-9	MMS (0.08%)	0	140	140	10	<0.0001
	Untreated	450	355	805	10	
Ankle1	Cis (0.25 mM)	331	512	843	10	0.07
	Untreated	473	856	1329	10	

Table 2.2. Mutagenizing agent assays. Genotype of each mutant is displayed, along with what treatment they were given and at what dose (see Materials and Methods for more information on implementation of assay). For each genotype and treatment, there was an untreated brood and a treated brood. Biological replicates represents how many vials were scored for each genotype/treatment. Numbers for mutant progeny, heterozygous progeny, and total progeny are shown. Treated and untreated classes were compared using unpaired t-test in Prism 8.

nucleases are cleaving the DNA that would normally be unwound by the helicase. An example of this is that when the helicase Fancm is absent, there is a large increase in mitotic recombination (Table 2.3). However, *Fancm mus312* double mutants experience no mitotic recombination (Table 2.3) (Kuo *et al.* 2014). To test if *Ankle1* experiences a similar phenotype, I examined mitotic crossovers in an *Ankle1; Fancm* double mutant. In the double mutant, crossovers are again decreased, which is not significantly different from *Fancm mus312* double mutants (Table 2.3) (p=0.58). Therefore, I predict that Ankle1 may act to resolve DNA stress due to the absence of *Fancm* to produce mitotic crossovers.

Genotype	Parental	Recombinant	Total
Fancm	2728	29	**2757**
Fancm mus312	909	0	**909**
Ankle1; Fancm	2555	4	**2559**

Table 2.3. Mitotic crossovers in *Ankle1*. Mitotic crossovers scored as in Materials and Methods. *Fancm mus312* data is from (Kuo *et al.* 2014). *Fancm mus312* is not significantly different from *Ankle1; Fancm* (*p*=0.58), statistical analysis done by fisher's exact test.

Discussion

Overall, these data show that *Ankle1* has no visible meiotic defects or sensitivity to the DNA-damaging agents I tested. Therefore, Ankle1 either does not have a role in creating meiotic crossovers or repair of DNA damage, or its role is redundant, so a mutant phenotype is not presented. However, Ankle1 appears to have a role in creating mitotic crossovers in the presence of DNA stress due to absence of the helicase Fancm.

We hypothesized that Ankle1 forms a complex with MUS312 and MEI-9-ERCC1. MEI-9 has shown to have roles in creating meiotic crossovers as well as repairing DNA after damage (Yildiz *et al.* 2004). I therefore hypothesized that we would see defects in meiotic recombination or sensitivity to DNA-damaging agents in *Ankle1* mutants. I did not observe any defects in meiotic nondisjunction or sensitivity to MMS, IR, or Cisplatin in *Ankle1* mutants, so I conclude that Ankle1 either does not play a role in these processes or its role is redundant. It is puzzling that we see an interaction between Ankle1 and Mei-9, yet *Ankle1* mutants do not show defects in activities that the MEI-9 complex is thought to play a role in. However, we can not rule out a complex with Ankle1, MEI-9, and MUS312 because Ankle1's activity may be redundant so we can not detect the defects.

However, surprisingly there is a decrease in crossovers in *Ankle1; Fancm* double mutants as compared to *Fancm* single mutants (Table 2.3). This result is similar to the

phenotype seen in *mus312 Fancm* double mutants, suggesting that MUS312 repairs DNA stress as mitotic crossovers in *Fancm* mutants (Kuo *et al.* 2014). Kuo *et al.* also examined *Fancm* double mutants with other members of the complexes discussed, including MUS81, SLX1, and MEI-9. *Fancm* mutants did not have a significant change in mitotic crossovers compared to *mei-9; Fancm* double mutants (Kuo *et al.* 2014). *Fancm* mutants with *Slx1* or *mus81* also did not show any change mitotic crossovers, but *mus81; Slx1 Fancm* triple mutants had a significant decrease in crossovers as compared to *Fancm* single mutants, suggesting SLX1 and MUS81 act together to form mitotic crossovers and that MUS312 is needed for this function (Kuo *et al.* 2014). The fact that *Ankle1; Fancm* has a significant decrease in crossovers as compared to *Fancm* single mutants suggest that Ankle1 complexes with MUS81, SLX1, and MUS312 to form mitotic crossovers. This is partially supported by the observation that Ankle1 interacts with MUS312 truncations through yeast two-hybrid, and the interactions between Ankle1 with MUS81 and SLX1 should also be explored in future studies.

Interestingly, there appears to be a different phenotype for *Ankle1* in mice. In mouse cells lacking the helicase *Blm*, Ankle1 deficiency did not decrease mitotic crossovers (Braun *et al.* 2016). Similar to my results, *Ankle1*-deficient mice showed no viability defects or detectable mutant phenotypes, nor did they experience sensitivity to various DNA-damaging agents (Braun *et al.* 2016). Therefore, it seems as though the mitotic crossover role of *Ankle1* in mice is non-existent or redundant, and Ankle1 in mice also is not involved in DNA damage repair.

CHAPTER 3: MEIOTIC MCM PROTEINS PROMOTE AND INHIBIT CROSSOVERS DURING MEIOTC RECOMBINATION[1]

Abstract

Crossover formation as a result of meiotic recombination is vital for proper segregation of homologous chromosomes at the end of meiosis I. In many organisms, crossovers are generated through two crossover pathways: Class I and Class II. To ensure accurate crossover formation, meiosis-specific protein complexes regulate the degree in which each pathway is used. One such complex is the mei-MCM complex, which contains MCM (mini-chromosome maintenance) and MCM-like proteins REC (ortholog of Mcm8), MEI-217, and MEI-218, collectively called the mei-MCM complex. The mei-MCM complex genetically promotes Class I crossovers and inhibits Class II crossovers in *Drosophila*, but it is unclear how individual mei-MCM proteins contribute to crossover regulation. In this study, we perform genetic analyses to understand how specific regions and motifs of mei-MCM proteins contribute to Class I and II crossover formation and distribution. Our analyses show that the long, disordered N-terminus of MEI-218 is dispensable for crossover formation, and mutations that disrupt REC's Walker A and B motifs differentially affect Class I and Class II crossover formation. In Rec Walker A mutants, Class I crossovers exhibit no change, but Class II crossovers are increased. However, in *rec* Walker B mutants, Class I crossovers are severely impaired, and Class II crossovers are increased. These results suggest that REC

[1] This chapter is adapted from previous work published in the journal *Genetics.* The original citation is as follows:
Hartmann M, Kohl K, Sekelsky J, Hatkevich T, 2019 Meiotic MCM Proteins Promote and Inhibit Crossovers During Meiotic Recombination. *Genetics,* https://doi.org/10.1534/genetics.119.302221

may form multiple complexes that exhibit differential REC-dependent ATP binding and hydrolyzing requirements. These results provide genetic insight into the mechanisms through which mei-MCM proteins promote Class I crossovers and inhibit Class II crossovers.

Introduction

To reestablish the diploid genome upon sexual fertilization, the genome of progenitor germ cells must be successfully reduced by half through meiosis. Accurate reduction of the genome at the end of meiosis I requires crossover formation between homologous chromosomes during meiotic recombination. Meiotic recombination is initiated by the formation of multiple double-strand breaks (DSBs); the majority of meiotic DSBs are repaired as noncrossovers, while a selected subset are repaired as crossovers between homologs (Lake and Hawley 2016).

Two distinct types of meiotic crossovers have been described: Class I and Class II. First defined in budding yeast (De Los Santos *et al.* 2003), Class I and Class II crossovers exist in most sexually reproducing organisms, but the relative proportions of each crossover type vary among organisms (Hollingsworth and Brill 2004). In *Drosophila*, most – if not all – crossovers are generated through the Class I pathway (Hatkevich *et al.* 2017), as shown through their dependence on the putative catalytic unit of the Class I meiotic resolvase MEI-9 (Sekelsky *et al.* 1995; Yildiz *et al.* 2002) and their display of crossover interference (Hatkevich *et al.* 2017). Most crossovers in *Drosophila* are also dependent upon a group of MCM- or MCM-like proteins, called the mei-MCM complex (Baker and Carpenter 1972; Grell 1978; Liu *et al.* 2000; Kohl *et al.* 2012).

The mei-MCM complex consists of REC (the *Drosophila* ortholog of MCM8), MEI-217, and MEI-218. REC appears to be a bona fide MCM protein, based on conservation of both the N-terminal MCM domain and the C-terminal AAA+ ATPase domain, which includes Walker A and B boxes that bind and hydrolyze ATP (Figure 3.1A). In

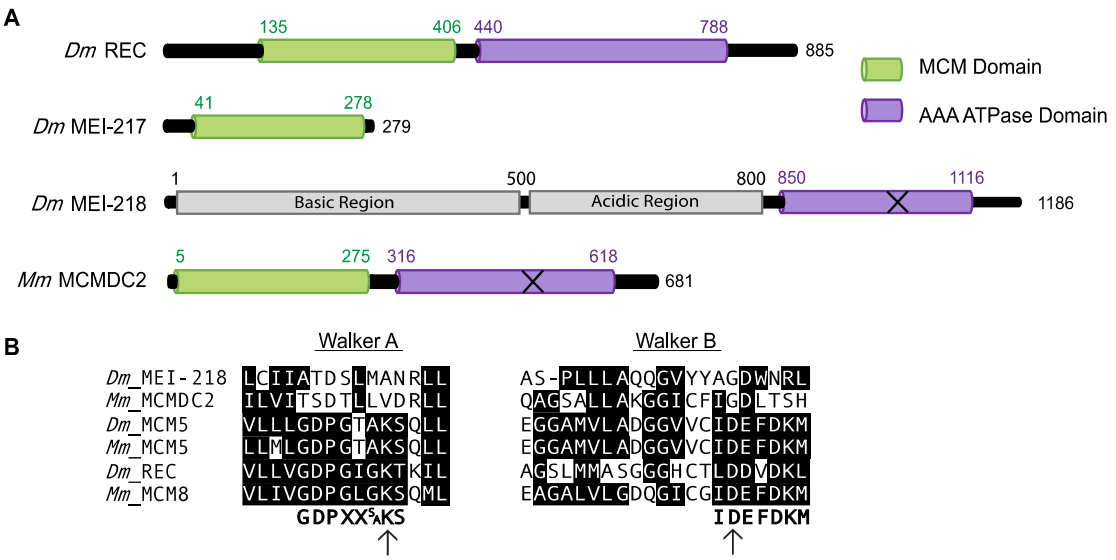

Figure 3.1. MCM protein structure and alignments. (A) Structural domains of *Drosophila melanogaster* REC, MEI-217, MEI-218 and *Mus musculus* MCMDC2. Structural domains identified using PHYRE 2 **(Kohl *et al.* 2012)**. "MCM domain" corresponds to protein data bank ID #c2vl6C and the AAA ATPase domains identified correspond to protein data bank ID #d1g8pa. The X on *Dm* MEI-218 and *Mm* MCMDC2 represents predicted inactive AAA ATPase domains. (B) Consensus sequence for Walker A motif **(Walker *et al.* 1982)**, and consensus sequence for Walker B motif **(Forsburg 2004)**. Identical or conserved amino acids are denoted with black background. Arrows denote the conserved catalytic residues.

contrast, MEI-217 and MEI-218 are highly divergent MCM-like proteins, and together resemble one full MCM protein. MEI-217 is structurally similar to the MCM N-terminal domain, though this similarity is not detected in BLAST or conserved domain searches (Kohl *et al.* 2012). The carboxy-terminus of MEI-218 has a domain related to the AAA+ ATPase domain, but key residues are not conserved, including the Walker A and B motifs that are critical for binding and hydrolyzing ATP, respectively (Iyer *et al.* 2004) (Figure 3.1B). Because key residues in the Walker A and B motifs are not conversed, MEI-218 may not exhibit ATPase activity or it may exhibit partial function. In addition, MEI-218 has a long N-terminal extension that is poorly conserved and predicted to be disordered. The function of this region is unknown, but gene swap studies suggest that it may contribute to differences in the recombination landscape among *Drosophila* species (Brand *et al.* 2018). For further

analysis and details regarding the evolution of the mei-MCM complex, see Supplemental Figures 3.2-3.4.

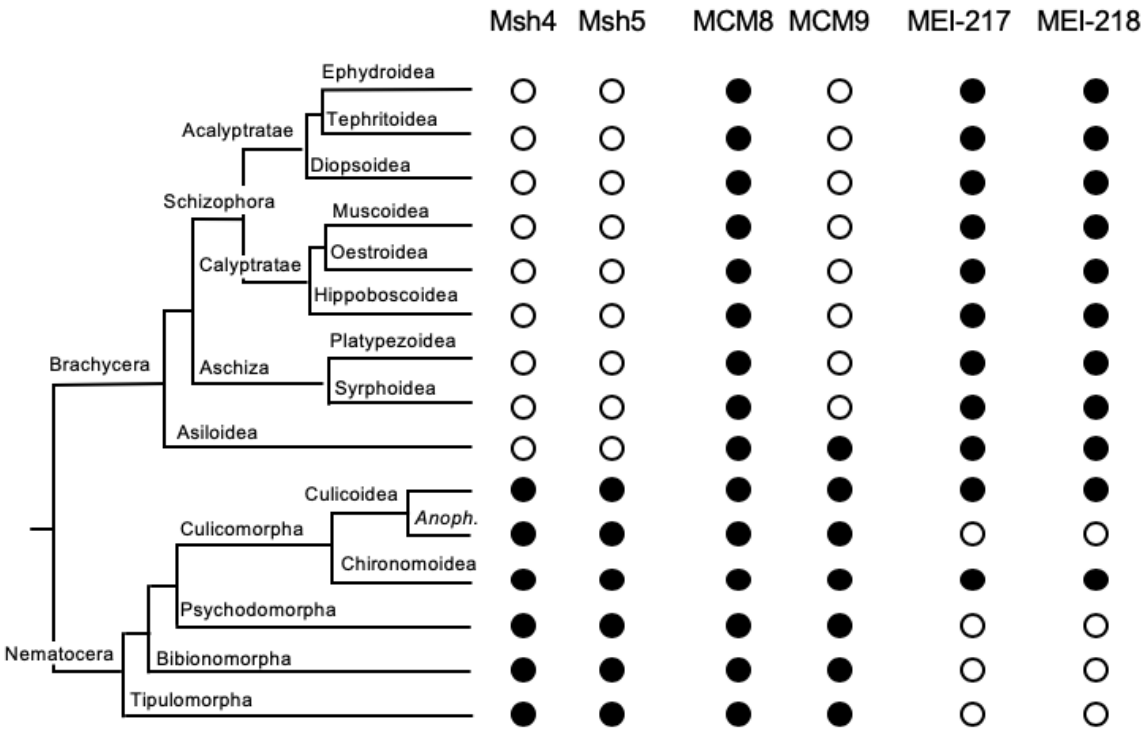

Figure 3.2. Occurrence of Msh4, Msh5, MCM8, MCM9, MEI-217, and MEI-218 in Diptera. The dendrogram on the left illustrates relationships among Dipteran taxa for which sufficient genome or transcriptome sequence is available to determine with reasonable confidence the presence or absence of genes encoding proteins relevant to this work. Circles to the right indicate presence (filled) or absence (open) of each gene/protein. For the suborder Brachycera, major superfamilies within Schizophora and the sister taxon Aschiza are shown, as well as the superfamily Asiloidea. For the suborder Nematocera, only infraorders are shown, except for Culicomorpha, where both superfamiles are indicated. Within the superfamily Culicoidea (mosquitoes), MEI-217 and MEI-218 are found in *Culex* and *Aedes* but are missing from all of the 20 *Anopheles* species whose genomes are sequenced.

It is hypothesized that the mei-MCM complex functionally replaces Msh 4/5 in *Drosophila* (Kohl *et al.* 2012). We do not find orthologs of Msh4, Msh5, or Mcm9 in species in the Dipteran sub-order Brachycera, suggesting that the structure and function of the *Drosophila* mei-MCM complex may have its origins in the ancestral founder of this lineage. Interestingly, Asiloidea appear to have retained an ortholog of MCM9. It may be informative to examine these species more thoroughly when additional sequences become available.

A

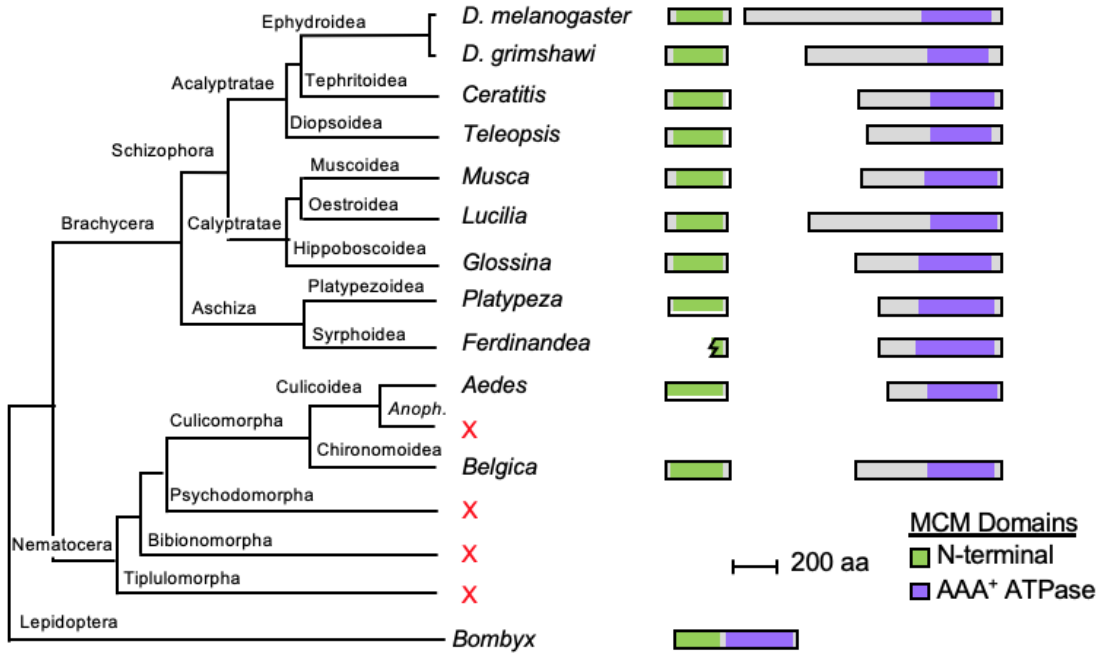

B

D. melanogaster
Q L E A C H L R I N *
CAACTGGAAGCATGTCATCTACGAATAAACTAGAGAAAAAG
M S S T N K L E K K

Ceratitis capitata
I F Q A W S V M T H *
ATATTTCAAGCATGGAGCGTAATGACACATTAGAAACCACG
M E R N D T L E T T

Musca domestica
E F Q A W N L T T I *
GAGTTTCAAGCATGGAACCTAACAACAATATAAGTACAGAT
M E P N N N I S T D

Platypeza anthrax
E F E S W H L T R T Q V *
GAATTTGAATCATGGCATTTGACAAGGACTCAAGTTTAGAT
M A F D K D S S L D

Aedes aegypti
W A F E E L *
TGGGCTTTCGAGGAATTGtaggatgatgATGGAGTCTACGCTA
M E S T L

Belgica antarctica
A T V *
GCCACCGTTtaatcattgccagtcactgtccatcATGTCGTTTT
M S F

Bombyx mori
K S I I I W S L E K I E Q C K A P M T H
AAATCCATTATAATATGGAGTTTGGAAAAGATTGAACAATGTAAAGCACCAATGACCCAT

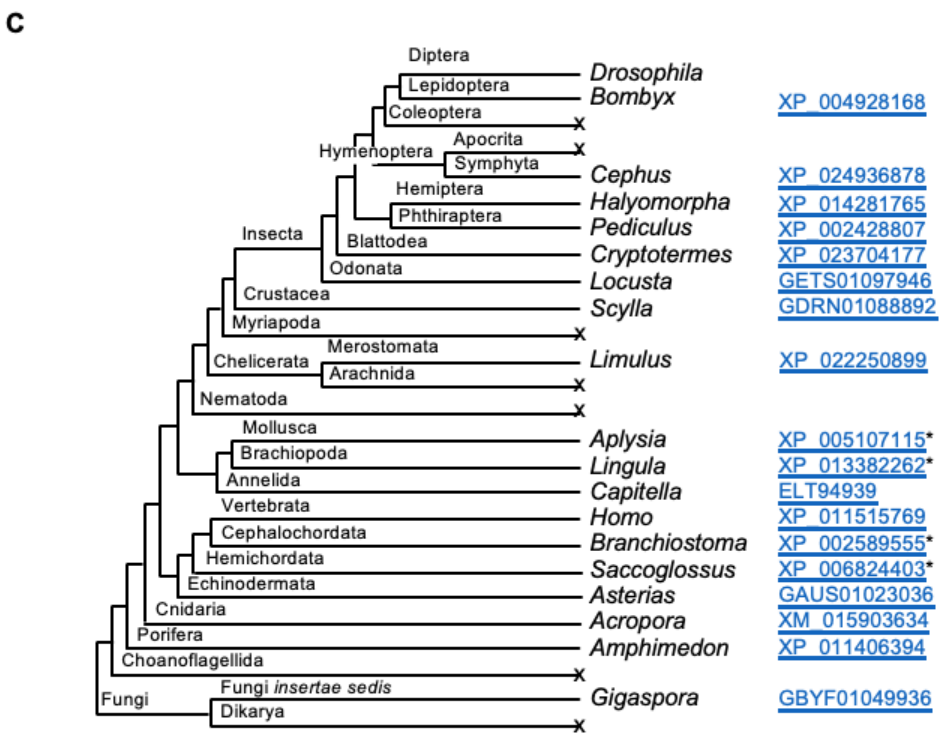

Figure 3.3. Structures of MEI-217 and MEI-218 in Diptera. (A) The dendrogram is the same as in Figure S1, with additional species to illustrate the variation in domain architectures. Domain architectures for representative species are to the right (the jagged N-terminal end in *Ferdiandea cuprea* indicates incomplete sequence). Domains were determined by PHYRE2 alignment to Protein Data Bank entry c5udb7 (a cryo-electron microscopy structure of *S. cerevisiae* MCM7). Accession numbers for the sequences included are listed below. Accession numbers that start with J are from Ensemble Metazoa genomic assemblies (found at http://metazoan.ensemble.org). The *Aedes*, *Musca*, and *Glossina* sequences are genomic contigs from Vectorbase (http://vectorbase.org). All other sequences are from NCBI (http://ncbi.nih.nlm.gov); those starting with a G are from the transcriptome shotgun assembly (TSA) database.

Species	Accession
Drosophila melanogaster	NM_167557.3
Drosophila grimshawi	XM_001992187.1
Ceratitis capitate	GAMC01014250.1
Teleopsis whitei	GBBQ01026862.1
Musca domestica	scf7180000644883
Lucilia cuprina	JRES01000755:1975-11359
Glossina morsitans	scf7180000644883
Platypeza anthrax	GCGU01008763.1
Ferdinandea cuprea	GCHQ01011487.1
Aedes aegypti	AAGE02016621.1
Belgica Antarctica	JPYR01000187:32247-35225
Bombyx mori	AK381112.1

(B) Junctions between open reading frames (ORFs) for the N-terminal and AAA+ ATPase domains are shown. At the top are three species from Shizophora and one from Aschiza, showing overlapping ORFs. Amino acids at the end of the N-terminal domain are shown in green above the DNA sequence (the position of the stop codon is highlighted in green); amino acids for the beginning of the AAA+ ATPase domain are in purple below the DNA sequence (the position of the start codon is highlighted in purple). Below that are two Nematocera species, showing separate but non-overlapping ORFs. Non-coding sequence between the ORFs is in lowercase text. At the bottom is a non-Diptera representative, the moth *Bombyx mori*. In this case, as in all other non-Dipteran species with an Mcmdc2 ortholog and in replicative MCM proteins, the two domains are on the same polypeptide, separated by a short linker.

(C) Distribution of Mcmdc2 in Opisthokonta. Dendrogram shows phyla, some sub-phyla, and several orders within the sub-phylum Insecta in which we can find clear orthologs of Mcmdc2 or in which there are sufficient genome or transcriptome sequences to suggest loss of Mcmdc2 with reasonable confidence. For those clades with an ortholog, a representative genus is listed, along with an accession number. Taxa in which we could not find any orthologs are indicated with an x. We have not found Mcmdc2 orthologs outside of Opisthokonta.

While most crossovers are generated through the Class I pathway in wild-type *Drosophila* and are mei-MCM dependent, mutants that lack the Bloom syndrome helicase (Blm) generate only Class II crossovers based on their independence of MEI-9 and lack of patterning (*e.g.*, interference) that is associated with Class I crossovers (Hatkevich *et al.* 2017). Blm is an ATP-dependent 3’-5’ helicase that exhibits vital anti-crossover functions in both meiotic and somatic DSB repair (Hatkevich and Sekelsky 2017). Interestingly, mutations in *mei-MCM* and *Blm* genes genetically interact. In *Blm* mutants, crossovers are reduced by 30% but in a *Blm rec* double mutant, crossovers are significantly increased compared to wild-type (Kohl *et al.* 2012). This suggests that the mei-MCMs may function to inhibit crossovers within the Class II pathway, in addition to their role promoting crossovers in the Class I pathway.

While the mei-MCMs function as a complex, little is known about how individual mei-MCMs contribute to Class I and II crossover regulation. Here, we investigate specific features of MEI-218 and REC to understand better how these proteins contribute to meiotic recombination. We find that the N-terminus of MEI-218 is dispensable for crossover

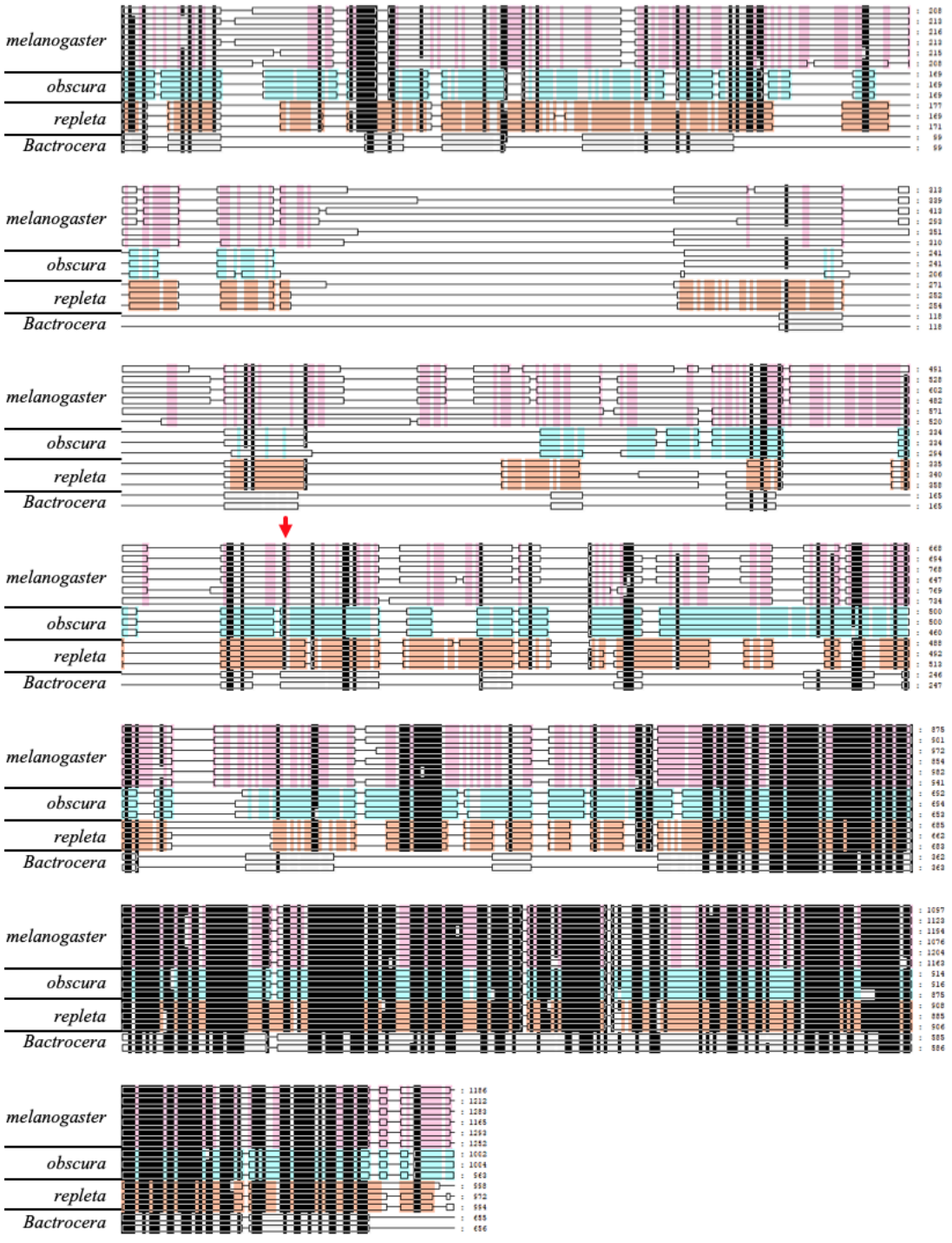

Figure 3.4. Sequence conservation and divergence in MEI-218. MEI-218 orthologs from 12 *Drosophila* species and two *Bactrocera* species (Tephritid fruit flies, also in the Acalyptratae subsection of Schizophora) are depicted. The red arrow indicates the start of the N-terminally-truncated MEI-218 analyzed in this work.

Species are, from top to bottom and sorted by species group as indicated on the figure:

melanogaster:	*Drosophila melanogaster*
	Drosophila sechelia
	Drosophila simulans
	Drosophila mauritiana
	Drosophila yakuba
	Drosophila erecta
obscura:	*Drosophila pseudoobscura pseudoobscura*
	Drosophila persimilis
	Drosophila miranda
repleta:	*Drosophila navojoa*
	Drosophila mojavensis
	Drosophila arizonae
Bactrocera:	*Bactrocera latifrons*
	Bactrocera dorsalis

Thin horizontal lines denote gaps introduced in the alignment process. Vertical lines indicate amino acid identity or similarity, using the Dayhoff PAM 200 matrix. Black is conserved among at least 11 sequences (*e.g.*, one mismatch in the 12 *Drosophila* species). Pink indicates conservation within the *melanogaster* species group, aqua within the *obscura* group, and orange within the *repleta* group. The red arrow denotes the start codon for the truncated MEI-218 described in the text.

Sequences were aligned in MEGA (v. 10.0.4) using the MUSCLE algorithm. Manual adjustments were done in GeneDoc v. 2.7.000. This visualization is the summary view produced by GeneDoc, with species groups with conservation mode shading enabled.

formation and general crossover distribution. By mutating key residues in REC's Walker A and B motifs (rec^{KA} and rec^{DA}, respectively), we found that rec^{KA} mutants exhibit no Class I crossover defect, while Class II crossovers are significantly increased. Surprisingly, rec^{DA} mutants exhibit a severe decrease in Class I crossovers and a significant increase in Class II crossovers. Our results suggest that the mei-MCMs function in multiple roles and may complex in a variety of configurations to properly regulate crossover formation.

Materials and Methods

Drosophila stocks

Flies were maintained on standard medium at 25°C. Some mutant alleles have been previously described, including $mei\text{-}9^{a}$ (Baker and Carpenter 1972; Yildiz *et al.* 2004), $mei\text{-}218^{1}$ and $mei\text{-}218^{6}$ (Baker and Carpenter 1972; McKim *et al.* 1996), Blm^{N1} and Blm^{D2}

(McVey *et al.* 2007), *rec*^{1} and *rec*^{2} (Grell 1978; Matsubayashi and Yamamoto 2003; Blanton *et al.* 2005). The maternal-effect lethality in *Blm*^{N1}/*Blm*^{D2} mutants was overcome by the *UAS::GAL4* rescue system previously described (Kohl *et al.* 2012).

Generating mei-218 transgenic alleles

The transgenes for *mei-218*$^{\triangle N}$ and *mei-218*^{FL} were constructed by cloning cDNA for *mei-218* into *P*{*attBUASpW*} (AddGene). Full-length *mei-218* included codons 1-1186; the *mei-218*$^{\triangle N}$ transgene included codons 527-1186. Transgenics were made by integrating into a phiC31 landing site in 2A on the *X* chromosome.

Generating rec^{KA} and rec^{DA} mutants

Annealed oligonucleotides were inserted into *Bbs*I-digested pU6-BbsI-chiRNA plasmid (Addgene). *rec*^{KA}: CTTCGCCGAGAAGGGATAGTAAAC; *rec*^{DA}: CTTCGTTGCAGTGCCTACAATCAG. Resulting plasmids were co-injected with repair template plasmid, consisting of synthesized gBlocks (IDT DNA) cloned into pBlueScript plasmid (sequences available on request). Injected larvae were raised to adulthood, and their male progeny were crossed to *TM3*/*TM6B* females (Bloomington Stock Center) to generate stocks, after which DNA was extracted for screening through PCR and restriction digest.

Nondisjunction assay

X-chromosome nondisjunction (NDJ) was assayed by mating virgin females to *y cv v f* / *T(1:Y)B*^{S} males. Each cross was set up as a single experiment with 20-50 separate vials. The progeny of each vial were counted separately. Viable nondisjunction progeny are *XXY* females with Bar eyes and *XO* males with Bar^{+} eyes and the phenotypes from *y cv v f* chromosome. Total (adjusted) represents the total with inviable exceptional progeny accounted for (*XXX* and *YO*). NDJ rates and statistical comparisons were done as in Zeng et al. 2010.

Crossover distribution assay

Crossover distribution on chromosome *2*L was scored by crossing virgin *net dpp$^{d\text{-}ho}$ dp b pr cn* / + female flies with mutant background of interest to *net dpp$^{d\text{-}ho}$ dp b pr cn* homozygous males. Each cross was set up as a single experiment with at least 25 separate vials scored. The first set of vials was flipped after three days of mating into vials of a new batch, although these were counted as one experiment. Batch effects for recombination assays have not been observed in repeated studies for multiple genotypes used in this study (Figure 3.5). These include wild-type (unpublished data), *Blm* (unpublished data), *rec* (Blanton *et al.* 2005; Kohl *et al.* 2012), *mei-9* (Sekelsky and Hawley 1995), and *mei-9; rec* (Blanton *et al.* 2005). All progeny were scored for parental and recombinant phenotypes. Crossover numbers in flies are shown as cM where cM = (number of crossovers / total number of flies) * 100. Chi-squared tests with Bonferroni correction were performed for each interval. For total cM, Fisher's Exact Test was used to compare total crossovers to total number of flies. Crossover distribution is represented as cM/Mb where Mb is length of the interval without transposable elements (TEs) because crossovers rarely occur within TEs (Miller *et al.* 2016).

Protein structure and alignment

Structural domains of proteins were determined by using PHYRE 2. All of the MCM regions identified correspond to the protein data bank ID #c2vl6C and the AAA ATPase domains identified correspond to protein data bank ID #d1g8pa. Alignment of the Walker A and Walker B motifs (Kohl *et al.* 2012) was done using MEGA 5 and aligned with the ClustalW program. Identical and conserved residues are shaded based on groups of amino acids with similar chemical properties.

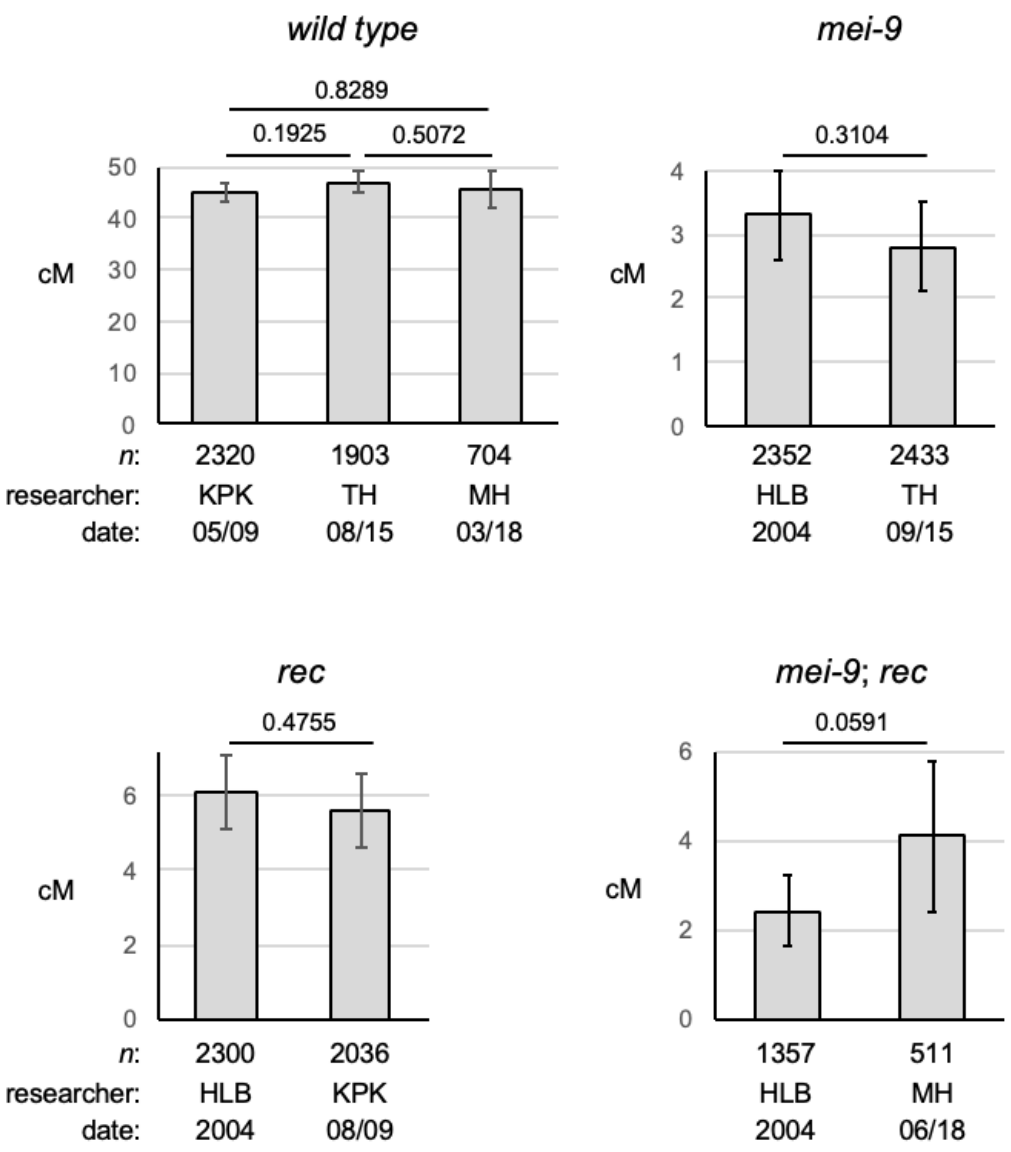

Figure 3.5. Reproducibility of recombination assays. Graphs shows the total number of cM for the *net* – *cn* intervals (*al* – *cn* for HLB assays; *al* is 0.2 cM to the right of *net*) for recombination assays in the same genotype scored by different researchers at different times. Error bars are 95% confidence intervals. *P* values are from Fisher's exact test on 2x2 contingency tables with total crossovers and parental flies for each genotype. Below each bar is the total number of flies scored (*n*), the researcher doing the scoring, and the date of the experiment. MH, KPK, and TH are authors of this work, with some data published in Kohl *et al.* 2012 and Hatkevich *et al.* 2017. HLB refers to data published in Blanton *et al.* 2005. The *mei-9*; *rec* MH experiment had six double crossovers and one triple crossovers. Because all of these were *b pr*$^{+}$ *cn* and no multiple crossover events were observed in the 2.7x larger HLB dataset, we suspect these were from some non-meiotic event(s); these flies were removed from this analysis.

Results and Discussion

The N-terminus of MEI-218 is dispensable for crossover formation

MCMDC2 is a distantly-related member of the MCM family of proteins that is unique in that the ATPase domain is predicted to be incapable of binding or hydrolyzing ATP. Orthologs in Dipteran insects are further distinguished by having the N-terminal and ATPase-like domains encoded in separate open reading frames. The two polypeptides, MEI-217 and MEI-218 interact physically, at least in *Drosophila melanogaster*, presumably reconstituting a single MCM-like protein. MEI-218 is also distinguished by possessing an N-terminal extension of variable length in different species. *Drosophila melanogaster* MEI-218 can be divided into three distinct regions (Figure 3.1A): an N-terminal tail (residues 1-500), a central acidic region (residues 500-800) and the C-terminal ATPase-related region (residues 850-1116) (Kohl *et al.* 2012; Brand *et al.* 2018). The N-terminal and middle regions are predicted to be disordered (Kohl *et al.* 2012) and are poorly conserved (Figure 3.4). Results obtained through gene swap experiments suggest that the N-terminal tail and central region regulate crossover number and distribution within *Drosophila* species (Brand *et al.* 2018).

To genetically examine the function of the N-terminus of MEI-218, we compared functions of a transgene that expresses a truncated form of MEI-218 that lacks the N-terminal 526 amino acids (*mei-218*$^{\Delta N}$) to a matched full-length transgene (*mei-218*^{FL}) (Figure 3.6A). Due to the relatively high conservation among *Drosophila* species, the middle region of mei-218 was retained for this experiment (Figure 3.4). Using the *UAS*/*GAL4* system (Duffy 2002), we expressed both constructs in *mei-218* null mutants using the germline-specific *nanos* promoter and measured crossovers along five adjacent intervals that span most of *2*L and part of *2R* (Figure 3.7; for simplicity, we refer to this chromosomal region as *2*L.)

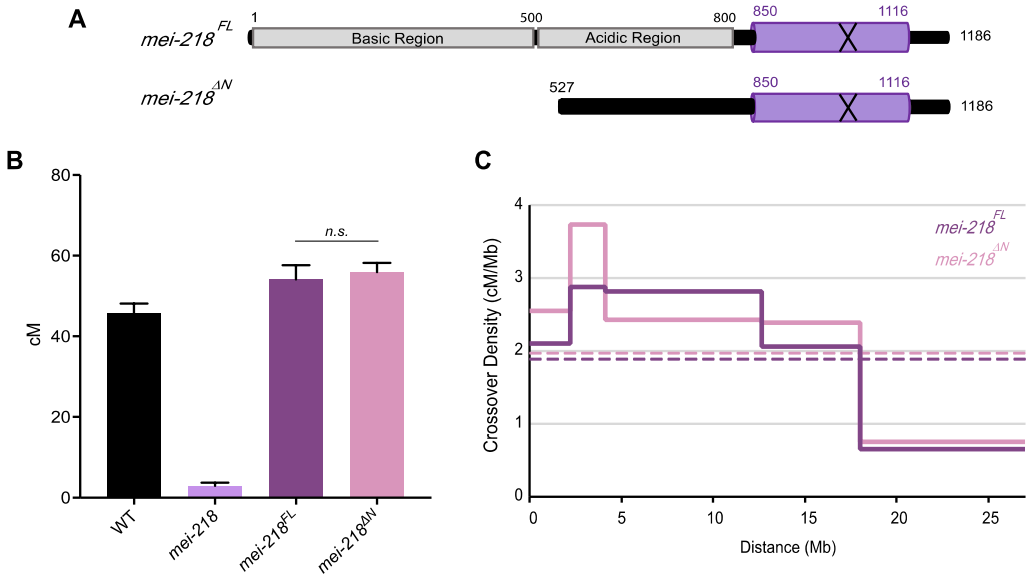

Figure 3.6. The role of MEI-218 N-terminus in crossover formation and distribution. Schematic of transgenes for full length *mei-218* and N-terminal deleted *mei-218*, in which the first 526 amino acids are absent. (B) Map units of WT (Hatkevich *et al.* 2017), *mei-218* (Kohl *et al.* 2012), *mei-218*^{FL} and *mei-218*$^{\Delta N}$. Map units represented as centimorgans (cM). Error bars indicate 95% confidence intervals. *n.s.* = not significant (p = 0.61). (C) Crossover distribution (solid lines) of *mei-218*^{FL} and *mei-218*$^{\Delta N}$ represented as cM/Mb. Mb is measured distance of defined interval, excluding centromere, pericentromeric heterochromatin and transposable elements. Dotted lines represent mean crossover density across *2*L. Figure S5 details the cross scheme of *mei-218* transgene experiments. Refer to tables S1and S3 for complete data sets.

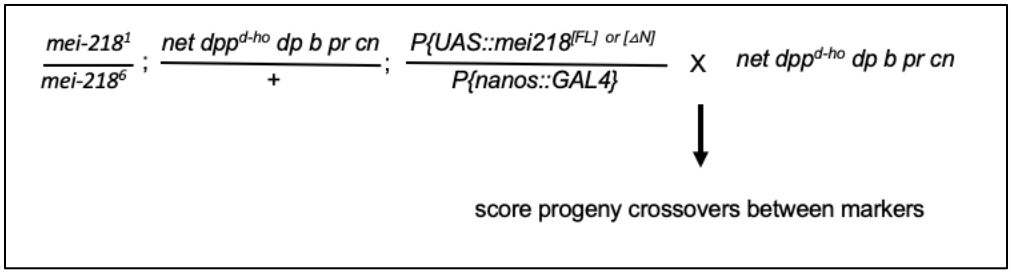

Figure 3.7. Cross scheme of *mei-218* overexpression. *mei-218*^{FL} or *mei-218*$^{\Delta N}$ are expressed from *UAS::Gal4* system on the third chromosome in the background of a *mei-218* null mutation. Recessive markers on chromosome 2 are used for crossover scoring. Virgin female progeny are crossed back to flies homozygous for the recessive marker chromosome.

In wild-type females, the genetic length of *2*L is 45.8 cM (Hatkevich *et al.* 2017) (Figure 3.6B), whereas *mei-218* mutants exhibit a severe decrease in crossovers, with genetic length of 2.92 cM (Kohl *et al.* 2012). Expression of *mei-218*^{FL} in *mei-218* mutants (*mei-218*^{FL}) fully rescues the crossover defect, exhibiting a genetic length of 54.1 cM. Unexpectedly, expression of *mei-218*$^{\triangle N}$ in *mei-218* mutants (*mei-218*$^{\triangle N}$) restored crossing over to the same level as in *mei-218; mei-218*^{FL} (55.9 cM; *n.s. p* = 0.61).

Brand *et al.* (2018) expressed *Drosophila mauritiana* MEI-217 and MEI-218 in *Drosophila melanogaster* and found that crossovers were increased in proximal and distal regions, resulting in an overall change in crossover distribution. We examined crossover distribution in *mei-218; mei-218*^{FL} and *mei-218; mei-218*$^{\triangle N}$ (Figure 3.6C). Overall, distributions are similar, with both genotypes exhibiting a strong inhibition of crossovers near the centromere (referred to as the centromere effect; Beadle 1932) and the majority of the crossovers placed in the medial-distal regions (Figure 3.6C).

We conclude that the N-terminal tail of MEI-218 is dispensable for both crossover formation and overall distribution on chromosome *2*L. This conclusion is supported by the observation that of 16 sequenced mutations in *Drosophila melanogaster mei-218*, 14 are nonsense or frameshift, and the only two missense mutations alter residues in the C-terminus (amino acids 845 and 1107) (Collins *et al.* 2012).

The reasons why the MCM domains have been separated into MEI-217 and MEI-218 polypeptides and why MEI-218 has an N-terminal extension are unknown, but this structure has been maintained for more than 250 million years of Dipteran evolution (Figure 3.3). Interestingly, MEI-218 is expressed moderately high in testes (Thurmond *et al.* 2019) even though males do not experience meiotic recombination. The predominant or exclusive transcript in males does not encode MEI-217 (Thurmond *et al.* 2019), the seemingly obligate partner for MEI-218 in female meiotic recombination. Males that lack *mei-218* are viable,

fertile, and do not exhibit elevated nondisjunction (Baker and Carpenter 1972; McKim *et al.* 1996). For these reasons, we speculate that an unknown function of MEI-218 (independent of MEI-217) in the male germline explains why its overall structure has been evolutionarily maintained.

REC ATPase motifs are required for crossover formation

Of the three known mei-MCM subunits, only REC harbors well-conserved Walker A and B motifs, suggesting that REC has ATP binding and hydrolysis activity (Kohl *et al.* 2012). It is unknown whether the mei-MCM complex utilizes REC's putative ATPase activity for its function *in vivo*. To test this, we used CRIPSR/Cas9 to introduce into *rec* mutations predicted to disrupt Walker A and B motif functions (Figure 3.8A). The Walker A mutation (rec^{KA}) results in substitution of a conserved lysine residue with alanine; this mutation in other AAA+ ATPases, including replicative MCMs, prevents binding of ATP (Bell and Botchan 2013). The Walker B mutation (rec^{DA}) results in substitution of a conserved aspartic acid with alanine; in MCMs and other AAA+ ATPases, this mutation destroys the ability to coordinate Mg^{++} for ATP hydrolysis (Bochman *et al.* 2008).

We assayed crossover frequency along *2*L in rec^{KA} and rec^{DA} mutants (Figure 3.8B). Surprisingly rec^{KA} ATP binding mutants exhibit a genetic length of 44.9 cM, which is not significantly different from wild-type ($p = 0.4016$), suggesting that ATP binding by REC is not required for crossover formation. Conversely, there is a severe reduction in crossovers in rec^{DA} mutants, with a genetic length of 1.6 cM ($p < 0.0001$), suggesting that REC's ability to hydrolyze ATP is required for crossover formation.

Because the genetic length of rec^{DA} is significantly lower than *rec* null mutants (Figure 3.8B, $p < 0.0001$), we hypothesized that rec^{DA} is an antimorphic mutation. To test this, we examined crossover levels and *X* chromosome nondisjunction (NDJ) in rec^{DA}/rec^{+} (Figure 3.8B and 3.8C, respectively). The genetic length of *2*L in rec^{DA}/rec^{+} is slightly lower

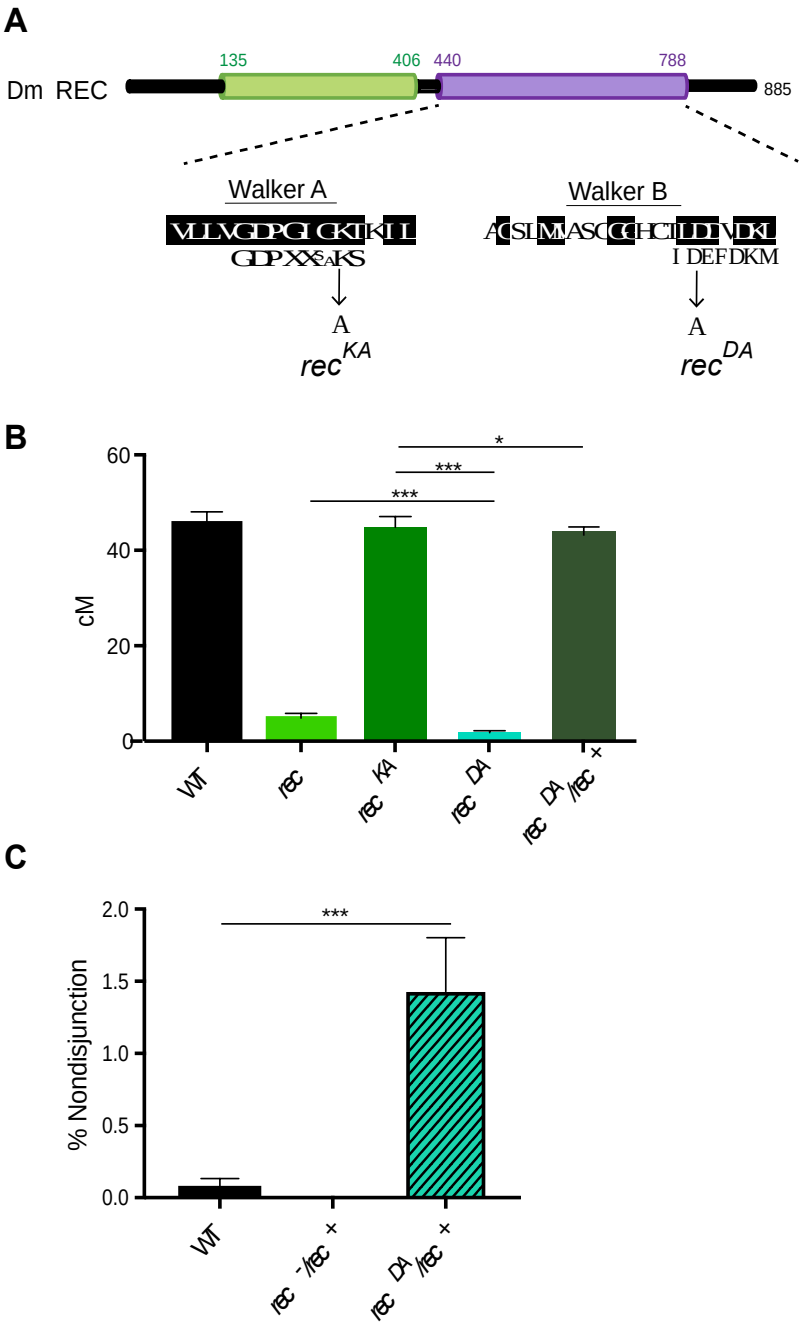

Figure 3.8. REC ATPase binding and hydrolysis requirements for crossover formation. Schematic representation of the mutated residues in *rec*^{KA} and *rec*^{DA}. (B) Map units of *WT* (Hatkevich *et al.* 2017), *rec*^{1}/*rec*^{2}, *rec*^{KA}, and *rec*^{DA}, *rec*^{DA}/*rec*$^{+}$. Map units represented as centimorgans (cM). Error bars show 95% confidence intervals. (C) Percent nondisjunction of *WT*, *rec*^{1}/*rec*$^{+}$, and *rec*^{DA}/*rec*$^{+}$. (D) Model of possible complex depicting the functional Walker B motif of REC protein interacting with a Walker A motif on a potential partner. * $p < 0.05$; ***$p < 0.0001$. Refer to tables 3.1 and 3.2 for complete data sets.

Interval	*mei-218*^{FL}	*mei-218*$^{\Delta N}$	Fold Change	*P* Value
net-ho	4.87 (1.53)	5.9 (1.08)	1.21	n.s.
ho-dp	5.79 (1.66)	7.49 (1.21)	1.29	<0.0001
dp-b	25.39 (3.1)	21.87 (1.91)	0.86	<0.0001
b-pr	11.71 (2.29)	13.55 (1.58)	1.16	n.s.
pr-cn	6.32 (1.73)	7.11 (1.18)	1.13	n.s.
Total *n*	759	1815		

Table 3.1. Meiotic crossovers on chromosome *2L* in *mei-218*^{FL} and *mei-218*$^{\Delta N}$. Crossover frequency shown as map units (centimorgans). Numbers in parentheses represent 95% confidence intervals. Fold change = *mei-218*^{FL} / *mei-218*$^{\Delta N}$. *P* values determined by chi-squared tests. Figure 2 shows distributions for *mei-218*^{FL} and *mei-218*$^{\Delta N}$.

Genotype	*XX* females	*XY* males	*XXY* females	*XO* males	Total *n*	NDJ
wild type (y w)	1551	1481	0	1	**3034**	0.07%
rec^{-} / *rec*$^{+}$	880	775	0	0	**1655**	0%
rec^{DA} / *rec*$^{+}$	1072	863	10	4	**1963**	1.43%

Table 3.2. Nondisjunction of *WT*, *rec*$^{-}$ / *rec*$^{+}$, and *rec*^{DA} / *rec*$^{+}$. *XX* females and *XY* males are normal, whereas *XXY* females and *XO* males are karyotypes genotypes resulting from nondisjunction. Total *n* calculates in exceptional progeny that do not survive (*XXX* and *XO*).

than wild-type, but not significantly different (43.9 cM and 45.8 cM, respectively; $p = 0.35$). For *X*-NDJ, both wild-type and *rec*$^{-}$/*rec*$^{+}$ mutants exhibit rates below 0.5%, while *rec*^{DA}/*rec*$^{+}$ mutants exhibit a significant increase to 1.4% NDJ ($p < 0.0001$). These data support the conclusion that *rec*^{DA} is weakly antimorphic and suggest that *rec*^{DA} results in an inactive mei-MCM complex that is antagonistic to the wild-type complex. In light of these interpretations, we propose that the mei-MCM complex binds to recombination sites independent of REC binding to ATP, and that REC-dependent ATP hydrolysis is required for the removal of the mei-MCM complex from these sites.

The phenotypes of *rec*^{KA} and *rec*^{DA} mutants suggest that REC's ability to hydrolyze ATP is required for crossover formation, whereas its ATP binding capability is dispensable. The disparate requirements for REC's ATP binding and hydrolysis are similar to those of other ATPase-dependent complexes. Rad51 paralogs, which form multi-protein complexes and contain Walker A and B motifs, are proposed to exhibit ATPase activity in *trans* between adjacent subunits, each of which contributes a Walker A or Walker B motif to the active site (Wu *et al.* 2004, 2005; Wiese *et al.* 2006). Because neither MEI-217 nor MEI-218 possess an ATPase domain that harbors conserved key enzymatic residues (Figure 3.1B) (Kohl *et al.* 2012), we propose that ATPase activity of the mei-MCM complex requires REC for ATP hydrolysis and an unknown mei-MCM protein for ATP binding. Alternatively, because REC is highly diverged, its Walker A and B motifs may function non-canonically. Biochemical studies are needed to test these hypotheses, but these may require identification of the putative missing subunit.

REC-dependent ATP hydrolysis is required for MEI-9-dependent crossovers

To gain insight into the crossover pathways that are used in *rec*^{KA} and *rec*^{DA} mutants, we examined whether these crossovers require the Class I endonuclease/resolvase. In *Drosophila,* the catalytic subunit of the putative Class I meiosis-specific endonuclease is MEI-9 (Sekelsky *et al.* 1995; Yildiz *et al.* 2002; Hatkevich *et al.* 2017). The *2*L genetic length within a *mei-9* mutant is 2.75 cM (Figure 3.9), demonstrating that at least 90% of crossovers are dependent upon MEI-9. However, the genetic length in *mei-9*; *rec* mutants is not significantly different than that of *rec* null single mutants (4.11 cM *vs* 4.66 cM, $p = 0.64$) suggesting that in the absence of REC, the resulting crossovers are likely independent of MEI-9. Similarly, it has been shown previously that *mei-218 mei-9* double mutants do not have reduced crossovers compared to *mei-218* single mutants (Sekelsky *et al.* 1995),

indicating that crossovers generated in the absence of the mei-MCM complex are MEI-9-independent.

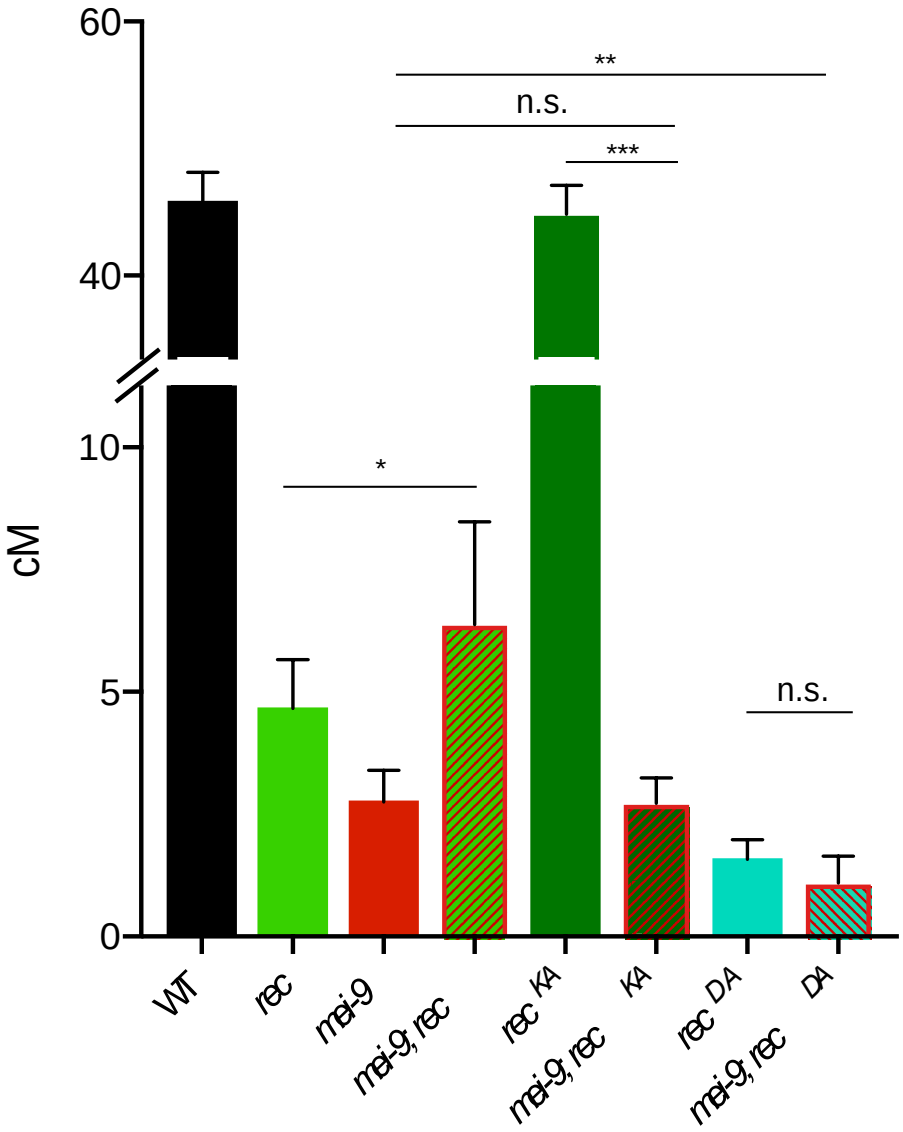

Figure 3.9. MEI-9-dependent crossovers in *rec^{KA}* and *rec^{DA}* mutants. Map units of *WT* (Hatkevich *et al.* 2017), *rec, mei-9, mei-9;rec, rec^{KA}, mei-9;rec^{KA}, rec^{DA},* and *mei-9;rec^{DA}.* Map units represented as centimorgans (cM). Error bars show 95% confidence intervals. * $p < 0.05$ ** $p < 0.001$ ***$p < 0.0001$; (*mei-9* vs *mei-9; rec^{KA}* $p = 0.94$) (*rec^{DA}* vs *mei-9; rec^{DA}* $p = 0.23$). Refer to Table 3.3 for complete data set.

Because *rec*^{KA} mutants exhibit the same distribution and number of crossovers as wild-type (Figure 3.8B), we hypothesized that *rec*^{KA} crossovers are dependent on MEI-9. To test this, we examined genetic length across *2*L in *mei-9; rec*^{KA} double mutants (Figure 3.9). Mutants for *mei-9; rec*^{KA} exhibit a genetic length of 2.72 cM, which is significantly decreased compared to the *rec*^{KA} single mutant ($p < 0.0001$), but not significantly different from *mei-9* single mutants ($p = 0.94$), showing that crossovers in *rec*^{KA} are indeed dependent upon MEI-9 nuclease. In contrast, we predicted that crossovers in *rec*^{DA} will be independent of MEI-9, similar to crossovers generated in *rec* null mutants. We observe that *mei-9; rec*^{DA} double mutants exhibit a genetic length of 1.1 cM, which is significantly lower than that of *mei-9* single mutants ($p < 0.001$). Importantly, crossing over in the *mei-9; rec*^{DA} double mutant is not significantly different than in *rec*^{DA} single mutants ($p = 0.23$), demonstrating that crossovers in *rec*^{DA} are independent of MEI-9 (Figure 3.9).

From these data we conclude that the crossovers in *rec*^{KA} mutants arise through the normal, MEI-9-dependent pathway, whereas mitotic nucleases generate the residual crossovers in *rec*^{DA} mutants. These data show that REC^{KA} functions normally in the Class I pathway, but this pathway is nonfunctional in *rec* null and *rec*^{DA} mutants. We suggest that the REC's ability to hydrolyze, but not bind, ATP is required for the formation of Class I crossovers.

REC ATPase motifs are required to prevent Class II crossovers

In wild-type *Drosophila*, most or all crossovers are generated through the Class I pathway (Hatkevich *et al.* 2017), and these crossovers are dependent upon the mei-MCM complex (Kohl *et al.* 2012). However, in *Blm* mutants, crossovers are generated exclusively through the Class II pathway (Hatkevich *et al.* 2017). In *Drosophila Blm* mutants, meiotic crossovers are decreased by 30%, suggesting that the Class II pathway is less efficient at generating crossovers than the Class I pathway, even though what may be the primary anti-

crossover protein, Blm helicase, is absent. It has previously been shown that loss of Blm suppresses the high nondisjunction of *mei-218* and *rec* mutants (Kohl *et al.* 2012). However, in *Blm rec* double mutants, crossovers are increased significantly compared to *Blm* single mutants (Kohl *et al.* 2012), suggesting that REC and/or the mei-MCM complex has an anti-crossover role in *Blm* mutants, and therefore in the Class II crossover pathway.

To further understand the role of REC in the Class II pathway, we investigated whether REC's predicted ATP binding or hydrolysis function is required for its Class II anti-crossover function. To do this, we measured the crossovers across *2*L in rec^{KA} and rec^{DA} in the background of *Blm* mutants. If REC ATP binding or hydrolysis is required for an anti-crossover role in Class II, then the genetic length of *Blm* rec^{KA} or *Blm* rec^{DA} double mutants will be similar to that of *Blm rec* double mutants. Conversely, if REC ATP binding or hydrolysis is not required, then double mutants will exhibit genetic lengths similar to that of *Blm* single mutants.

Interestingly, *Blm* rec^{KA} mutants exhibit a genetic length of 43.3 cM, which is not significantly different than *Blm rec* mutants ($p = 0.10$) but significantly higher than *Blm* single mutants ($p < 0.0001$; Figure 3.10). Similarly, *Blm* rec^{DA} double mutants have a recombination rate of 53.4 cM, which is not significantly different from *Blm rec* double mutants ($p = 0.52$), but significantly higher than *Blm* single mutants ($p < 0.0001$). These results suggest that REC's predicted abilities to bind and hydrolyze ATP are both required for the inhibition of crossovers at REC-associated Class II recombination sites. Therefore, it appears that REC forms different complexes within the Class II pathway and Class I pathway. It is unknown whether this Class II REC-associated complex requires the other mei-MCM proteins, and additional genetic studies will be valuable to discern this.

In summary, the mei-MCMs are a family of diverged proteins that help to establish the recombination landscape in *Drosophila melanogaster* by promoting Class I crossovers

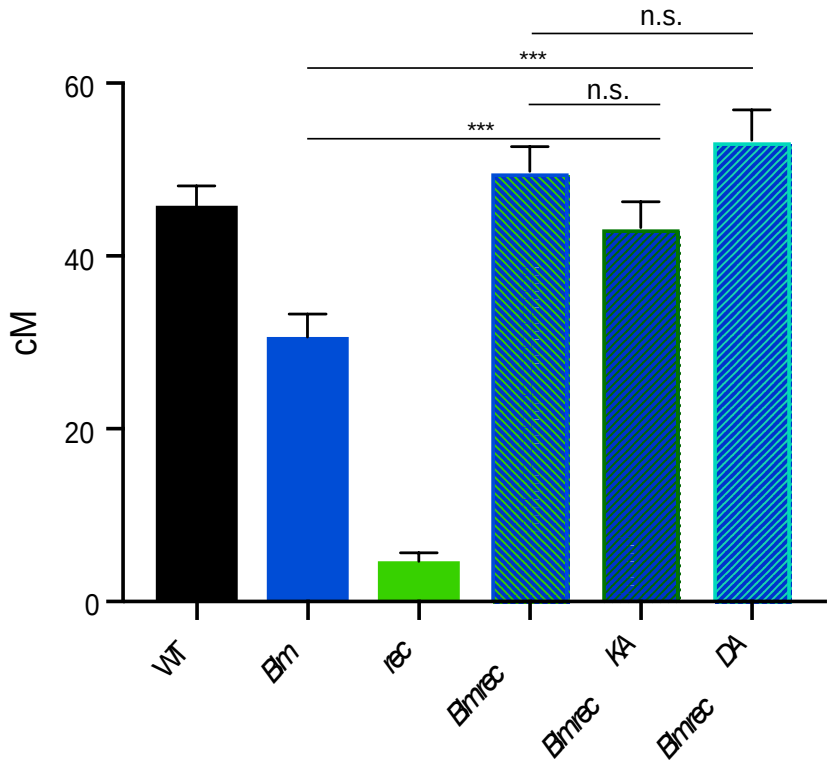

Figure 3.10. Requirements of REC ATPase activity in Blm function. Map units of *WT* (Hatkevich *et al.* 2017), *Blm* (Kohl *et al.* 2012), *rec, Blm rec* (Kohl *et al.* 2012), *Blm* rec^{KA}, and *Blm* rec^{DA}. Map units represented as centimorgans (cM). Error bars show 95% confidence intervals. Refer to Table 3.3 for complete data set. *** $p < 0.0001$. (*Blm rec* vs *Blm* rec^{KA} $p = 0.10$) (*Blm rec* vs *Blm* rec^{DA} $p = 0.52$).

and inhibiting Class II crossovers. Results obtained in this study have further elucidated meiotic recombination roles for two mei-MCM proteins, MEI-218 and REC. While the N-terminus of MEI-218 is dispensable for crossover formation (Figure 3.6), REC's predicted ability to bind and hydrolyze ATP exhibit differential requirements for regulating Class I and Class II crossover formation. From our genetic analyses, we suggest that the Walker B motif of REC, but not the Walker A motif, is required for promoting the formation Class I, MEI-9 dependent crossovers (Figures 3.8 and 3.9). The weakly antimorphic phenotype of rec^{DA} demonstrates that an impaired REC Walker B mutant renders a poisonous complex – a complex in which we propose cannot be released from recombination sites. Both Walker A

and Walker B motifs block crossovers in the Class II pathway, suggesting that REC forms different complexes to execute its pro- and anti-crossover functions. Biochemical and cytological studies are needed to support or refute these hypotheses.

Progeny		Genotype Being Assayed															
		WT	*mei-218*	*mei-218* ^{FL}	*mei-218* $^{\Delta N}$	*rec*	*rec*^{KA}	*rec*^{DA}	*rec*^{DA} / *rec*$^{+}$	*mei-9*	*mei-9; rec*	*mei-9;* *rec*^{KA}	*mei-9;* *rec*^{DA}	*Blm*	*Blm rec*	*Blm rec*^{KA}	*Blm rec*^{DA}
Parental		2376	1693	396	942	2129	1061	3452	1597	2366	490	3650	1360	844	705	684	445
SCO	1 (*net-ho*)	176	4	24	75	8	54	3	73	6	0	7	0	23	31	27	13
	2 (*ho-dp*)	290	6	33	93	10	100	5	137	11	3	13	1	22	29	35	10
	3 (*dp-b*)	1099	16	168	315	53	464	29	679	40	11	43	5	89	136	116	98
	4 (*b-pr*)	154	18	65	168	13	94	12	201	8	5	20	5	104	103	95	78
	5 (*pr-cn*)	39	7	29	80	20	44	6	30	2	2	19	4	61	87	78	64
DCO	1 and 2	1	0	0	0	0	0	0	0	0	0	0	0	1	0	4	0
	1 and 3	11	0	3	13	0	7	0	4	0	0	0	0	4	11	4	0
	1 and 4	10	0	4	11	0	4	0	2	0	0	0	0	2	7	0	3
	1 and 5	2	0	6	8	0	0	0	2	0	0	0	0	1	0	3	2
	2 and 3	6	0	3	13	0	3	0	3	0	0	0	0	1	5	1	6
	2 and 4	7	0	6	18	0	1	0	9	0	0	0	0	2	7	5	2
	2 and 5	13	0	1	12	0	2	0	3	0	0	0	0	2	2	1	4
	3 and 4	19	0	10	38	0	14	0	14	0	0	0	0	5	19	5	18
	3 and 5	17	0	8	18	0	4	0	7	0	0	0	0	7	21	17	12
	4 and 5	2	0	2	11	0	3	0	3	0	0	0	0	2	8	9	10
TCO		0	0	1	0	0	0	0	0	0	0	0	0	1	10	7	7
Total *n*		**4222**	**1744**	**759**	**1815**	**2233**	**1855**	**3507**	**2764**	**2433**	**511**	**3752**	**1375**	**1171**	**1181**	**1091**	**774**

Table 3.3. Crossovers in each interval on chromosome *2L* for all mutants discussed. Each row shows the number of parental (P), single (SCO), double (DCO), and triple (TCO) crossovers for each genotype and each mutant discussed in the article. Total *n* represents all parental and recombinant flies scored for each genotype. Wild-type data are from Hatkevich *et al.* 2017. Data for *mei-218 Blm*, and *Blm rec* are from Kohl, Jones, and Sekelsky 2012. The *mei-9*; *rec* experiment had six apparent double crossovers and one triple crossovers. Because all of these were *b pr*$^{+}$ *cn* and no multiple crossover events were observed in the 2.7x larger dataset of Blanton *et al.* (2005) we suspect these were from some non-meiotic event(s); these flies were removed from analysis.

CHAPTER 4: THE ABSENCE OF CROSSOVERS ON CHROMOSOME 4 IN *DROSOPHILA MELANOGASTER*: IMPERFECTION OR INTERESTNG EXCEPTION?[2]

Abstract

Drosophila melanogaster chromosome *4* is an anomaly because of its small size, chromatin structure, and most notably its lack of crossing over during meiosis. Earlier ideas about the absence of crossovers on *4* hypothesize that these unique characteristics function to prevent crossovers. Here, we explore hypotheses about the absence of crossovers on *4,* how these have been addressed, and new insights into the mechanism behind this suppression. We review recently published results that indicate that global crossover patterning, in particular the centromere effect, make a major contribution to the prevention of crossovers on *4*.

Preface: Opposing Views of *Drosophila* Geneticists on Chromosome *4*

As a graduate student, I (JS) did my graduate research under the direction of the late Bill Gelbart at Harvard University. My rotation project was to inject a *P* element transgene construct and then screen for and map any integrants. One integration did not map to the *X*, *2*, or *3*, so I told Bill it must have landed on *4*. Bill instructed me to autoclave the stock immediately so as not to contaminate the lab with something associated with the fourth chromosome. “God gave flies the fourth chromosome so they wouldn’t be perfect,” he said. Bill’s position was based on the absence of crossovers on *4*, which prevented one from doing

[2] This chapter is adapted from previous work published in the journal *Fly.* The original citation is as follows:
Hartmann M, Sekelsky J, 2017 The absence of crossovers on chromosome 4 in *Drosophila melanogaster*: Imperfection or interesting exception? *Fly,* DOI: 10.1080/19336934.2017.1321181

"real" genetics involving that chromosome. My postdoctoral advisor, Scott Hawley, has the opposite relationship with *4* and has made numerous contributions to understanding unique aspects of the biology of this chromosome, particularly how it segregates in meiosis in the absence of chiasmata (Hawley *et al.* 1993). Intentionally or not, Bill and Scott's positions helped spark my own interest in chromosome *4*.

The Absence (and Presence) of Crossovers on *4*

Much of the attraction to chromosome *4* stems from its lack of crossovers, which has been a puzzle for 90 years. In his influential book *The Theory of the Gene*, T.H. Morgan presented a map of three chromosome *4* genes in the order *bent* (*bt*) - *shaven* (*sv*) - *eyeless* (*ey*) (Morgan 1928). Both the order and relative distances were wrong; *bt* is adjacent to *ey* in the middle of *4*, and *sv* is toward the distal end. The errors occurred because the presumed recombinants were actually cases of nondisjunction (Morgan *et al.* 1926; Patterson and Muller 1930). True crossovers on *4* have been observed, but only under special conditions. Perhaps most notable were the studies of Sturtevant, who found that crossovers are "greatly elevated" in diplo-*4* triploid females (Morgan *et al.* 1945). He used this finding to build a genetic map of *4*, reporting 3.0 map units between the most proximal and distal genes known (*ci* and *sv*) (Sturtevant 1951). Additionally, it has been reported that heat shock results in crossovers on chromosome *4* (Grell 1971), but it is unknown if these are true meiotic events. Although these cases support the possibility of crossover formation on *4*, they do not seem to provide insight into the mechanisms regulating crossover inhibition on *4* in a normal meiosis.

Previous hypotheses for why *4* lacks crossovers have focused on the unusual physical characteristics of this chromosome, including its small size, repetitive sequence, and heterochromatic structure, but studies reported recently by Hatkevich *et al.* have contributed new insights regarding the regulation of recombination on *4* (Hatkevich *et al.* 2017). Hatkevich *et al.* provide support for the idea that the meiotic crossover patterning processes that

establish crossover distributions characteristic of chromosomes *X, 2,* and *3* also prevent crossovers on *4.* Here, we review and assess the idea that the absence of crossovers on *4* stems from its physical characteristics and how crossover patterning processes may play a role.

Can Unique Physical Properties of *4* Explain the Absence of Crossovers?

The fourth chromosome in *Drosophila melanogaster* is much smaller than the other chromosomes, and is often referred to as the "dot chromosome" due to its observed small size in metaphase spreads. It has been suggested that crossovers on chromosome *4* in *Drosophila melanogaster* do not occur due its physical size. Interestingly, Chino and Kikkawa observed that the small chromosome in *Drosophila virilis*, which is similar in size to *Drosophila melanogaster* chromosome *4*, does have meiotic crossovers (Chino and Kikkawa 1932). This discrepancy between the two species may be explained by the fact that *D. virilis* has a much higher rate of crossing over on other chromosomes compared to *D. melanogaster*. For example, the *X* is the same physical size in *D. virilis* and *D. melanogaster*, but *D. virilis* has about three times as many crossovers on the *X* (Chino 1929). These data lead Chino and Kikkawa to hypothesize that a combination of the fourth's small size and the overall low crossover rate in *D. melanogaster* results in such a low probability of crossovers that they are undetectable.

To address the argument that we have not seen crossovers on *4* due its small size and low rate of crossing over, we can make comparisons with data from another chromosome (Figure 4.1). The assembled sequences of proximal *2L* and *4* have similar chromatin domains based on ChIP studies from several *Drosophila* cell lines (Roy *et al.* 2010). In the GBrowse chromatin tracks on Flybase (Gramates *et al.* 2017), most of chromosome *4* is classified as heterochromatin. Proximal *2L* is similarly classified as heterochromatin from approximately 22 Mb to the end of the assembly. Chromosome *4* is about 4-5 Mb, of which 1.2 Mb is assembled

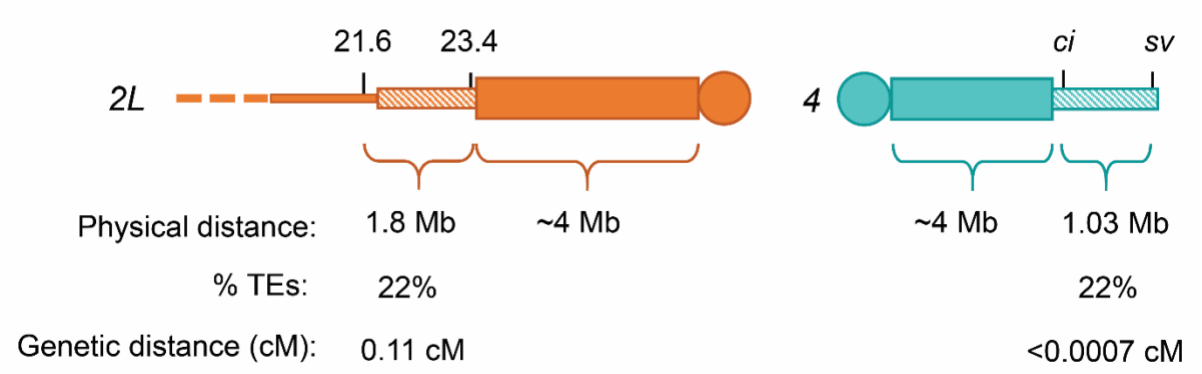

Figure 4.1. Comparison of proximal 2L and 4. Heterochromatin distances are as reported in Adams et al. (Adams et al. 2000) and Sun et al. (Sun et al. 2000). Distance of euchromatin and percentage transposable elements are from the v6.0 Drosophila melanogaster assembly (Hoskins et al. 2015). Genetic distance for 4 is from Sandler and Szauter (Sandler and Szauter 1978). The distance for proximal 2L interval was calculated from our unpublished data described in the text; flies with crossovers between pr and cn were collected and crossover sites were more finely mapped by genotyping with the SNP/indel markers shown (numbers represent positions of on the v6.0 assembly. Chromosomes not drawn to scale.

in the genome sequence (Locke and McDermid 1993; Sun *et al.* 2000; Hoskins *et al.* 2015). The pericentric heterochromatin on *2L* makes up approximately 5.4 Mb. As on *4*, most of this is composed of highly repeated tandem (satellite) sequences, but 1.5 Mb adjacent to proximal *2L* euchromatin has been assembled in the genome sequence (Adams *et al.* 2000; Hoskins *et al.* 2015). A common interval on *4* where crossover events are scored is from *ci* to *sv,* which spans 1.03 Mb. The *ci* to *sv* interval and the sequenced region of proximal *2L* are approximately the same distance from the centromere, providing a good comparison between *2L* proximal crossovers and crossovers on *4.*

We have identified SNPs and indels from the genome assembly that span the assembled heterochromatin proximal to the centromere to more finely map crossovers near the centromere. Figure 4.1 shows the location of two of these SNPs/indels, at 21.6 Mb and 23.4 Mb (v6.0 assembly). We collected crossovers between *pr* and *cn* and then genotyped them for these two genetic markers. We recovered eight crossovers in the 21.6Mb – 23.4Mb interval region from 7,399 flies scored (unpublished data). This gives a genetic distance of

0.11 cM ("map units" are traditionally used to describe recombination frequencies in *Drosophila*; we use the equivalent but more widely used centiMorgan, cM, here). Using the comparison between proximal *2L* and *4*, the *ci – sv* interval on *4* would have an expected genetic distance of 0.06 cM. Based on the number of flies scored for crossovers on *4,* it would be very unlikely that the crossovers were simply missed. In one notable example, Sandler and Szauter (Sandler and Szauter 1978) found no crossovers among 58,702 flies, yielding an upper limit of 0.0007 cM. From this comparison, we can infer that the small size of chromosome *4* and rate of recombination are not the only factors preventing crossovers.

If size alone does not account for the lack of crossovers on *4,* perhaps the sequence makeup of *4* contributes to crossover prevention. A large fraction of the region that has been assembled in the genome sequence consists of transposable elements (TEs): 22% of the *ci – sv* interval in the v6.0 assembly (Slawson *et al.* 2006; Riddle *et al.* 2008). In some organisms, recombination rates are lower in regions of high TE density and absent within TEs themselves (Dolgin and Charlesworth 2008). Miller *et al.* demonstrated that only one of 541 *Drosophila* crossovers they mapped through whole-genome sequencing was within a TE(Miller *et al.* 2016), suggesting crossovers are reduced within TEs but not completely absent. The *2L* region described above, from 21.6 Mb to 23.4 Mb, is 22% TE in the reference genome, similar to the *ci – sv* interval on *4* (but it should be noted that we do not know TE structure and density on the chromosomes used in the experiments reported here). Since these two intervals are comparable in size and transposable element density, we would expect them to have a similar recombination rate and, thus, genetic distance. Therefore, it is unlikely that TE density alone is responsible for preventing *4* crossovers.

Another aspect of the makeup of chromosome *4,* and closely related to the factor of heterochromatic sequences, is chromatin structure. Chromatin structure modifications have been studied in the context of chromosome *4,* although there are data on the other autosomes

that suggest chromatin structure could play a role in preventing crossovers. For example, in suppressors of variegation (*Su(var)* mutants), chromatin structure is modified so that heterochromatin is in a more open state, and found that *Su(var)* mutants resulted in an increase in crossovers proximal to the centromere on both chromosomes *2* and *3* (Westphal and Reuter 2002). However, these studies did not look at crossovers on chromosome *4.* It would be interesting to see if *Su(var)* mutations resulted in crossovers on *4*, which would support a role for chromatin structure in the prevention of crossovers on *4.*

In summary, the physical properties of *4*, including size, TE content, and chromatin structure could potentially play a role in preventing crossovers on *4,* but these are not likely the only factors involved, and perhaps not even major factors.

The Centromere Effect and the Absence of Crossovers on *4*

A different perspective on the reasons for the absence of crossovers on *4* was investigated by Hatkevich *et al.* –that the absence of crossovers on *4* is a result of meiotic crossover patterning (Hatkevich and Sekelsky 2017). Meiotic recombination begins with the introduction of DNA double-strand breaks (DSBs) in the DNA. Some DSBs are repaired as crossovers, but most become non-crossovers. Pathway choice is very highly regulated, but the mechanisms involved are poorly understood.

The major meiotic crossover patterning phenomena are interference, assurance, and the centromere effect. Sturtevant, when he first demonstrated the use of meiotic recombination frequencies to make a map of genes on the *Drosophila melanogaster X* chromsome*,* also noted that a crossover on one chromosome reduces the likelihood of another crossover in an adjacent interval, a phenomenon he and Muller later termed interference (Sturtevant 1913a, 1915). While interference applies to crossover distribution along a chromosome, assurance describes distribution among chromosomes, in that there is a tendency to have at least one crossover on every chromosome pair, regardless of size.

Assurance was first noticed by Darlington and Dark (Darlington and Dark 1932) in studies of chiasmata in the grasshopper *Stenobothrus parallelus*. From these and similar studies, Owen (Owen 1949) suggested that each bivalent has an "obligatory chiasma". Since interference and assurance were discovered, they have been described in many other organisms, including plants, fungi, flies, nematodes, and mammals (Jones and Franklin 2006; Berchowitz and Copenhaver 2010; Wang *et al.* 2015). Since there are no crossovers on *4*, neither interference nor assurance is applicable to explain the lack of crossovers; however, the third patterning phenomenon – the centromere effect – might contribute to this absence. The centromere effect is the suppression of crossovers in the centromere-proximal euchromatin. Like interference, the centromere effect was first described in *Drosophila* (Beadle 1932), and its mechanism remains mysterious.

To determine whether crossover suppression on *4* is due to proximity to the centromere, Osborne (Osborne 1999) used *T(1;4)w*^{m5}, which swaps the distal portions of the *X* and *4* (Figure 4.2). The *4*^{P}*X*^{D} element of this translocation has the centromere and proximal heterochromatin of chromosome *4*, a block of heterochromatin thought to be derived from the *X*, and the distal end of the *X* through the *white* (*w*) gene (Hawley *et al.* 1992). The *X*^{P}*4*^{D} element has most or all of the *4* gene-containing region (Bolen (Bolen 1931) thought the *4* break was between *bt* and *ey*, but Hawley (Hawley *et al.* 1992) says it is within the pericentric heterochromatin of *4*) attached to the *X* at 3C2, placing chromosome *4* gene sequences far from the *X* centromere. Osborne asked whether crossovers were able to occur in the chromosome *4* sequences that are now further from the centromere, and, conversely, if crossing over was abolished on the portion of the *X* translocated onto the centromere of *4*. To generate heterozygous markers, He first induced mutations in *y* and *w* on the *4*^{P}*X*^{D} chromosome and in *ey* and *sv* on the *X*^{P}*4*^{D} chromosome. This allowed him to score crossing over in flies homozygous for *T(1;4)w*^{m5} but heterozygous for mutations in these four genes. Interestingly, Osborne observed crossing over between *ey* and *sv* when

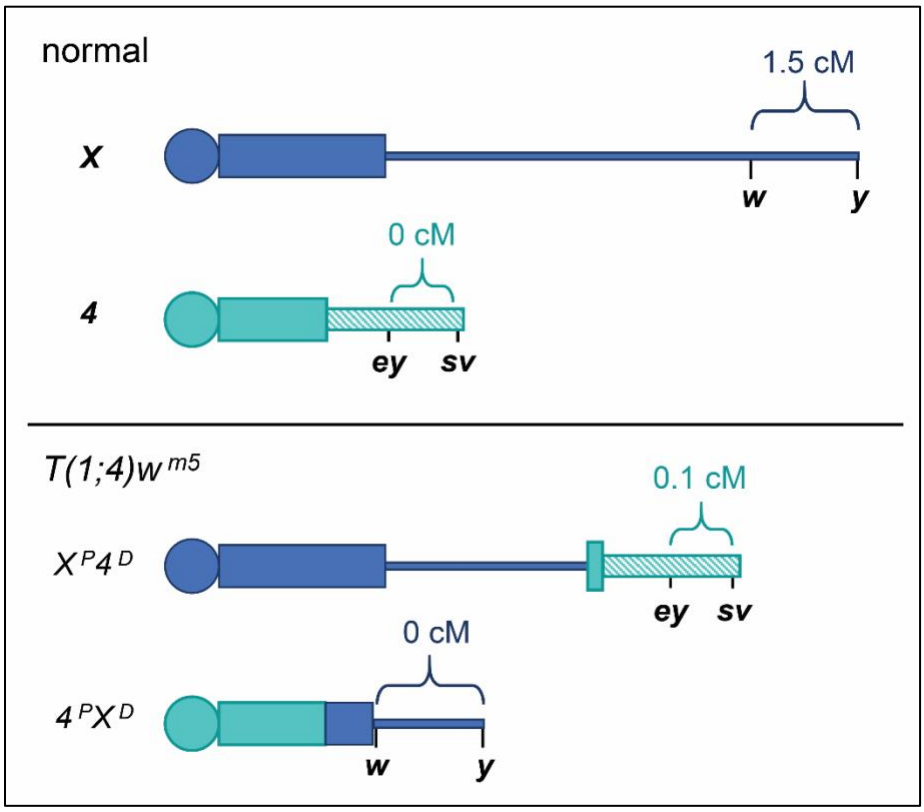

Figure 4.2. Representation of *T(1;4)w*^{m5}. Representation of *T(1;4)w*^{m5} with markers that Osborne used to measure recombination. The *y* – *w* distance on the wild-type *X* chromosome is the standard value based on recombination maps (Lindsley and Zimm 1992). The values in the *T(1;4)w*^{m5} experiment are from Osborne's data (Osborne 1999). For clarity, we flipped the orientation of the *X* chromosome from the standard map. Not drawn to scale.

they were on the end of the truncated *X*, but there were no detectable crossovers between *y* and *w* when they were translocated adjacent to the centromere of *4* (Figure 4.2). These results are consistent with the centromere effect largely contributing to crossover prevention on *4,* and argues against the hypothesis that size, sequence content, and chromatin structure are the main barriers to crossovers.

Eliminating crossover patterning allows crossovers on *4*

Crossovers have a characteristic distribution, forming mainly in the middle of each chromosome arm. In contrast, non-crossover gene conversion events detected in whole-

genome sequencing are distributed more evenly along each major chromosome arm(Comeron *et al.* 2012; Miller *et al.* 2016). Chromosome *4* at first seems to be an exception to this meiotic crossover patterning because it has no crossovers; however, Comeron (Comeron *et al.* 2012) reported finding non-crossover gene conversion events on *4*, so we can infer that DSBs are made on *4*; these DSBs on *4* are actively prevented from becoming crossovers through meiotic patterning processes. How could the absence of crossovers on *4* result from meiotic patterning? Since *4* is very small, the euchromatin is located very near the centromere, so perhaps the entirety of the chromosome is under the influence of the centromere effect. In our mapping of crossovers on *2L* (Figure 4.1), crossovers do occur in the one Mb interval adjacent to the proximal heterochromatin. However, this does not necessarily mean we would expect crossovers to occur in the euchromatic regions of the fourth for two reasons. First, the telomere effect (a crossover suppression at the distal ends of each chromosome, much weaker than the centromere effect) could be acting together with the centromere effect. Second, the centromere effect differs among chromosome arms(Miller *et al.* 2016), and is possibly stronger on *4*.

Hatkevich *et al.* (Hatkevich *et al.* 2017) showed that crossover patterning is lost in the absence Blm, a helicase involved in multiple DNA repair pathways (Adams *et al.* 2003; McVey *et al.* 2007). In studying meiotic phenotypes of *Blm* mutants, Hatkevich *et al.* found that interference, assurance, and the centromere effect were all absent or severely reduced. Interestingly, they also reported the occurrence of crossovers on *4* in a *Blm* mutant.

Why does loss of Blm lead to loss of crossover patterning and the presence of crossovers on *4*? In many organisms, there are two pathways that can generate meiotic crossovers (Kohl and Sekelsky 2013) (Figure 4.3). The major pathway produces “Class I” crossovers that exhibit meiotic patterning. The second pathway is minor, perhaps mostly resolving problems that arise during repair by the major pathway. The “Class II” crossovers produced by this minor pathway are not patterned: They do not experience interference,

assurance, or the centromere effect (Hatkevich *et al.* 2017). In *Blm* mutants, all crossovers appear to be Class II, suggesting that Blm is required to chaperone DSBs into the pathway that produces Class I crossovers under the influence of crossover patterning. Hatkevich *et al.* concluded that the absence of crossovers on *4* is due to meiotic patterning processes, with the centromere as the major contributor to this absence.

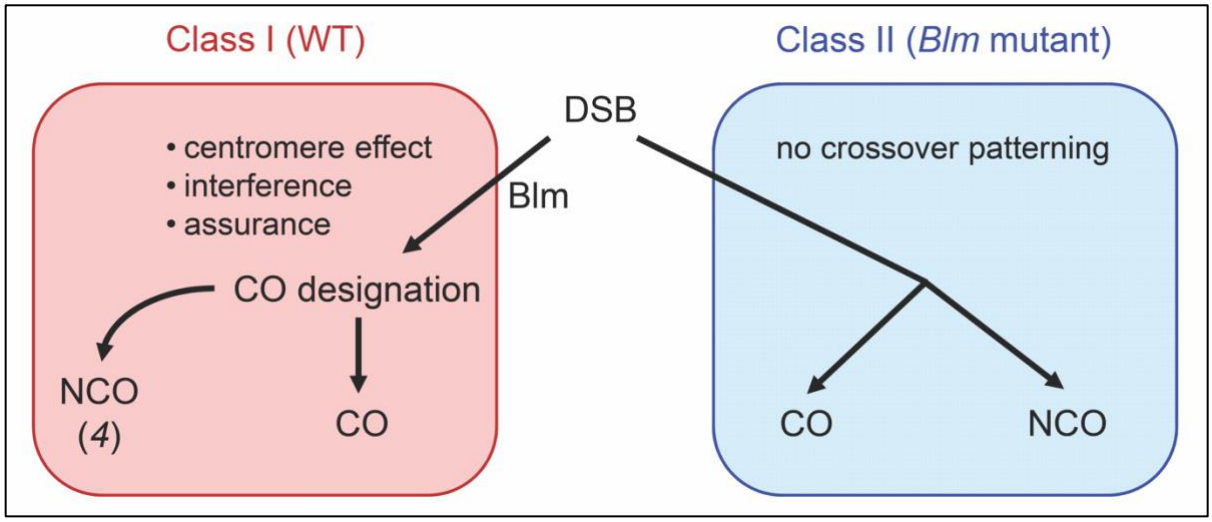

Figure 4.3. Use of the pathway that generates Class I crossovers requires Blm. In wild type flies, crossover patterning processes contribute to designating which DSBs become crossovers, resulting in observance of the centromere effect, interference, and assurance, as well as the absence of crossovers on *4*. In a *Blm* mutant, crossovers arise from a backup pathway and are not patterned, resulting in a random distribution of COs and NCOs across the genome, including on chromosome *4*.

Conclusions and Future Directions

There are many factors that could potentially contribute to the absence of crossovers on chromosome *4,* but until recently, only a few of the most basic physical characteristics of *4* have been studied in the context of crossover prevention. Based on recent studies, Hatkevich *et al.* suggest that it may not be the physical properties of *4* that prevent crossovers, but that the key regulator of this crossover suppression is likely the meiotic patterning of crossovers. Hatkevich *et al.* show that Blm directs double-strand break repair down the Class I pathway toward crossovers that experience meiotic patterning. Without

Blm, meiotic patterning is abolished and thus crossovers are permitted on *4*. There are still lingering questions such as whether any of the physical feature of *4*, such as the small size, repetitive sequence content, or heterochromatic chromatin states, play a role in meiotic patterning. Additionally, the Hatkevich *et al.* paper raises questions about what Blm is actually doing in meiosis and how interference, assurance and the centromere effect are enforced. Finally, although the data from Osbourne and Hatkevich *et al.* reviewed above make a strong case for the hypothesis that crossover prevention on *4* results largely from the centromere effect, we know essentially nothing about how the centromere effect is conferred. In considering mechanism, however, Sturtevant's classic mapping of *4* crossovers in triploids may provide a clue (Sturtevant 1951). Perhaps the increased number of centromeres (11 in diplo-*4* triploids versus 8 in normal diploids) dilutes the strength of the effect on each centromere. Redfield studied crossing over on chromosomes *2* and *3* in diploid and triploid females (Redfield 1930, 1932). She reported that triploids had elevated crossovers in the middle of each chromosome (*i.e.*, where the centromere is located) and reduced crossovers away from the central region (crossovers were also elevated near each end of chromosome *2*). Thus, it appears that centromere effect is sensitive to the number of centromeres. It will be interesting to confirm with conclusion through other manipulations and to further investigate the nature of this interesting phenomenon.

CHAPTER 5: CENTROMERE-PROXIMAL MEIOTIC CROSSOVERS IN *DROSOPHILA MELANOGASTER* ARE SUPPRESSED BY BOTH HIGHLY-REPETITIVE HETEROCHROMATIN AND THE CENTROMERE EFFECT[3]

Abstract

Crossovers are essential in meiosis of most organisms to ensure the proper segregation of chromosomes. The lack or improper placement of crossovers can result in nondisjunction and aneuploidy in progeny. Crossovers near the centromere can cause nondisjunction; centromere-proximal crossovers are suppressed by what is termed the centromere effect, but the mechanism is unknown. Here, we investigate contributions to centromere-proximal crossover suppression in *Drosophila melanogaster*. We mapped a large number of centromere-proximal crossovers and find that crossovers are essentially absent from the highly-repetitive (HR)-heterochromatin surrounding the centromere but occur at a low frequency within the less-repetitive (LR)-heterochromatic region and adjacent euchromatin. Previous research suggested that flies that lack the Bloom syndrome helicase (Blm) lose meiotic crossover patterning, including the centromere effect. Mapping of centromere-proximal crossovers in *Blm* mutants reveals that the suppression within the HR-heterochromatin is intact, but the centromere effect is lost. We conclude that centromere-proximal crossovers are suppressed by two separable mechanisms: the HR-heterochromatin effect, which completely suppresses crossovers in the HR-heterochromatin,

[3] This chapter contains work that has been submitted to the journal *Genetics* and is available on bioRxiv and the citation is as follows:
Hartmann M., J. Umbanhowar, and J. Sekelsky, 2019 Centromere-proximal meiotic crossovers in Drosophila melanogaster are suppressed by both highly-repetitive heterochromatin and the centromere effect. *bioRxiv*. https://doi.org/http://dx.doi.org/10.1101/637561

and the centromere effect, which suppresses crossovers with a dissipating effect with distance from the centromere.

Introduction

Crossovers are essential for the proper segregation of homologous chromosomes in meiosis, which is evidenced by the fact that chromosomes lacking a crossover commonly segregate improperly in meiosis I (Koehler *et al.* 1996a). However, it is not only the presence of crossovers that is important, but also their proper placement along the chromosome. Koehler et al. also showed that apparent meiosis II nondisjunction events occurred primarily in oocytes that experienced a centromere-proximal crossover (Koehler *et al.* 1996a). Similarly, cases of human trisomy 21 that appear to have arisen from meiosis II nondisjunction are associated with an increase in centromere-proximal crossovers (Koehler *et al.* 1996b; Lamb *et al.* 1996). It has long been known that crossovers near the centromere are reduced in many organisms; this has been referred to as the centromere effect (or the spindle-fibre effect before centromeres were defined) (Beadle 1932).

Meiotic recombination is initiated by DNA double-strand breaks (DSBs), each of which can be repaired to give crossovers or noncrossover products through a tightly-controlled decision (Lake and Hawley 2016; Miller *et al.* 2016). In addition to the centromere effect, interference and assurance also govern crossover patterning. Interference is the phenomenon where one crossover suppresses the occurrence of another crossover in nearby (A. H. Sturtevant 1913; reviewed in Berchowitz and Copenhaver 2010). Assurance is the phenomenon in which each pair of homologous chromosomes almost always receive at least one crossover regardless of size (Mather 1937; Wang *et al.* 2015). The effect of these crossover patterning phenomena on DSB repair results in the typical crossover distribution where most crossovers occur in the middle to distal end of the chromosome and are decreased near the centromere. The mechanisms of these phenomena are largely

undescribed and remain elusive. In this study, we use *Drosophila melanogaster* to gain insight into the centromere effect and how crossovers are suppressed in the centromere-proximal regions.

Approximately one third of each *Drosophila* chromosome is composed of highly-repetitive, peri-centromeric satellite sequence arrays that are heterochromatinized. There have been studies that suggest heterochromatin plays a role in decreasing crossovers in the pericentric regions. It has been proposed that there are no crossovers within heterochromatin simply due to the tightly packed chromatin not being accessible to proteins that either make DSBs or repair them into crossovers. Support for this comes from cytological studies where Mehrotra and McKim (2006) observed no DSBs colocalizing with the heterochromatic mark HP1. Additionally, dominant suppressor of position-effect variegation, *Su(var)* mutations, that likely cause heterochromatin to assume a more open structure, allow an increase in crossovers within the pericentromeric heterochromatin (Westphal and Reuter 2002). These results support the idea that suppression of crossovers near the centromere is due to exclusion of DSBs in heterochromatin.

However, early studies on the centromere effect involving chromosome rearrangements in *Drosophila* show that centromere-proximal crossover suppression extends beyond heterochromatin into the euchromatin. Mather (1939) showed that a euchromatic region moved closer to the centromere, but nearer to a smaller amount of heterochromatin, experienced a greater decrease in crossovers than did a region moved slightly farther away from the centromere, but nearer to a larger amount of heterochromatin. He suggested that the decrease in crossovers was due to proximity to the centromere rather than the proximity to heterochromatin. Yamamoto and Miklos (1978) studied *X* chromosomes in *Drosophila* that had large deletions of the pericentromeric heterochromatin, and showed that the larger the deletion, the farther the decrease in crossovers spread into

the euchromatin. They concluded that centromere-proximal crossover suppression does not depend on the amount of heterochromatin, but on distance from the centromere. Nonetheless, the question still remains whether heterochromatin has the ability to decrease crossovers in adjacent euchromatic regions; we address that question in this work.

Heterochromatin is not homogeneous and may not behave uniformly throughout. In polytene chromosome spreads, heterochromatin has two distinct appearances that have been described: alpha-heterochromatin is the small, densely staining region of the chromocenter that is highly underreplicated in this tissue, whereas beta-heterochromatin is more diffusely staining and is moderately replicated (Gall 1973; Ashburner 1980; Laird *et al.* 1987; Miklos and Cotsell 1990). Heterochromatin is not homogeneous based on sequence composition. Regions of pericentric heterochromatin adjacent to the euchromatin are composed of blocks of transposable elements (TEs) with varying amounts of repeats and interspersed unique sequence. This has made it possible to assemble these regions in the reference genome (Hoskins *et al.* 2015). Chromatin domains identified in cell lines show that much of this sequence is heterochromatic or transcriptionally silent (Filion *et al.* 2010; Thurmond *et al.* 2019). In contrast, sequences closer to the centromere are highly repetitive, consisting largely of blocks of tandemly-arrayed satellite sequences. These have not been assembled to the reference genome, but long-read sequencing has permitted assembly of some satellite arrays (Khost *et al.* 2017). We will refer to the two types of heterochromatin as highly-repetitive (HR)-heterochromatin and less-repetitive (LR)-hetero-chromatin.

In this study, we investigate the role of the two types of heterochromatin and the centromere effect in suppressing pericentromeric crossovers. We show that centromere-proximal crossover suppression is mediated by both a (HR)-heterochromatin effect and the centromere effect. The HR-heterochromatin effect is restricted to the highly-repetitive

heterochromatin, which presumably does not allow double strand breaks to occur and therefore, no crossovers can be formed in these regions. This study allows some insight into chromosome characteristics that could be contributing factors to the centromere effect and supports the idea that the centromere effect is a protein mediated meiotic mechanism.

Materials and Methods

Drosophila stocks

Flies were maintained on standard medium at 25°C. Mutant alleles that have been previously described include Blm^{N1} and Blm^{D2} (McVey *et al.* 2007). Blm^{N1}/Blm^{D2} mutants experience maternal-effect lethality, which was overcome using the *UAS::GAL4* system with the *mat*α driver as previously described (Kohl *et al.* 2012).

Phenotypic crossover distribution assay

Crossover distribution on chromosome *X* was scored by crossing *y sc cv v g f* • y^+ / *M{3xP3-RFP.attP'}ZH-20C* to *y sc cv v g f* • y^+ males, where • y^+ is a duplication of y+ onto the right arm of the X. Crossover distribution on chromosome *2*L was scored by crossing virgin *net* $dpp^{d\text{-}ho}$ *dp b pr cn* / + female flies to *net* $dpp^{d\text{-}ho}$ *dp b pr cn* homozygous males. Crossover distribution on chromosome *2*R was scored by crossing *net* $dpp^{d\text{-}ho}$ *dp b pr cn vg*/ + to *net* $dpp^{d\text{-}ho}$ *dp b pr cn vg* homozygous males. Crossover distribution on chromosome *3* was scored by crossing virgin *ru h th st cu sr e ca* / + females to *ru h th st cu sr e ca* homozygous males. Crossovers between *px* and *sp* were scored by crossing virgin *px sp* / + to homozygous *px sp* males and scoring crossovers. Additionally, *px* bw^D *sp* / + , and *px sp* / bw^D were crossed to *px sp* homozygous males for scoring this interval in a bw^D background. Crossovers in *Blm* mutants were scored same way as chromosome *2*L in wild-type. Each cross was set up as a single experiment with at least 20 vials set up and flipped after three days. After three more days, parents were emptied from second round of vials. All progeny were scored for parental and recombinant phenotypes for five days from all vials. Crossover

numbers in flies are shown as cM where cM = (number of crossovers / total number of flies) * 100. Fisher's Exact Test was used to compare total COs to total number of flies. See Table 5.1 for phenotypic crossover distribution data.

Genotype	Chromosome	Genome Location (Mb)	cM/Mb
WT	X	0.40	3.23
WT	X	5.96	3.81
WT	X	10.92	3.93
WT	X	13.73	2.01
WT	X	17.23	1.83
WT	X	22.80	0.00
WT	2L	0.08	2.05
WT	2L	2.43	3.75
WT	2L	4.48	3.03
WT	2L	13.82	1.70
WT	2L	20.07	0.26
WT	2R	7.78	0.26
WT	2R	12.88	1.40
WT	2R	17.89	3.40
WT	2R	22.49	3.47
WT	3L	1.37	3.23
WT	3L	8.68	2.81
WT	3L	16.05	0.31
WT	3L	16.50	0.19
WT	3R	11.20	0.17
WT	3R	18.09	0.99
WT	3R	21.23	2.10
WT	3R	29.81	3.65
Blm	2L	0.08	1.17
Blm	2L	2.43	1.21
Blm	2L	4.48	0.86
Blm	2L	13.82	1.31
Blm	2L	20.07	0.57

Table 5.1. Phenotypic crossover mapping in WT and *Blm*. Phenotypic crossover data for WT and Blm. Data shows genotype, chromosome, genome location of the phenotypic marker (Mb) and the crossover density (cM/Mb) calculated for that interval.

SNP/indel crossover mapping

Crossovers were finely mapped near the centromere using SNP/indels between isogenized strains. First, centromere-proximal crossovers were identified by phenotypic markers on the

chromosome. For all chromosomes, crosses were set up between a wild-type chromosome and a chromosome with recessive markers; females heterozygous for these were collected and crossed to males homozygous for the recessive markers, and progeny were scored. Crossovers were collected between f and y+ on the X chromosome, between b and vg on chromosome 2, and between h and e on chromosome 3. Illumina whole-genome sequencing was performed on each isogenized strain and genomes were assembled to the Drosophila melanogaster reference sequence, Dm6 (Hoskins *et al.* 2015), using BBMap (version 37.93, Bushnell 2014). SNPs and indels were called in comparison to the reference sequence using SAMtools mpileup (Sversion 1.7, Li et al. 2009; Li 2011), and then compared between strains using VCFtools (version 0.1.14, Danecek et al. 2011). Primers were designed to amplify only the wild-type chromosome so that each SNP/indel could be genotyped. See Table 5.2 for list of primers and locations. See table 5.3 and 5.4 for crossover distribution results from fine mapping for WT and *Blm,* respectively.

Drosophila whole mount ovary immunofluorescence

About ten three- to five- day old virgins were kept in a vial with yeast paste overnight with a few males. Ovaries were dissected in phosphate buffered saline (PBS) and incubated for 20 minutes in fixative buffer (165 µL fresh PBS, 10 µL NP-40, 600 µL heptane, 25 µL 16% paraformaldehyde). Ovaries were washed three times in PBST (1x PBS + 0.1% Tween-20), then incubated in blocking solution (PBST + 1% BSA). Then ovaries were incubated in primary antibody diluted in blocking solution at 4° C. Ovaries were then washed three times in PBST and incubated in secondary antibody diluted in blocking solution. After antibody incubation ovaries were washed three times quickly in PBST and mounted with DAPI Fluoromount-G (Thermo Scientific). Antibodies for H3K9me3 (Active Motif, 39161) and C(3)G (Anderson *et al.* 2005) were used.

Chromosome	Location	Forward Primer Sequence	Location	Reverse Primer Sequence
X	22649701	GATCTTTGCAATCCACGGAAG	22649922	CGCCAGAATCATGGCTGTG
X	21400408	CAGTCGACACGGCCTTCAC	21400805	GGACTACAGGAGAACTGAG
X	20596878	CGTCGTAGCTTTACATGAC	20597242	CGATCTCTGTTCCAGTGC
X	20065852	GTTGAAACTTAATGGTCTTCTTAAAG	20066087	CTGGCCTTTCATCACGTTTG
X	19541473	CAAAATGTTTATAGATGTCACAG	19541898	CTTCAAACGAGGCAACCGTGC
X	18947554	CCACATGGCCCTGTAATC	18948141	CTTTAAGAGAATCACGCAGTG
X	18552184	CACGTTGCGCAAGTTGCC	18552373	GCACAGAGTGGCCATGATATG
X	18152965	CATGGATCGGCGAGAATCC	18153356	AAGCGCTAGTTGCTGGCTG
X	17476509	CGTCTCTTTTGCCGCCTATG	17477114	TTCGTTCAAGGTTGTGTGTTAC
2L	14707226	GCGAGCCTGAAGGTTATCG	14707459	CGTGTAATCATCTCCTACC
2L	15866603	GTAGCTACCACCTGGATTAG	15867237	CACAGCCCATTTCTCAAG
2L	16339184	GATACGCTTCGCTGTGAATAAC	16339575	GTCCGGGATCTAGTGGTGC
2L	16583646	GCCAATGCTGGGTCCACTC	16584204	CAGACACGCCACGAGGATGAC
2L	16809718	CGTCTGTCTGTACGTTATTC	16810155	TCCTTCATTAAAGCAATCGC
2L	17153268	GGGTTGCCAATTCTGCTTC	17153555	AAAGCCAGCCAACGGAACT
2L	17492746	CATCAGCTAATGGCAGGAGTTTG	17493189	GACTCAAGCCAGTCGAGCG
2L	17836891	CGCGAACTTCTCACACTC	17837185	AACAGCTCTGGCGGGAAATC
2L	19070295	GCACGCACATGGTCAACTC	19070868	CATGTGGACAATTGGAACC
2L	20041502	CCATTCGGATCCACTTGCG	20042067	CCACTTTCTGCTCTCCGC
2L	20618378	GCCTGCGGCCGTGTCATG	20618548	CATGTTGCCAACGATTCCGG
2L	21108908	GTAATCAGCTGTTGAAAAC	21109483	GAATTCGGCGTTCCTTAATCG
2L	21675849	GGACTAATACCATTGTAAAG	21676016	CCTATACTGGCCAGTCTCC
2L	22073133	TACTCTAAGATTAGTGGATAT	22073251	TGACTACCGCACTTTCAAC
2L	23424573	TTTGTTTGACTAACATTGGA	23424795	TTAGGACGAAACACAATTGG
2R	639629	GGAAGTTAGAGCTCAGACACAA	640253	GACTCTCTAATTCGTGGAC
2R	1097861	GCTCTCCCGCTCTATTAGC	1098657	GTAAATTGGGTAAACATCGTCA
2R	2598095	GAAGGAGACAATTAAAATCAC	2598893	AGCAATCTACCCTACCAAGG
2R	3076813	CTCAAACCGCGTAGCCATC	3077426	ACACTTCCCTGTGGAATTCTT
2R	4377398	CTAGATGTTTCCTACAGTTTC	4377786	GATACCCGTTACTGAGTGTGG
2R	5043317	CAAACCTGTAAGTCTGCAC	5043483	TTCTTATATCTACCGTAAAATGC

2R	5476458	GATGACCTCCAGTGCGAATC	5476859	GTCGTCAAGTGATGCTGCAC
2R	6111492	GTAGAAGTAGAAGATCGACG	6112190	GAAGGTTGTGGCCTGACTC
2R	6784660	CAAGTGCTGGGTCAATGTG	6785039	GATGTTTTCCGGCCCATTTC
2R	7459353	GCTAAAGTCTAGGCATATTTG	7459964	CAGAAGATTCGACGAAGCC
2R	7989635	AGTGTGGTGCCGTGTGGC	7990035	GATCGCTGGAACAGGTTG
2R	8338722	GACTTGGACTTTCTTAAGTCTTAC	8338935	CCTGCAAGAAATTAGCGCCTG
2R	8769813	GGATTTTGAACATAGCCTTACG	8770212	CCAGCTGCCAGACGATTAAG
2R	9280320	GTTGCTTTTGGCACCATCCAATC	9280938	GTCTTGAGCTTCCACTTTCTCC
2R	10020451	GTGCCGCGTCCGCTTATC	10020784	CCAAATGGGATTTACTTGTCGTG
2R	10794962	GTGTCTATGCGTGCCTGTTTTTGTG	10795211	CGATGAGCAGACTTTGGGCAGC
2R	11889879	GTTCATTGTCCAAGTGTGAGC	11890485	GTCAGCGTTTGCCTTGCTTTTGCC
2R	12284348	CCCAAGATATTTTCCCTTTTACCG	12285113	GCAGGATATGGATGTGGTTTC
3L	9732472	ATCAACTCATAGAAAGCTTCC	9733062	CACAATGCTCTAAAGCAATGC
3L	11349437	CATTACATACAATCCAGCAACC	11349993	GTGTAACACAGCAAGTGCGC
3L	12647591	GCACCAACACGATCCTCAATG	12647997	TAGCCCCATAACAAGGTTTCC
3L	13799750	CTATCTTCTTTGGCCCTTATTC	13799988	GTGTTTGAATGTGCGAGTGTC
3L	14867724	GTGGTATAACTACTGGTCATGC	14868335	CAAATTGCATCGCCATACGAAAC
3L	15446067	ACACAGAAAGCTCGTGGTG	15446468	GTGGCTTTGGAAGACATGC
3L	17006414	GGTGTCTCGTTGAGCTTCCGTT	17006615	GTTGATAGCAGTGTATGGCG
3L	17507475	CAAAATGGAGCAACAGGTTGG	17507899	CATCGCCATTGCTCTTCGTC
3L	18590308	CATCACAGCATCTGCATGC	18591113	GCTTATTCGTGGGGATGTTGAG
3L	18948357	GAAGGAGGCTGGGAGCCAAAAG	18948563	CATGCGAGAAATCGAAATTCAG
3L	20462623	GTAATCAAATCATGGCTGTTC	20463199	GTTGCGCAGTTGCATGTGAG
3L	21082261	GATTTTTCTTGCTTTCCTCGAC	21082465	GTACGAATATCGAACGAATAC
3L	21501188	CCAGTATACCAAAGACCCTAG	21501580	CCACTGTCACCGTAGCTG
3L	21997309	ATCCTTCTTATGGGGTGGCAG	21997682	GTTTTGACCCGTCCCACACG
3L	22980628	TGCTTTAGTGACACTTCCTCATTG	22980989	CTATAAAGCGATAGCTTGAAGG
3L	23632568	GGAACATAATTCAACCAAATTCG	23633162	GCTGTAAACTCTTCCGTGC
3L	24515924	GCTAGGAGGCAGGATGGAATACTAC	24516307	CTTCATCAGCTCCACCGCTC
3L	25068055	GAAAATCCACGCGTAAGCTGCC	25068669	CTTCAGATACCGTGATATGGATTG
3L	26003222	GTTTGTTGACCCATGTTGTC	26003611	GAATCCTGAGAGGATTGTGC

3L	26699659	GCCTTGACAGTGTTCATCAG	26700239	GGATTCTGCGGTGACATC
3L	27398795	GCGTCATCTGGATGCCAC	27399291	CTCTGTACGCTTCCGTTATTCCTAA
3R	1153007	CATCCAAAGCATCCGTTACTGTC	1153418	CGAGAATAGTGAAGAGGAAGAAGCG
3R	1521153	CGCTTCGATCATCTTCCGC	1521700	GATAATGTGACAGACCATGTG
3R	2080717	CAATCTTTGTAAATTAGGTCTCA	2080936	CTATCGATGACAAATACCCAATTC
3R	2460409	GTAAGAGGAAGCACAAAGGTATCC	2460800	CATATCCATCTTACATAATCGTCG
3R	3526413	GACAAACTAACGGGATACGC	3526605	CTTACTGCTCCGCTACCTC
3R	4622421	GCGTTTGCGGTCAGTTGACATTC	4623036	CGCAGCTCGAACTATCACTAAG
3R	4966057	GCGTATTAAACTGATCGCCAGG	4966844	GATCAACACCATCCGCCGATTC
3R	5584425	GCTTGCACGTTGGAGTTGCTTG	5584877	CTCGCCATAATCTTCCGAAAC
3R	5989386	GACCCTCTGCAAAATGTCGAAG	5989567	CCGATGTCGATGCCTTTGCC
3R	6604707	GCGCACAACAGCATTTGCAG	6605100	CTGCACCCAGCTTGTCCATC
3R	7026906	GTTCCCATTCGGCGCCTTTTC	7027518	GAACGCAAGTCGGCAAAGACG
3R	7503742	TATTGTACCTTCCCAAGTGACC	7504533	CTTCCATGGCTGCATTTGATC
3R	7977701	GCGAAATGAACGCGGTGAAG	7978303	TTTAGTGTGTGCCAATACATGA
3R	9062678	CTGAAAGATACAAACTGTACCGACC	9063061	CTTGGCAGGTTGACTTATCGAC
3R	9497822	GTCTGTGGAGCGAGTACGAAGA	9498450	CCTTCAAGCGAACTCAACTG
3R	10000797	GTGCTTGTACCGCTTCACATT	10000965	CACCCATCAAGAGCATAATGAAC
3R	10543465	CCTTGCCAGCATTCAACC	10543855	GCGTGCTATATGTCTGACCAAC
3R	12038967	GGAAATTTCCCCAAAAACCGAC	12039148	CCACTTTCATGCCAAATTTCG
3R	13964694	ACGTATGCAATTCTTATTCGAAC	13965268	CATGCTGCTCCGTTCATCG
3R	14915739	GCCAGCCGGGTTGAATATC	14916114	CATAAGTCAACCCGTGAGTAG
3R	15933596	CGTTGTAGCGACTTCGTC	15933796	TAGCTATATCATCGAGAATCG
3R	17012997	GTAAGTGGGCGTTTCAACCG	17013362	CCATGGACCTGTTTTGTGCG
3R	18507653	AGCTGATCAGGTGTTTGTTCAT	18507838	CTGGCATTGACAACCGAATAGC
3R	18968137	GGTGGATTCGCTTATCGTACGAC	18968292	CCTGCTCTGCTTCAGTCACAACTTG
3R	19559552	GCCACTCACTCTGCGAATGG	19559961	CAAGGGAATGGCATCTTCTGCAGC
3R	20054762	CTGTACTGAGGTTATACTTTAC	20055162	GATGGGATTGGGGGACTCAAAG
3R	20512391	GATCCGTTCGGTGGACAGCACTG	20512983	GCTATTGATACTGAAACTTAAATG

Table 5.2. Primers used in fine mapping of crossovers. All primers used for SNP/indel mapping designed to amplify one of the isogenized strains used in each cross. Chromosome and genomic location, sequence of each primer is displayed.

Chromosome	Interval Width (Mb)	Crossovers	Genes	TEs	Flies
X	1.249293	1	52	200	1595
X	0.80353	19	74	88	1595
X	0.531026	20	74	44	1595
X	0.524379	23	102	40	1595
X	0.593919	38	60	21	1595
X	0.39537	23	51	7	1595
X	0.399219	11	53	5	1595
X	0.676456	16	69	11	1595
X	0.243571	9	18	6	1595
2L	1.35144	3	46	220	7399
2L	0.397284	5	40	136	7399
2L	0.566941	2	198	163	7399
2L	0.49053	7	85	26	7399
2L	0.576876	16	77	83	7399
2L	0.971207	16	137	28	1460
2L	1.233404	14	194	26	1460
2L	0.344145	4	16	7	1460
2L	0.339478	3	42	8	1460
2L	0.34355	4	40	9	1460
2L	0.226072	10	40	5	1460
2L	0.244462	11	22	1	1460
2L	0.472581	15	65	12	1460
2L	1.159377	35	150	20	1460
2L	0.883247	28	108	10	1460
2R	0.639629	0	4	3	15115
2R	0.458232	0	16	20	15115
2R	1.500234	0	3	5	15115
2R	0.478718	3	13	10	15115
2R	1.300585	6	20	400	15115
2R	0.665919	8	18	297	15115
2R	0.433141	45	51	229	15115
2R	0.635034	42	80	128	15115
2R	0.673168	44	118	31	15115
2R	0.674693	22	58	8	15115
2R	0.323443	12	118	15	2389
2R	0.555926	9	73	14	2389
2R	0.431091	5	98	7	2389
2R	0.510507	16	120	22	2389
2R	0.740131	32	114	11	2389
2R	0.774511	50	173	24	2389
2R	1.094917	18	82	4	2389
2R	0.994753	30	132	13	2389
3L	0.701205	0	3	3	3744
3L	0.699136	14	10	7	3744

3L	0.696437	0	4	5	3744
3L	0.935167	0	10	12	3744
3L	0.552131	0	8	3	3744
3L	0.883356	0	14	162	3744
3L	0.65194	0	16	416	3744
3L	0.983319	0	122	98	3744
3L	0.496121	1	89	26	3744
3L	0.418927	1	69	23	3744
3L	0.619638	1	93	26	3744
3L	1.514266	17	258	49	3744
3L	0.358049	6	67	9	3744
3L	1.583894	20	192	41	3744
3L	0.505954	17	76	7	3744
3L	0.447426	1	116	9	796
3L	0.606967	5	113	5	796
3L	0.578343	4	70	13	796
3L	1.067974	7	105	19	796
3L	1.152159	28	146	11	796
3L	1.298154	38	224	13	796
3L	1.616965	42	201	13	796
3L	1.056713	27	177	17	796
3R	0.368146	0	1	6	3744
3R	0.559564	0	1	0	3744
3R	0.379692	10	1	6	3744
3R	2.162012	0	90	162	3744
3R	0.343636	0	40	39	3744
3R	0.618368	2	81	22	3744
3R	0.404961	1	87	18	3744
3R	0.615321	0	80	20	3744
3R	0.422199	3	56	12	3744
3R	0.476836	1	94	19	3744
3R	0.473959	0	56	22	3744
3R	1.084977	10	197	18	3744
3R	0.435144	2	51	4	3744
3R	0.502975	10	104	3	3744
3R	0.542668	6	74	8	3744
3R	0.652127	9	80	7	3744
3R	0.843375	13	141	7	2310
3R	1.925727	29	309	56	2310
3R	0.951045	35	126	11	2310
3R	1.017857	25	153	14	2310
3R	1.079401	21	148	8	2310
3R	1.077806	28	158	16	2310
3R	0.41685	26	66	10	2411
3R	0.460484	48	54	4	2411
3R	0.591415	32	65	9	2411

3R	0.49521	17	75	5	2411
3R	0.457629	28	1	11	2411
3R	0.717409	37	127	12	2411

Table 5.3. Fine mapping of crossovers, gene density and TE density. Fine mapping data and data used for modeling analyses. Data includes chromosome, interval width (Mb), number of crossovers in that interval, number of genes, and number of transposable elements (TEs), and total number of flies scored in each experiment. For each arm, data goes from most proximal to centromere to most distal.

Chromosome	Interval Width (Mb)	Crossovers	Flies
2L	1.35144	3	1070
2L	0.964225	11	1070
2L	0.49053	1	1070
2L	0.576876	7	1070
2L	2.204611	40	1070
2L	0.344145	1	1070
2L	0.339478	3	1070
2L	0.34355	2	1070
2L	0.226072	3	1070
2L	0.244462	7	1070
2L	0.472581	5	1070
2L	1.159377	7	1070
2L	0.883247	15	1070

Table 5.4. *Blm* mutant fine mapping. Fine mapping data for *Blm* mutant used in modeling analyses and mapping distribution. Data includes chromosome, interval width, number of crossovers in that interval, and total flies scored for this experiment.

Generation of fluorescence in situ hybridization (FISH) probes

BAC clone (BAC PAC RPCI-98 library) DNA was extracted using a MIDI-prep kit (Clontech #740410). The probe for the *bw* locus was Clone BACR48M01. BAC DNA was used in nick-translation reaction to create biotinylated probes. Nick translation reaction: 5 µL 10X DNA Pol I buffer, 2.5 µL dNTP mix (1 mM each of dCTP, dATP, dGTP), 2.5 µL biotin-11-dUTP (1 mM), 5.0 µL 100 mM BME, 10 µL of freshly diluted dDNase I, 1 µL DNA Pol I, 1 ug of template DNA, water up to 50 µL. The reaction was incubated in thermocycler at 15° C for four hours. The probe was purified using PCR purification kit (Qiagen) and quantified using

Qubit (Thermofisher Q32854), then diluted to 2ng/µL in hybridization buffer (2X saline-sodium citrate (SSC) buffer, 50% formamide, 10% w/v dextran sulfate, 0.8 mg/mL salmon sperm DNA).

AACAC oligonucleotide probe was obtained from Integrative DNA Technologies (IDT, www.idtdna.com). Sequence: Cy3-AACACAACACAACACAACACAACACAACACAACAC.

Drosophila whole mount ovary IF-FISH

Ovaries were dissected as described above, incubated in fixative buffer for four minutes (100 mM sodium cacodylate (pH7.2), 100 mM sucrose, 40 mM potassium acetate, 10 mM sodium acetate, 10 mM EGTA, 5% paraformaldehyde), washed four times quickly in 2XSSCT (5mL 20X saline sodium citrate (SSC), 50 µL Tween-20, up to 50 mL water), washed 10 minutes in 2X SSCT + 20% formamide, 10 minutes 2X SSCT + 40% formamide, then two times 10 minutes in 2X SSCT + 50% formamide. Ovaries were pre-denatured by incubating at 37° C for 4 hours, 92° C for 3 minutes, 60° C for 20 minutes. Probe(s) was added and ovaries were incubated in a thermocycler at 91° C for three minutes then overnight at 37° C. Ovaries were then washed with 2X SSCT + 50% formamide at 37° C for 1 hour, then in 2X SSCT + 2-% formamide for 10 minutes at room temperature (RT), then in 2X SSCT quickly four times. Ovaries were then incubated in blocking solution (6 mg/mL NGS in 2X SSCT) for four hours, then washed quickly three times in 2X SSCT. Ovaries were incubated overnight in primary antibody diluted in 2X SSCT at room temperature, then washed three times quickly in 2X SSCT, incubated with secondary antibody diluted in 2X SSCT for two hours, then washed three times quickly in 2X SSCT. Ovaries were then incubated with streptavidin (1.5 µL of 488-conjugated streptavidin diluted in 98.5 µL detection solution [0.5 mL 1M Tris, 400 mg BSA, water to 10 mL]) for one hour at room temperature, washed two times quickly in 2X SSCT, one hour in 2X SSCT, then three hours

in 2X SSCT. Ovaries were then mounted in DAPI fluoromount. In this work, primary antibody for C(3)G (Anderson *et al.* 2005) was used.

Imaging and quantification

Images of whole-mount germaria were taken using a Zeiss LSM710 confocal laser scanning microscope using 40x oil-immersion objective. Images were saved as .czi files and processed using FIJI (ImageJ). Distance between foci for Figure 3 was measured using FIJI. Distances were compared using unpaired t-test.

Statistical methods

We conducted an analysis of crossover density using a model averaging approach (Burnham *et al.* 2011). In this approach, models of varying composition and complexity are weighted according to their ability to fit the data parsimoniously, then averaged to construct predictions and inference. A benefit of this approach is lack of picking one best model when uncertainty exists among a set of candidate models. Similarly, there are no hard *p*-value cutoffs which can be used to artificially exclude weak, but potentially important variables. All statistical analyses were completed using the R language (version 3.6; R Core Team 2019).

The count of crossovers in each chromosome section was modeled with negative binomial regressions fit using maximum likelihood using the MASS library (version 7.3-51.4; Venables and Ripley 2002). All models use a log link function to relate the linear combination of predictor variables to the mean number of crossovers. All models also include an offset variable (a variable whose slope is assumed to be one) of the log(# of number of flies X length of chromosome section). This offset accounts for the different sampling involved in each observation and can be thought of changing the model to one fitting the density of crossovers per fly per section. Prior to fitting, all quantitative variables were centered and standardized by dividing by 2 times the standard deviation of the variable.

The most complex or “global model” included, in addition to the offset, linear additive effects of the density of transposable elements and gene density and a quadratic response to distance from the centromere (distance from the centromere is calculated as distance from the end of the genome assembly for each chromosome arm):

Log(mean # of crossovers) ~ (distance from centromere + distance from centromere^2 + transposable element density + gene density)* chromosome identity + log(offset(Fly number * width of chromosome section))

All subsets of this model that included the quadratic effect of distance only when there was a linear effect of distance, were fit. Model selection and averaging were conducted using the MuMIn library (version 1.4.36; Barton 2019). We fit all possible submodels of the global. This led to 150 models being fit. We used the corrected Akaike Information criterion, AICc, as our measure of model performance and selected a final model set based on a 95% confidence set and then calculated model averaged estimates of coefficients and their standard errors. Models which had higher AICc than nested models were excluded based on the recommendation of Richards *et al*. to avoid including overly complex models that do not improve model performance (Richards *et al.* 2011).

Results

Pericentromeric crossover distribution

To gain a deeper understanding of the centromere effect, we sought to more finely map centromere-proximal crossovers. Crossovers near the centromere have classically been mapped using phenotypic markers in the euchromatin on either side of the centromere. Additionally, whole-genome mapping has been used to more precisely map crossovers within the genome (Sturtevant 1915; Miller *et al.* 2016). However, these methods have caveats that do not allow us to fully understand the distribution of centromere-proximal

crossovers. Using phenotypic markers to map crossovers limits resolution to only the most centromere-proximal markers used. Whole-genome mapping provides precise locations of crossovers, but only a handful of centromere-proximal crossovers have been mapped using this method. For example, from whole-genome sequencing of 98 flies only one crossover was mapped between the markers *pr* and *cn* that flank the chromosome *2* centromere (Miller *et al.* 2016). We therefore develop a method to map a high quantity of crossovers with more precision than phenotypic mapping allows, allowing us to gain a better understanding of the relationship of crossover distribution in euchromatin and the two types of heterochromatin (LR-heterochromatin and HR-heterochromatin).

We collected proximal crossovers using phenotypic markers between isogenized *Drosophila* chromosomes then more finely mapped these using SNP and indel markers to intervals that range from 0.23 Mb to 1.9 Mb. We mapped approximately 160-300 crossovers per chromosome arm. This mapping shows that crossovers are decreased near the centromere and increase in frequency with distance from the centromere (Figure 5.1). Interestingly, we see a low frequency of crossovers in the assembled LR-heterochromatin, but crossover frequency goes down to nearly zero in the highly repetitive heterochromatin on every chromosome arm. Of 37,219 total flies scored (including crossover and noncrossover progeny), only three progeny, all on chromosome *2*, experienced a crossover between the most centromere-proximal SNPs/indels used in our mapping. These crossovers may have occurred within LR-heterochromatin, either proximal to our most proximal markers or in sequences not included in the genome assembly. Alternatively, they may have been within HR-heterochromatin or unique sequences within HR-heterochromatin. We cannot exclude the possibility that these crossovers are mitotic in origin. While we cannot rule out that double crossovers occur within the HR-heterochromatin region, we believe this to be highly unlikely due to the near absence of even single crossovers. The fact that we do see a

small amount of crossovers in the less-repetitive heterochromatin was surprising because it has been shown that DSBs do not colocalize with heterochromatic markers (Mehrotra and McKim 2006; see Discussion).

Fine mapping gives a clearer understanding of crossover distribution near the centromere, but to begin understanding the contribution to this distribution, we explored a mutant that does not experience centromere-proximal crossover suppression.

A centromere effect mutant separates the centromere effect and the HR-heterochromatin effect

If the centromere effect is genetically controlled, we would anticipate it being possible to identify mutants that do not experience suppression of crossovers near the centromere. Hatkevich *et al.* identified a mutant that they hypothesized does not experience the centromere effect (Hatkevich *et al.* 2017). *Drosophila* Blm helicase, like *S. cerevisiae* Sgs1, has been proposed to direct DSBs down the meiotic DSB repair pathway to allow the proper crossover patterning (De Muyt *et al.* 2012; Zakharyevich *et al.* 2012; Hatkevich *et al.* 2017). It is hypothesized that *Blm* mutants do not have the centromere effect based on a flat distribution of crossovers and a measure of the strength of the centromere effect (Hatkevich *et al.* 2017). That study only mapped crossovers using phenotypic markers in the euchromatin on either side of the centromere so we aimed to examine the loss of the centromere effect in *Blm* mutants using the SNP/indel mapping approach. Importantly, *Blm* mutants appear to have normal heterochromatin as evidenced by H3K9me3 staining colocalizing with DAPI dense, heterochromatic regions (Figure 5.2A).

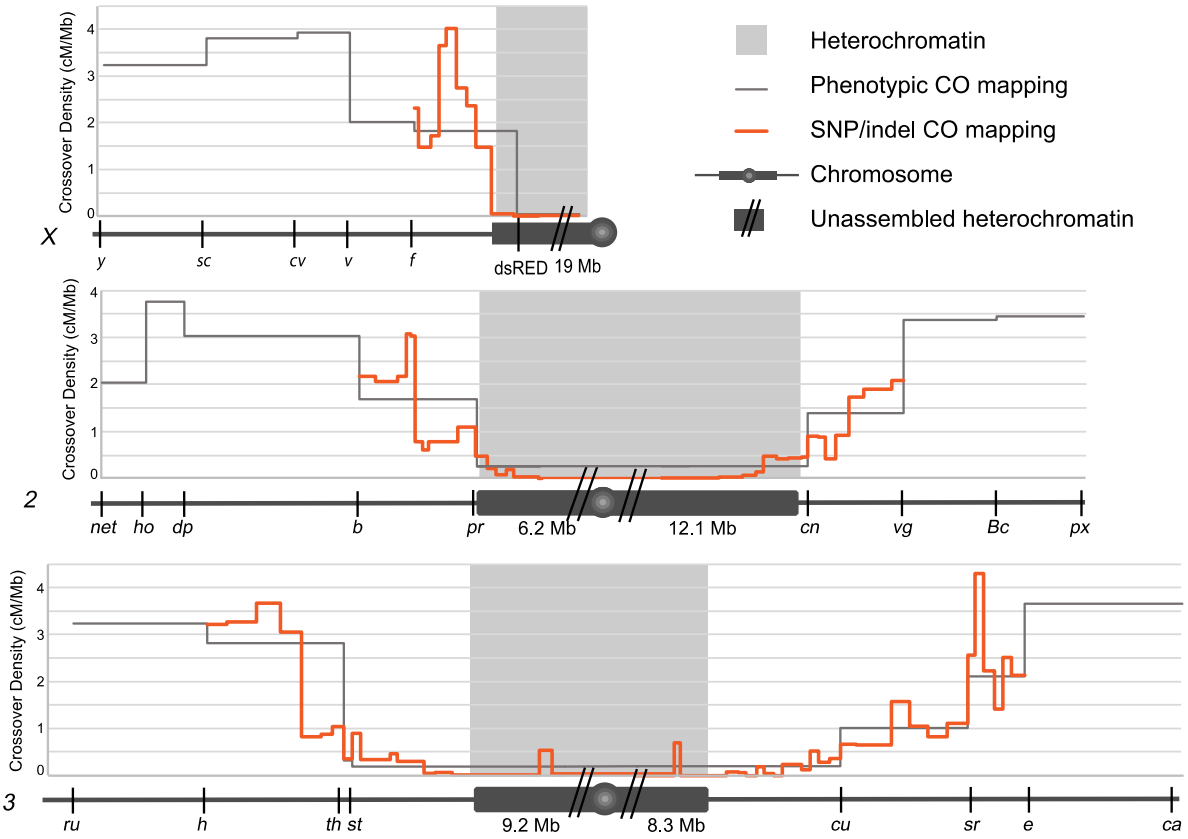

Figure 5.1. Fine mapping of centromere-proximal crossovers. Chromosomes are represented under each graph (*X, 2, 3*) with euchromatin (dark gray line), heterochromatin (dark gray box), unmapped heterochromatin (dark gray box with two slashes), and the centromere (dark gray circle). Predicted amount of heterochromatin is displayed underneath chromosome for each chromosome arm (values obtained from Hoskins et al. 2002). Heterochromatin boundaries (light gray blocks) are based on H3K9me2 ChIP array boundaries shown in Riddle *et al.* 2011). Phenotypic markers used for mapping crossovers are indicated on each chromosome. Crossover density (cM/Mb) is plotted for crossovers scored between phenotypic markers (gray line) and for crossovers scored using SNP/indel mapping (orange line). Chromosome *X* n=160, Chromosome *2* n=415, Chromosome *3* n=622). For full data set, see Tables 5.1 and 5.3.

SNP/indel mapping of *Blm* mutants reveals a relatively flat distribution of crossovers throughout the chromosome arm and into the assembled heterochromatin (Figure 5.2B). *Blm* mutants experience no crossovers within the HR-heterochromatin, as in wildtype. From these results, we hypothesize that the suppression of crossovers can be separated into two phenomena: the HR-heterochromatin effect, defined as the virtual absence of crossovers

within highly-repetitive heterochromatin, and the centromere effect, which has a dissipating effect with distance from the centromere. We hypothesize that the HR-heterochromatin effect is likely due to the absence of DSBs in this region, whereas the centromere effect is likely a regulation of DSB repair outcome.

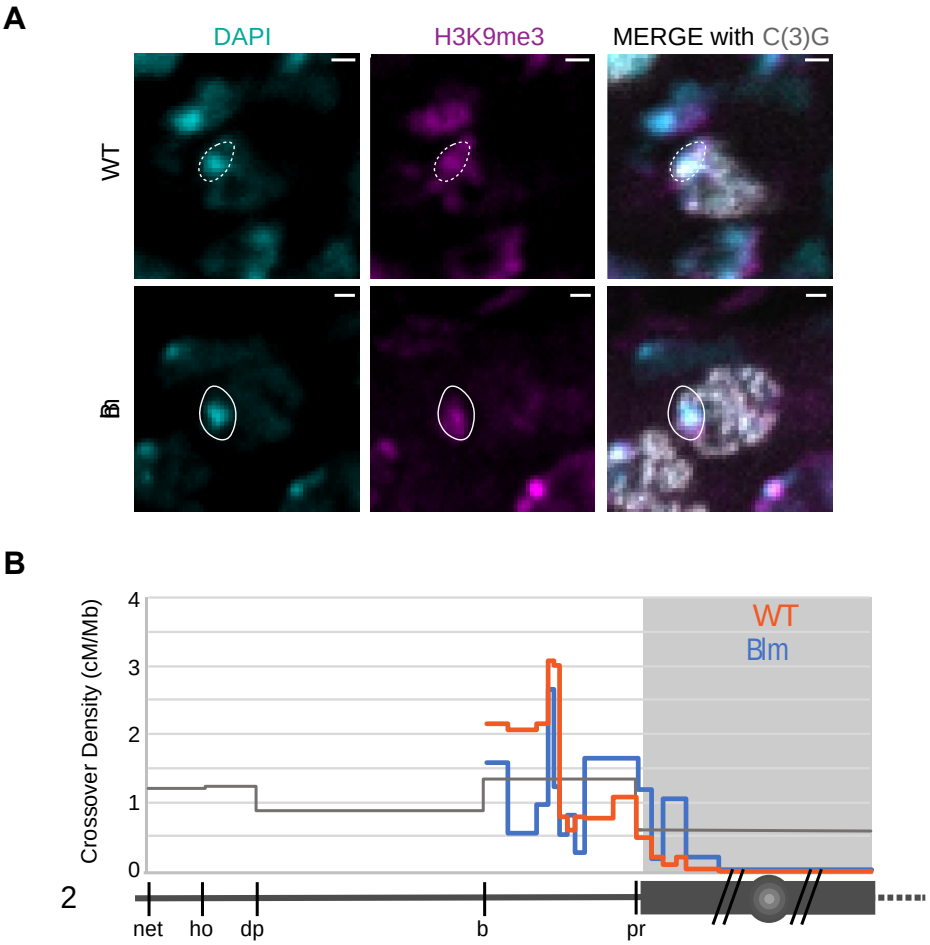

Figure 5.2. Fine mapping of centromere-proximal crossovers in *Blm* mutants. (A) Heterochromatin staining in *Blm* mutants and WT. DAPI staining for DNA is shown in the left panels, H3K9me3 staining for heterochromatin shown in the middle panels, and the right panels are merged images. The dotted circle outlines a DAPI region that overlaps with heterochromatin showing that *Blm* mutants have normal localization of heterochromatin. (B) SNP/indel mapping as shown in Figure 5.1 for chromosome *2* with euchromatin (dark gray line), heterochromatin (dark gray box), unmapped heterochromatin (dark gray box with two slashes), and the centromere (dark gray circle). Phenotypic markers are depicted under the chromosome. Plotted on the graph is crossover density (cM/Mb) for phenotypic markers (gray), WT SNP/indel mapping (orange), and *Blm* SNP/indel mapping (blue). Heterochromatin shown by light gray box. For full data sets, see Tables 5.1 and 5.4.

Heterochromatin alone does not produce a centromere effect

We sought to test whether the HR-heterochromatin effect and centromere effect can be separated by measuring recombination around a heterochromatic locus that is not located near the centromere. We do this by using the bw^D mutation, which has an insertion of about 2Mb of heterochromatin in the *bw* locus on distal chromosome *2*R (Slatis 1955; Dernburg *et al.* 1996) (Figure 5.3A). This mutation causes dominant suppression of the *bw* gene by pairing with its homolog and causing localization near the pericentromeric heterochromatin of chromosome *2* (Henikoff and Dreesen 1989; Dreesen *et al.* 1991; Henikoff *et al.* 1995; Dernburg *et al.* 1996). We used this tool to answer two questions: First, does an insertion of heterochromatin located far from the centromere suppress crossovers in adjacent intervals? Second, does spatial proximity to pericentromeric heterochromatin within the nucleus suppress crossovers?

We first asked whether the heterochromatic insertion of bw^D causes nuclear localization of the locus near clustered pericentromeric heterochromatin in meiotic cells in the same fashion as it does in somatic cells. We used a probe for the *bw* locus and a probe for a repeat in the pericentromeric heterochromatin of chromosome *2* (AACAC), as well as a marker of meiotic cells, C(3)G, a component of the synaptonemal complex (Figure 5.3B). We then measured the distance between the two foci in meiotic cells and see that the distance between the *bw* locus and AACAC heterochromatin locus is significantly shorter in bw^D compared to WT ($p < 0.001$) (Figure 5.3C). This suggests that the heterochromatic insertion in bw^D does localize near the pericentromeric heterochromatin in meiotic cells.

We measured recombination between phenotypic markers on either side of the *bw* locus, *px* and *sp*. The *px* gene is located at 2R:22.5 Mb; *sp* is not mapped to the genome but is between *or* at 2R:24.0 Mb and *Kr* at 2R:25.2 Mb, so the distance between *px* and *sp* is between 1.5-2.7 Mb (Thurmond *et al.* 2019). If the heterochromatic insertion in bw^D leads to

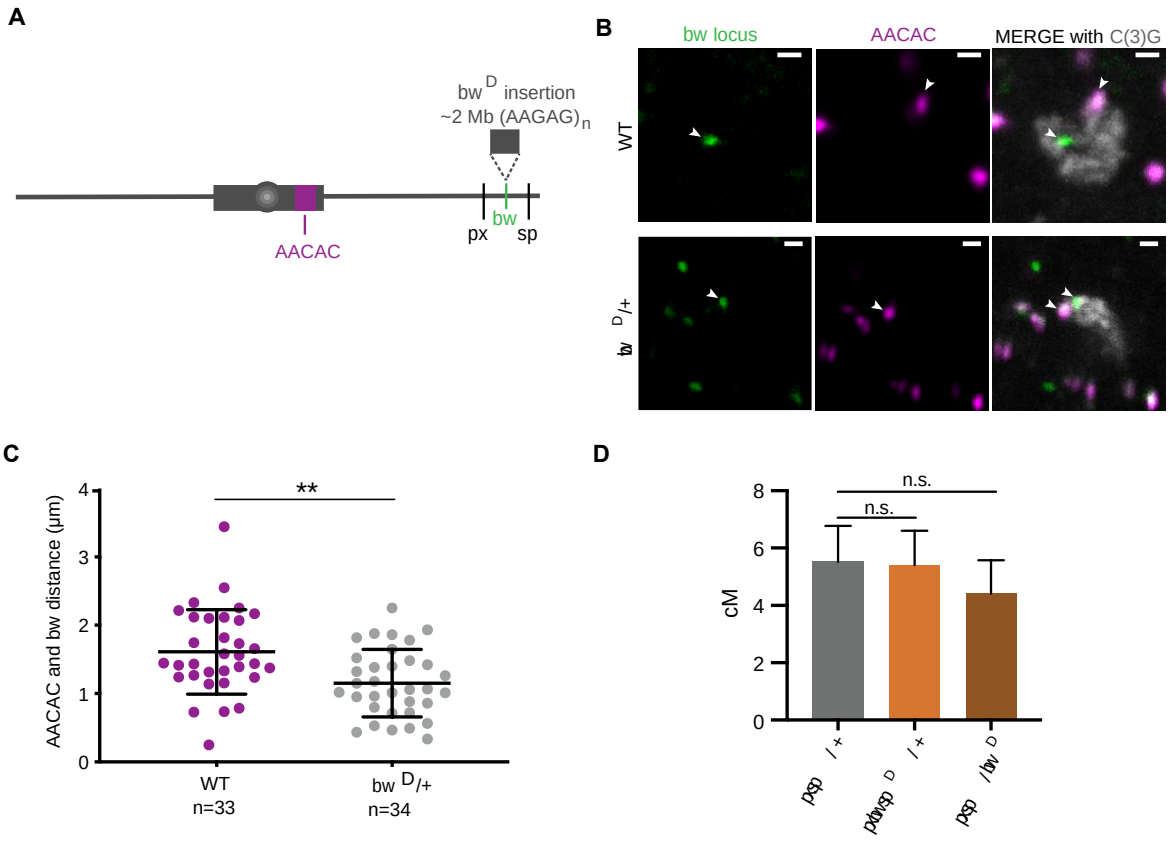

Figure 5.3. Insertion of a block of heterochromatin does not decrease crossovers. (A) Schematic of the *bw*^{D} mutation and AACAC locus used for staining. (B) Representative staining for *bw* locus (left panels), AACAC locus (middle panels), and C(3)G to identify meiotic cells (merged with foci in the right panels). White arrows point to the foci in all images. (C) Quantification of the distance between foci in WT and *bw*^{D}/+. (** $p < 0.001$). (D) Recombination between *px* and *sp* represented in cM for *px sp* / + (5.52 cM n= 1287), *px bw*^{D} *sp* / + (5.4 cM n= 1363), *px sp* / *bw*^{D} (4.4 cM n= 1197). Error bars represent 95% confidence intervals. (*px sp* / + versus *px bw*^{D} *sp* / +, n.s. $p = 0.86$) (*px sp* / + versus *px sp* / *bw*^{D}, n.s. $p=0.32$). For full data set, see Table 5.5.

suppression of crossovers in adjacent regions we would expect to see a decrease in crossovers between *px* and *sp*. We assume there are no crossovers within the heterochromatin of the *bw*^{D} mutation since we measured crossovers in *bw*^{D} heterozygous background. Surprisingly, there was not a significant difference in number of crossovers with the *bw*^{D} insertion being either *cis* or *trans* to *px* and *sp* ($p = 0.86$ and $p = 0.32$) (Figure 5.3D), suggesting that the heterochromatin insertion does not cause a decrease in crossovers in

the adjacent regions and that spatial proximity to the pericentromeric heterochromatin compartment of the nuclease does not have a strong effect on crossing over.

Genotype	Crossover	Parental	Total
px sp / +	71	1287	**1358**
px bw^D sp / +	73	1363	**1436**
px sp / bw^D	53	1197	**1250**

Table 5.5. Crossovers in WT and *bw^D*. Crossovers for WT (*px sp* / +) and *bw^D* heterozygotes (*px bw^D sp* / +) (*px sp / bw^D*). For each genotype, number of progeny with a crossover, the number of parental, and total number of flies are shown.

Examination of contributions to the centromere effect

The results with *bw^D* suggest that the centromere effect is not due solely to proximity to pericentromeric heterochromatin, so we asked whether other genomic features contribute to the centromere effect. Transposable element (TE) density and gene density have been suggested to influence crossover rates genome-wide in other organisms (Bartolome *et al.* 2001; Bartolome and Maside 2004; Kent *et al.* 2017). TEs are middle-repetitive elements found throughout the genome but are most abundant within LR-heterochromatin adjacent to euchromatin (Yamamoto *et al.* 1990; Carmena and González 1995). Conversely, genes are less abundant in the LR-heterochromatin than in the euchromatin. In *Arabidopsis thaliana* crossovers are negatively correlated with TE density and positively correlated with gene density (Giraut *et al.* 2011). Therefore, we searched for correlations between crossover distribution and distance from the centromere, TE density and gene density.

Figures 5.4A and B show TE and gene density overlaid with our SNP/indel mapping of proximal crossovers. We modeled how distance from the centromere, TE density, and gene density contribute to the variation seen in crossover distribution (Figure 5.4C). Two

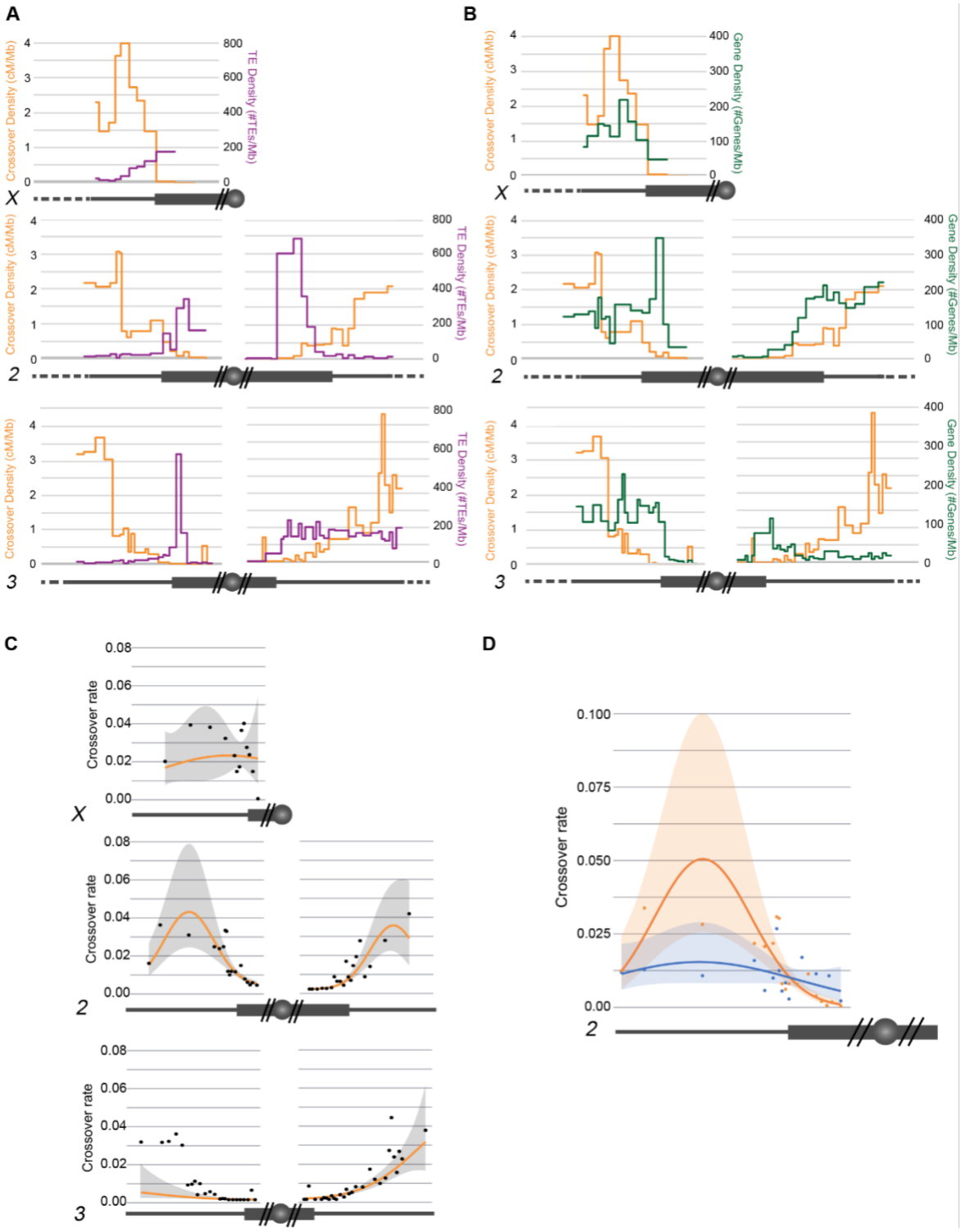

Figure 5.4. Distribution of TE and gene density. Chromosomes are depicted under each graph (*X, 2, 3*) with euchromatin (dark gray line), heterochromatin (dark gray box), unmapped heterochromatin (dark gray box with two slashes), and the centromere (dark gray circle). (A and B) Crossover distribution from SNP/indel mapping (orange) represented on left axis as cM/Mb. (A) Transposable element (TE) density (purple) plotted on right axis as

number of TEs/Mb. (B) Gene density (green) plotted on right axis as number of genes/Mb. (C) Crossover rate in relation to distance from the centromere. Observed data are plotted along with modeled marginal relationship with distance from the centromere. For the marginal predictions, gene density and transposable element density were set at their mean value across each chromosome. (D) Crossover rate in relation to distance from the centromere for chromosome *2*L for *Blm* mutant and WT. Observed data are plotted along with modeled marginal relationship with distance from the centromere. For the marginal predictions, gene density and transposable element density were set at their mean value across each chromosome. For statistical analyses, see Tables 5.6-5.9.

Chromosome	Estimate	SE	Lower 95	Upper 95
Distance from centromere				
2L	1.179	0.152	0.881	1.477
2R	1.865	0.282	1.312	2.418
3L	1.291	0.237	0.825	1.756
3R	1.38	0.152	1.082	1.677
X	0.363	0.378	-0.378	1.104
Squared distance from centromere				
2L	-0.461	0.039	-0.537	-0.386
2R	-0.412	0.131	-0.668	-0.156
3L	-0.285	0.127	-0.533	-0.036
3R	-0.292	0.115	-0.517	-0.068
X	-0.251	0.186	-0.616	0.114
Gene Density				
2L	0.005	0.025	-0.044	0.054
2R	0.768	0.158	0.459	1.077
3L	0.037	0.27	-0.492	0.565
3R	-0.313	0.141	-0.59	-0.036
X	0.316	0.155	0.012	0.619
TE Density				
2L	-0.505	0.075	-0.653	-0.357
2R	0.422	0.141	0.145	0.698
3L	-6.845	1.866	-10.501	-3.188
3R	-0.812	0.231	-1.264	-0.36
X	-0.342	0.261	-0.853	0.169

Table 5.6. Model averaged standardized effect sizes for each chromosome. Model averaged parameter estimates along with estimated standard errors and 95% confidence intervals for wild type analysis. All variables were standardized by two times their standard deviation prior to model fittings. Model averaged parameters and variance estimates were based on zero values for parameters if they were not included in model.

Chr	X	X
Dist	X	X
$Dist^2$	X	X
Gene Dens	X	X
TE Dens	X	X
Chr * Dist	X	X
Chr * $Dist^2$		X
Chr * GD	X	X
Chr * TE	X	X
df	22	26
Likelihood	-341.4	-335.2
∆ AICc	0	1.44
weight	0.673	0.327

Table 5.7. 95% confidence set for wild type chromosome analysis. Summary of models in 95% confidence set for wild type chromosome analysis. X indicates parameter was included in model. Interactions (*) indicate separate parameter estimated for each chromosome.

models were selected in the 95% confidence set (Tables 5.6 and 5.7). All predictor variables were included in this final set indicating statistically important effects of distance from the centromere, TE density and gene density that varied across chromosomes. Unless otherwise stated, all effects mentioned have 95% confidence intervals that do not overlap zero. For all chromosomes except *X*, distance from the centromere had a positive effect and a negative squared distance term. Two chromosome arms, *2R* and *X*, had positive effects of gene density; on *3R*, a negative effect was found with 95% confidence intervals just overlapping zero, suggesting a potential negative effect. In general, standardized effect sizes for gene density were lower than for distance from the centromere. For TE density all chromosomes but *X* had 95% confidence intervals that did not overlap zero. The effect was dramatically negative in *3R* with a negative standardize effect size of magnitude over three times greater than the next effect size. Other chromosomes had smaller magnitude effect size, being negative for *2L*, *3L*, and *3R*, but positive for *2R*. This modeling shows that TE and gene density do decrease the variation seen in the model; however, they do not fully

explain the model produced and there is leftover effect of distance from the centromere. These results support the idea that centromere-proximal crossover distribution is dictated not only by genomic features such as TE or gene density, but that there is some factor suppressing crossover rate that decreases with distance from the centromere.

Chromosome	Estimate	SE	Lower 95	Upper 95
Distance from centromere				
Wild Type	1.818	0.118	1.586	2.049
Mutant	0.439	0.318	-0.183	1.062
Squared distance from centromere				
Wild Type	-0.784	0.026	-0.835	-0.734
Mutant	-0.198	0.162	-0.517	0.12
TE Density				
Wild Type	-0.073	0.042	-0.155	0.009
Mutant	0.047	0.141	-0.228	0.323

Table 5.8. Modeled averaged parameters for mutant comparison. Model averaged parameter estimates along with estimated standard errors and 95% confidence intervals for 2L mutant analysis. All variables were standardized by two times their standard deviation prior to model fittings. Model averaged parameters and variance estimates were based on zero values for parameters if they were not included in model.

We applied the same modeling methods to the *Blm* mutant to understand if *Blm* mutants truly do not have a centromere effect and to what extent TE and gene density play a role in crossover distribution in *Blm* mutants (Figure 5.4D). Two models were selected in the 95% confidence set (Tables 5.8 and 5.9). There was no effect of gene density in either wild type or mutant, consistent with analysis of the wild-type chromosomes. In the wild type, all remaining modeled effects (distance, distance^2 and TE density) had 95% confidence intervals that did not overlap zero. In the mutant, no effect size had confidence intervals that didn't overlap zero, suggesting that none of them were valuable predictors of crossover rate. While we cannot prove zero effect, the best estimated effect of distance in the mutant is less than one quarter that of the wild-type (Table 5.8). These results support the hypothesis that *Blm* mutants experience a much weaker centromere effect, if any, and that the crossover

distribution in *Blm* is not demonstrably under the influence of distance from the centromere or chromosome characteristics. Importantly, these results provide more evidence that centromere-proximal crossover suppression is mediated both by the HR-heterochromatin effect and an effect whose strength varies with distance to the centromere.

Chr	X	X
Dist	X	X
$Dist^2$	X	X
TE Dens		X
Chr * Dist	X	
Chr * $Dist^2$	X	
Chr * TE		X
df	7	7
Likelihood	-106.8	-108.7
Δ AICc	0	3.85
weight	0.873	0.127

Table 5.9. 95% confidence set for 2L mutant chromosome analysis. 95% confidence set for 2L mutant chromosome analysis. X indicates variable(s) was in fit model. Interactions indicate separate parameter estimated for each chromosome.

Discussion

Two Contributions to Suppression of Proximal Crossovers

Our mapping of a large number of proximal crossovers in both wild-type flies and *Blm* mutants leads us to propose a model for centromere-proximal crossover suppression (Figure 5.5). In this model crossovers are completely suppressed in HR-heterochromatin due to the absence of DSBs. Adjacent to this region the centromere effect strongly suppresses crossovers, but that suppression dissipates with distance from the centromere until a region in the euchromatin where crossovers rise steeply to peak around the middle of each chromosome arm (orange line). In the *Blm* mutant (blue line), the HR-heterochromatin effect is still intact but the centromere effect is lost: crossover density is relatively even throughout the assembled LR-heterochromatin and euchromatin. We conclude that

pericentromeric crossover suppression is achieved by both HR-heterochromatin suppression and a centromere effect, and these two processes are separable.

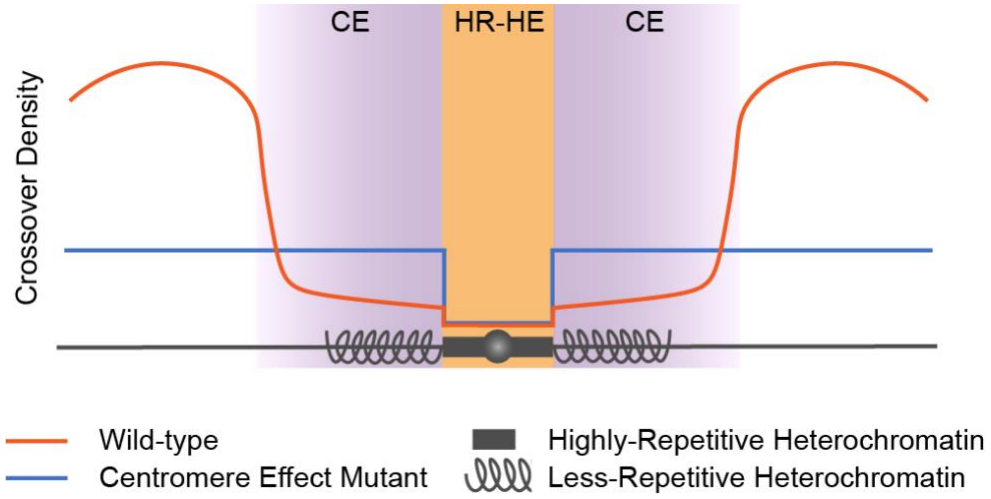

Figure 5.5. Model of the Centromere Effect and HR-Heterochromatin effect. The HR-Heterochromatin Effect (HR-HE) (orange) and Centromere Effect (CE) (purple) are both responsible for suppressing crossovers in the pericentromeric region. The HR-HE completely suppresses crossovers in the highly-repetitive heterochromatin (dark gray box), but does not have an effect outside of this region. The CE starts in the less-repetitive heterochromatin (spiral gray lines) and extends into the euchromatin of each arm (straight gray lines). Representative crossover distribution is shown for WT (orange) and a centromere effect mutant (blue).

Heterochromatin effect suppresses crossovers

Heterochromatin has long been thought to contribute to centromere-proximal suppression of crossovers, but the specifics of where this suppression occurred were unknown until now. In this study, we used a centromere effect mutant (*Blm*) that still has normal heterochromatic marks to show that the heterochromatin effect impacts the highly-repetitive heterochromatin but not the adjacent less-repetitive heterochromatin. This was a surprising result because a previous cytological study found that a marker of DSBs never colocalized with a heterochromatin marker (Mehrotra and McKim 2006). It is possible that, although DSBs do occur within less-repetitive heterochromatin, they are at a lower density

than in euchromatin (perhaps by being excluded from TE sequences) so the sample size in the previous study was insufficient to detect these relatively rare events.

We used bw^D to test whether HR-heterochromatin distant from the centromere exerts a centromere effect. The lack of an effect on crossing over between *px* and *sp* suggests that HR-heterochromatin is not sufficient to reduce crossovers in flaking regions. We could not assay the effects of homozygosity for bw^D because homozygotes were inviable, even for chromosomes with the closely-spaced markers *px* and *sp* recombined onto bw^D. Slatis (1955) conducted similar experiments and reported a decrease in crossovers in flies heterozygous and homozygous for bw^D. This may suggest that HR-heterochromatin does affect adjacent euchromatin even when distant from the centromere. However, Slatis also reported a decrease in bw^D heterozygotes, in contrast to our findings; the reasons for this difference are unknown. After the genomic location of *sp* is determined, it would informative to revisit these studies and map crossovers between *px*, bw^D, and *sp* more precisely.

Why can crossovers occur within the less-repetitive heterochromatin, but not the highly-repetitive heterochromatin? One reason could be differential access of DSB machinery to the DNA. Perhaps HR-heterochromatin is more densely packed than LR-heterochromatin and does not allow access of the DSB machinery. Additionally, there could be different heterochromatic marks or protein machinery in these regions that differentially regulate DSBs or crossover formation. Future studies could be aimed at determining functional differences between LR- and HR-heterochromatin.

In the centromere effect mutant, *Blm*, we show that crossovers do not occur within the highly-repetitive heterochromatin, but they do occur outside of that boundary at a higher frequency than wildtype crossovers. This suggests that DSBs are still occurring within the less-repetitive heterochromatin at a rate similar to the euchromatin, but that in wildtype, they are more frequently being converted to noncrossovers instead of crossovers. However,

Westphal and Reuter reported an increase in centromere-proximal crossovers in *Su(var)* mutants, which presumably cause heterochromatin to assume a more open structure (Westphal and Reuter 2002). This result suggests that the closed structure of heterochromatin can suppress crossovers, but that is in opposition to the result we see with the centromere effect mutant that still has normal heterochromatic marks, but allows more crossovers within the heterochromatic region. There are two possible explanations that could explain these opposing results. The first is that the *Blm* mutation is altering heterochromatin structure in a way that we did not detect cytologically. In this case, it would be interesting to look at distribution of heterochromatin marks in meiotic cells of the mutant, but this is currently not feasible because we do not have a way of isolating meiotic cells for studies such as ChIP analysis of heterochromatic marks. Additionally, in the *Su(var)* mutants, perhaps the opening of heterochromatin in both the less- and highly-repetitive heterochromatin allows crossovers to occur within the highly-repetitive heterochromatin. This could show us separation of the centromere effect and HR-heterochromatin effect by retaining the centromere effect but disrupting the HR-heterochromatin effect. It would be informative to conduct our SNP/indel mapping on crossovers in a *Su(var)* mutant.

Blm mutants also experience crossovers on chromosome *4,* which normally never has crossovers (Hatkevich *et al.* 2017). We hypothesized that chromosome *4* does not have crossovers because of a very strong centromere effect, which is lost in *Blm* mutants (Hartmann and Sekelsky 2017); the results reported here support this hypothesis. It would be interesting to finely map crossovers on chromosome *4* in *Blm* mutants to determine if there is a flat distribution and see if there is a separable HR-heterochromatin effect on this chromosome as well (this would require a marker to the left of the centromere).

Recombination and genomic features

The relationship between gene density, TE density, and recombination rate has been a long-standing discussion (reviewed in Kent *et al.* 2017). It is difficult to parse out these relationships because there are many factors influencing distribution of TEs, genes, and crossovers. It has been argued that the distribution of TEs and genes is in part dictated by recombination. For example, higher recombination could be favored in regions of high gene density to promote greater genetic diversity within populations. Conversely, lower recombination rates in regions of high TE density could help to prevent ectopic recombination between similar TE sequences in different genomic locations. The high density of TEs in proximal or heterochromatic regions could actually result from the low recombination rate preventing removal of TEs (Bartolome and Maside 2004). Recombination might also be directly silenced within TE sequences. Miller *et al.* (Miller *et al.* 2016) reported that crossovers can occur within TEs, but less frequently than would be expected. It has been suggested that active silencing of TEs could lead to the silencing or suppression of recombination around those regions (Kent *et al.* 2017). Therefore, it is difficult to determine whether or how TE density and gene density affect recombination rates. Our data support results seen previously in that TE density is increased in areas of low recombination and gene density is increased in areas of high recombination. When we factor these variables into models of crossover distribution, we see a strong impact of TE density on crossover rate. One caveat of our studies is that transposable elements have been shown to vary between different strains of *Drosophila* and we have based these analyses off the transposable element distribution within the *Drosophila melanogaster* reference sequence (Ananiev *et al.* 1984; Rahman *et al.* 2015). With advances in long-read sequencing technology, it might be possible in the future to do studies similar to ours but in strains in which LR-heterochromatin has been assembled *de novo*.

Conclusion

In conclusion, we find that centromere-proximal crossover suppression is a result of two separable mechanisms: an HR-heterochromatin effect that suppresses crossovers in highly-repetitive pericentromeric heterochromatin, and the centromere effect that suppresses proximal crossovers in a manner that dissipates with increasing distance from the centromere. The HR-heterochromatin effect is likely due to the absence of DSBs with satellite sequences, presumably a direct consequence of chromatin structure. In contrast, the mechanism of the centromere effect is unknown. This work is the first in-depth examination of the centromere effect since it was first described, and these findings provide the groundwork for future mechanistic studies of the centromere effect.

CHAPTER 6: DISCUSSION AND FUTURE DIRECTIONS

In the research detailed throughout this dissertation, I attempt to gain insights into proteins involved in meiotic crossover pathways and the mechanisms that govern crossover patterning. This research has helped us better define the meiotic crossover pathways and where proteins act in these pathways, and has also led to a clearer understanding of crossover patterning. Our work on the centromere effect was some of the first work that has helped understand the centromere effect since it was first described in 1932. Even though we did not elucidate the exact mechanisms behind the centromere effect, the fact that we discovered that centromere-proximal crossovers are suppressed by two separable mechanisms is novel and important in setting the stage for further mechanistic studies. Our results are important in the field of heterochromatin because they suggest that there are environments that have been characterized as heterochromatic, but can actually behave differently from each other. Modeling of crossover patterning is an important field, and our research helped form models of crossover patterning that can be useful to a wide variety of organisms.

Highlighted Findings

Through this research I have gained insights into the factors involved in the formation and patterning of meiotic crossovers. I began this work with the hypothesis that Ankle1 was an endonuclease involved in the formation of meiotic crossovers. I determined that *Ankle1* mutants have no defects in viability, fertility, nondisjunction, and no sensitivity to DNA damaging agents. Ankle1's meiotic role may be redundant so mutant phenotypes are not

detected in this mutant. However, I did detect that Ankle1 may play a role in creating mitotic crossovers in the presence of DNA stress. I also saw an interaction of Ankle1 with both MEI-9 and MUS-312. From these data, I conclude that Ankle1 plays a role in creating mitotic crossovers in the presence of DNA stress, and that we cannot rule out a meiotic role for Ankle1.

I continued my research on proteins involved in forming meiotic crossovers by studying the mei-MCM complex, which includes REC, MEI-217, and MEI-218. By examining the role of REC in both class I and class II crossovers, we discovered that REC plays different roles in these pathways and could possibly form two different complexes. REC contains Walker A and Walker B motifs to hydrolyze ATP and we used mutations of these motifs to determine if these are critical for REC's function in class I and class II pathways. We found that REC's Walker A motif is dispensable for crossover formation in the class I pathway, but that REC's Walker B motif is necessary.

REC was also predicted to have a role in preventing Class II crossovers because *Blm rec* double mutants experience more crossovers than *Blm* single mutants. We asked whether the Walker A and B motifs are needed for the anti-crossover activity of REC in the class II pathway. Interestingly, both the Walker A and B motifs are necessary for REC's anti-crossover function in the class II pathway. Therefore, the mei-MCM complex helps to establish meiotic crossover patterning and REC's roles are to help establish class I crossovers and prevent class II crossovers.

Following the examination of proteins involved in meiotic crossovers, my main project focused on uncovering the mechanism behind the crossover patterning phenomenon, the centromere effect. The centromere effect has classically been defined as the suppression of crossovers near the centromere, but my work has changed and clarified how centromere-proximal crossovers are suppressed. I discovered that centromere-proximal

crossover suppression is actually a result of two separable mechanisms by mapping crossovers in both wild-type and *Blm* mutants. Centromere-proximal crossovers are suppressed by both highly-repetitive heterochromatin and the centromere effect. I hypothesize that highly-repetitive heterochromatin is inaccessible to DNA double strand break proteins and that the centromere effect is a protein-mediated meiotic mechanism, but more work is needed to elucidate the true mechanisms behind these two factors of crossover suppression.

Future Directions

Ankle1

I hypothesized that Ankle1 was an endonuclease involved in creating meiotic crossovers in a complex with MUS312 and MEI-9. Even though I was able to show through yeast two-hybrid that Ankle1 interacted with MUS312 and MEI-9, we did not observe a meiotic crossover defect in this mutant. I also did not observe sensitivities to DNA damaging agents in this mutant. However, there is still the possibility that Ankle1 plays some role in the mitotic crossover pathway due to the result we observe with *Fancm* mutants. As previously discussed, we see that crossovers in *Ankle1; Fancm* double mutants are decreased, similar to *Fancm mus312* double mutants. Therefore, it appears that Ankle1 may play a role in mitotic crossovers and may interact with MUS312 in this role. This role and other possible roles of Ankle1 could be explored by biochemical analyses.

Ankle1 possesses a GIY-YIG nuclease domain, so it would be informative to test Ankle1's biochemical activity on different types of substrates. This could be accomplished by expressing Ankle1 in the Baculovirus Expression system, purifying the protein, and then performing nuclease assays. Nuclease activity with different types of substrates including Holliday junctions, replication forks, 5' and 3' flaps could be examined. Additionally, Ankle1 could be expressed with MUS312 alone and also MUS312 with MEI-9 to determine if a

stable complex can be formed and purified when two or all three components are expressed together. Then these complexes could also be tested with nuclease assays to determine if the proteins function together to perform nuclease activity.

Another informative study could be an immunoprecipitation of Ankle1 and detect MUS312 and MEI-9 with antibodies as well as do mass-spec to identify any other proteins that might be interacting with Ankle1. This could also be informative because other interacting proteins could give insights into other functions of Ankle1.

mei-MCM

There are many future studies that could impact the study of mei-MCMs in crossover patterning. The first and possibly most difficult would be to obtain the mei-MCM complex in soluble form after expressing these proteins, which has been attempted by our lab with no success. In Hartmann *et al.* (2019), we suggest that there is another component to this complex yet to be identified. Perhaps this missing component is necessary to render the complex stable enough to be expressed together. Therefore, identifying that factor and expressing it along with the other units of the mei-MCM complex would be a very important experiment. Being able to express this factor would give us important insights into the biochemical function of the complex as well as give a platform to examine mutations. Mutations in the REC Walker A and B motifs were made and analyzed in Hartmann *et al.* (2019), however, it is unknown if Walker A and B function have ATP binding and hydrolysis activity as in other proteins or even if these mutations actually abolish the ATP binding and hydrolysis activity of REC as predicted. Being able to experimentally prove that these mutations affect ATP binding and hydrolysis would be support for the conclusions that we draw from the genetic data.

In *Blm rec* double mutants, crossovers are increased compared to *Blm* single mutants, suggesting that REC plays a role in inhibiting Class II crossovers (Kohl *et al.* 2012).

To test whether REC's Walker A and Walker B functions are needed for this role, we examined REC Walker A and B mutations in a *Blm* mutant background (Hartmann *et al.* 2019). We observed that both the Walker A and B motifs are necessary for the anti-crossover function of REC in the class II pathway. It is possible that REC forms a different complex to regulate Class II pathways and future analysis of REC complexes in *Blm* mutants could give important insight into proteins involved in Class II crossover and noncrossover formation. Also testing whether MEI-218 functions similarly to REC in the Class II pathway would give us some insight into whether this complex is similar to the Class I complex. Measuring crossovers in a *mei-218; Blm* double mutant would allow us to determine if *mei-218* also affects crossovers in the Class II pathway.

We made an interesting observation that MEI-218 is expressed moderately highly in male testes (Thurmond *et al.* 2019; Hartmann *et al.* 2019). This is unexpected because males do not experience meiotic recombination, and *mei-218* mutant males are viable, fertile, and do not experience nondisjunction. We hypothesize that there is an unknown function, possibly non-meiotic role, of MEI-218 in males. It would be a difficult, yet interesting study to follow up on the function of MEI-218 in males.

Centromere-proximal crossovers

The *Blm* mutant allowed us to observe a separation of the highly-repetitive (HR-) heterochromatin effect and the centromere effect by eliminating the centromere effect and maintaining the HR-heterochromatin effect. Studying a mutant that instead decreases the HR-heterochromatin effect while presumably maintaining the centromere effect could be very informative. I propose that suppressors of variegation *Su(var)* mutants may be such mutants. *Su(var)* mutants are dominant suppressors of variegation and are predicted to open up heterochromatin structure and have been shown to have an increase in crossovers between centromere-proximal crossovers (Westphal and Reuter 2002). However, finely

mapping crossovers in these mutants would be informative because if the HR-heterochromatin effect is a result of tightly packed heterochromatin not being accessible to DSB machinery, we would expect to see an increase in crossovers in this HR-heterochromatin region instead of just the surrounding regions, like we see in the *Blm* mutant. The distribution of the crossovers could also be examined computationally to determine if the crossovers have a flat distribution or still increase in frequency with distance from the centromere. In the *Blm* mutant, which does not have a centromere effect, crossovers increase outside of the HR-heterochromatin boundary, but have a flat distribution throughout the remainder of the chromosome arm. In a *Su(var)* mutant, if crossovers increase dramatically and have a near flat distribution, this would indicate that the centromere effect is indeed partially due to heterochromatin structure. However, if crossovers were increased but still had an increasing frequency with distance from the centromere, that would suggest that the centromere effect has a role outside of chromatin compaction, but that even compaction of less-repetitive (LR-) heterochromatin still plays a role in crossover suppression outside of the HR-heterochromatin effect. Finally, there is the possibility that crossovers do not change at all in the LR-heterochromatin region and only are increased in the HR-heterochromatin region. This result would suggest that the centromere effect is completely separate from chromatin compaction and that LR-heterochromatin is not compacted enough to inhibit DSB machinery from accessing the DNA. Being able to distinguish whether the centromere effect is completely separate from or is still subject to chromatin compaction would provide very important insight into the mechanism of the centromere effect.

One of the caveats to the fine mapping I performed in our isogenized strains is that we assembled those sequences to the reference genome and therefore do not know the precise locations of transposable elements (TEs) in our stocks because those sequences

will automatically assemble to where they are in the reference genome. Miller *et al.* (2016) show that crossovers occur less frequently in transposable elements than would be expected. For more accurate interval measurements and crossover density calculations, TEs should be mapped precisely in our isogenized strains. For this to occur, a *de novo* assembly must be performed. We have begun experiments to perform long-read sequencing on our isogenized strains in order to perform this *de novo* alignment and be able to assemble these middle-repetitive regions. The sequencing platform we are using is the nanopore sequencing method. Knowing precise locations of transposable elements and crossovers will help us better understand the relationship between the two.

Current genome sequences do not have complete assembly of heterochromatic sequences because it is too repetitive. There are methods being developed to help assemble these sequences (Chang and Larracuente 2019). Having a clearer idea of how much heterochromatin is contained on each chromosome arm would be a valuable addition to my studies of centromere-proximal crossovers. It is known that heterochromatin amount varies per chromosome arm and the amount of heterochromatin has been estimated from cytological studies (Yamamoto *et al.* 1990). Knowing the precise amount of heterochromatin and comparing that with crossover distribution on each chromosome arm could be interesting to see if there is any correlation between amount of heterochromatin and crossover distribution.

Being able to sequence heterochromatin would also be informative for the studies of crossovers using the bw^D mutation. The bw^D mutation has been reported to consist of heterochromatin from polytene staining (Dernburg *et al.* 1996), however the precise amount of heterochromatin is unknown. Being able to sequence through this region and around it in bw^D would allow us to finely map crossovers around this region. Finely mapping crossovers here will show us what crossover distribution looks like around the locus instead of only

being able to quantify crossovers between two markers on either side. This will allow us to see if crossover density decreases around the heterochromatin insertion or stays at the same level throughout the interval. Additionally, it would allow us to determine if crossovers occur within the heterochromatic region in homozygous bw^D. We were unable to obtain homozygotes from our stock, but Dernburg *et al.* (1996) were able to obtain homozygous flies, so we could try a different stock. Being able to precisely map crossovers around a heterochromatic insertion would give us a better idea of how heterochromatin affects crossover rate in adjacent intervals.

It was striking that we found that heterochromatin behaves differently apparently based on how repetitive it is. Highly-repetitive heterochromatin appears to completely suppress crossovers presumably by not allowing double-strand breaks to occur in those regions. However, less-repetitive heterochromatin allows crossovers at a low frequency. It has been shown that heterochromatin domains form via phase separation (Strom *et al.* 2017). These studies were done in *Drosophila* embryos, so it would be interesting to examine liquid properties of heterochromatin domains in meiotic cells. In *Drosophila,* the centromeres of meiotic chromosomes cluster together in one or two foci, which is termed centromere clustering (Carpenter 1975). Therefore, it is highly likely that phase separation occurs within heterochromatin of meiotic cells, and this could be an interesting phenomenon to explore further. Heterochromatin likely forms via phase separation because heterochromatin protein 1 (HP1) contains intrinsically disordered regions in its N-terminal tail, which are characteristic of proteins that undergo liquid-liquid de-mixing (Strom *et al.* 2017). Perhaps the phase separation is what is creating these two types of heterochromatin- the type that does not experience crossovers and the type that can experience crossovers. For instance, if HP1 deposition differs between these two types of heterochromatin, it would cause a different environment around highly-repetitive (HR-) heterochromatin than around

less-repetitive (LR-) heterochromatin. To test this, HP1 ChIP-seq data could be examined around these regions and compared to the crossover density distributions.

An interesting experiment to test the difference between chromatin compaction and DNA sequence with regards to crossover density would be to artificially create heterochromatin in non-repetitive DNA sequences that are not adjacent to the centromere. It was shown in *Drosophila* that recruiting HP1 to open chromatin using the LacI-LacO tethering system caused open chromatin to adopt a more closed chromatin structure (Danzer and Wallrath 2004). This system could be used to form heterochromatin domains within non-repetitive sequences and then map crossovers around this region. This would be similar to the bw^D experiment, however, it would allow us to see if crossovers can occur within a heterochromatinized state that has normal sequence rather than highly-repetitive sequence. This would allow us to better understand if heterochromatic suppression of crossovers is due to compaction of chromatin or the highly-repetitive nature of the sequence.

Besides heterochromatic suppression of crossovers, I also found that the centromere effect is a second mechanism that suppresses crossovers with a suppressive effect that dissipates with distance from the centromere. We determined that the centromere effect was not only a result of genomic features such as TE density or gene density dictating crossover density, but that there is some other factor that changes with distance from the centromere, which is what we call the centromere effect. As of now, we do not understand the mechanism of the centromere effect, and this could be of interest for further study. We find that the *Blm* mutant does not have a centromere effect, which leads us to hypothesize that the centromere effect is mediated by proteins in the crossover pathway. Interestingly, the centromere effect seems to be separable from the other crossover patterning mechanisms interference and assurance. It was shown that in *Drosophila,* mutations in *mei-41*, the

ortholog of the checkpoint kinase ATR, show a centromere effect, but not interference and assurance (Brady *et al.* 2018). This result suggests that meiotic patterning processes are regulated at different times and that the centromere effect may be the first crossover patterning mechanism to be established. Interestingly, *Blm* mutants have severely altered meiotic progression as visualized in *Drosophila* germaria (unpublished data, Figure 6.1). Figure 6.1A shows the progression of meiosis in a *Drosophila* germarium. C(3)G, a component of the synaptonemal complex (SC), builds between homologous chromosomes of meiotic cells, and then disappears from all cells except the one designated oocyte. SC formation is severely delayed in *Blm* mutants and where wild-type normally has one designated oocyte by the end of the germarium, *Blm* mutants will often have multiple cells that have maintained SC by that point (Figure 6.1B). This suggests that meiotic timing is

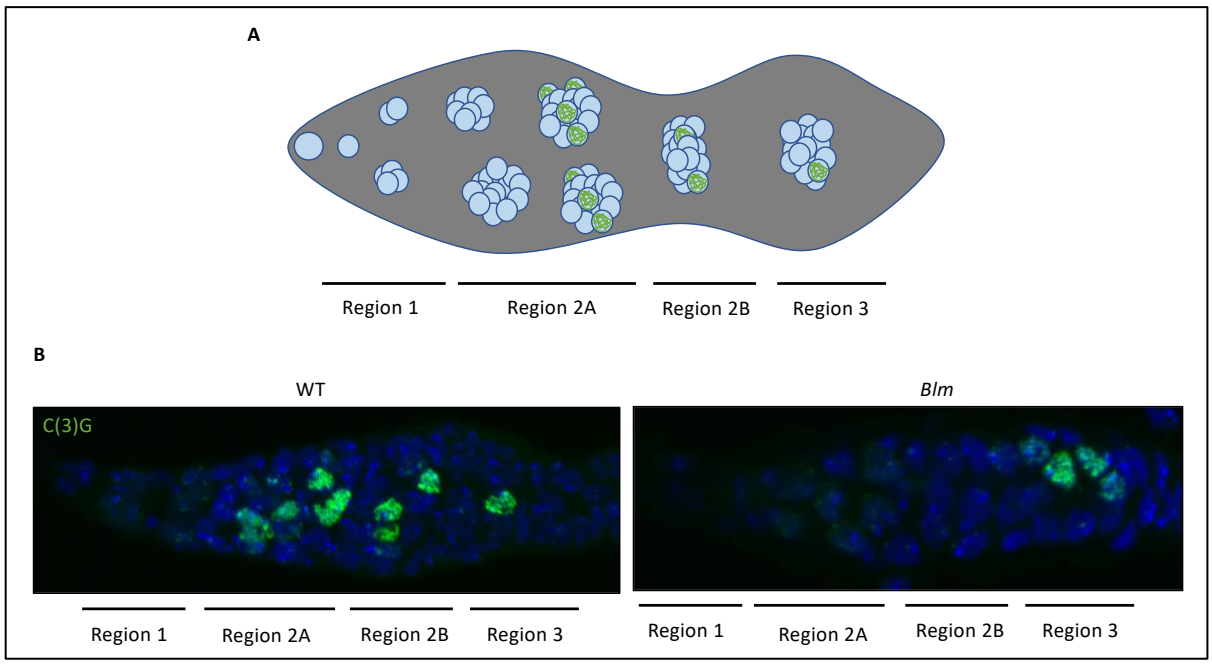

Figure 6.1. Meiotic progression in *Blm* mutants. (A) Schematic of meiotic progression in a *Drosophila* germarium. Blue circles are cells with the germline stem cell on the far left, which undergoes mitotic divisions until forming a 16 cell cyst. C(3)G (green) begins to form between homologous chromosomes of meiotic cells until one oocyte persists at the end of the germarium and meiotic recombination. (B) Staining for DNA (blue) and C(3)G (green) in wild-type and *Blm* mutants.

disrupted in *Blm* mutants and could be one of the factors leading to mis-regulation of crossover patterning mechanisms including the centromere effect.

My study of the mechanism of centromere-proximal crossover suppression lead to the discovery that it is a result of two separable mechanisms: complete suppression of crossovers by highly-repetitive heterochromatin and the centromere effect. This is an exciting and important discovery, however, it opens up many more questions to be answered about crossover regulation. Mainly, what are the mechanisms behind these two effects of crossover suppression? Does highly-repetitive heterochromatin completely suppress crossovers because of its repetitive nature, or its closed chromatin nature? Can DSBs even form within highly-repetitive heterochromatin? We predict that the centromere effect is a protein-mediated mechanism, but what meiotic proteins are involved and how are they regulated? Understanding centromere-proximal crossover suppression is important to the meiosis field because aneuploid diseases and miscarriages are correlated with an increase in crossovers near the centromere. Therefore, understanding how crossover distribution is regulated will aid the field in understanding how mistakes occur leading to nondisjunction and could even provide insights into how to prevent these mistakes. Additionally, crossover distribution is of particular interest to the evolutionary fields because understanding where crossovers are likely to occur within a genome can give important insight into how genomes evolve over time and why they are structured in particular ways.

REFERENCES

Adams M. D., S. E. Celniker, R. A. Holt, C. A. Evans, D. Jeannine, *et al.*, 2000 The Genome Sequence of Drosophila melanogaster. Science (80-.). 287: 2185–2194.

Adams M. D., M. McVey, and J. J. Sekelsky, 2003 Drosophila BLM in double-strand break repair by synthesis-dependent strand annealing. Science (80-.). 299: 265–267. https://doi.org/10.1126/science.1077198

Allers T., and M. Lichten, 2001 Differential timing and control of noncrossover and crossover recombination during meiosis. Cell. https://doi.org/10.1016/S0092-8674(01)00416-0

Ananiev E. V., V. E. Barsky, Y. V. Ilyin, and M. V. Ryzic, 1984 The arrangement of transposable elements in the polytene chromosomes of Drosophila melanogaster. Chromosoma 90: 366–377. https://doi.org/10.1007/BF00294163

Andersen S. L., D. T. Bergstralh, K. P. Kohl, J. R. LaRocque, C. B. Moore, *et al.*, 2009 Drosophila MUS312 and the Vertebrate Ortholog BTBD12 Interact with DNA Structure-Specific Endonucleases in DNA Repair and Recombination. Mol. Cell 35: 128–135. https://doi.org/10.1016/j.molcel.2009.06.019

Andersen S. L., H. K. Kuo, D. Savukoski, M. H. Brodsky, and J. Sekelsky, 2011 Three structure-selective endonucleases are essential in the absence of BLM helicase in Drosophila. PLoS Genet. 7. https://doi.org/10.1371/journal.pgen.1002315

Anderson L. K., S. M. Royer, S. L. Page, K. S. McKim, A. Lai, *et al.*, 2005 Juxtaposition of C(2)M and the transverse filament protein C(3)G within the central region of Drosophila synaptonemal complex. Proc. Natl. Acad. Sci. 102: 4482–4487. https://doi.org/10.1073/pnas.0500172102

Argueso J. L., J. Wanat, Z. Gemici, and E. Alani, 2004 Competing crossover pathways act during meiosis in Saccharomyces cerevisiae. Genetics. https://doi.org/10.1534/genetics.104.032912

Ashburner M., 1980 Some aspects of the structure and function of the polytene chromosomes of the Diptera. Insect Cytogenet. 10: 65–84.

Baker B. S., and A. T. Carpenter, 1972 Genetic analysis of sex chromosomal meiotic mutants in Drosophilia melanogaster. Genetics.

Baker B. S., A. T. C. Carpenter, and P. Ripoll, 1978 The utilization during mitotic cell division

of loci controlling meiotic recombination and disjunction in Drosophila melanogaster. Genetics 90: 531–578.

Bartolome C., X. Maside, and B. Charlesworth, 2001 On the Abundance and Distribution of Transposable Elements in the Genome of Drosophila melanogaster. Mol. Biol. Evol. 19: 926–937.

Bartolome C., and X. Maside, 2004 The lack of recombination drives the fixation of transposable elements on the fourth chromosome of Drosophila melanogaster. Genet Res 83: 91–100. https://doi.org/10.1017/S0016672304006755

Barton K., 2019 MuMIn: Multi-Model Inference

Beadle G. W., 1932 A possible influence of the spindle fibre on crossing-over in Drosophila. Genetics 18: 160–165.

Bell S. D., and M. R. Botchan, 2013 The minichromosome maintenance replicative helicase. Cold Spring Harb. Perspect. Biol. https://doi.org/10.1101/cshperspect.a012807

Berchowitz L. E., K. E. Francis, A. L. Bey, and G. P. Copenhaver, 2007 The role of AtMUS81 in interference-insensitive crossovers in A. thaliana. PLoS Genet. https://doi.org/10.1371/journal.pgen.0030132

Berchowitz L. E., and G. P. Copenhaver, 2010 Genetic interference: don't stand so close to me. Curr. Genomics 11: 91–102. https://doi.org/10.2174/138920210790886835

Blanton H. L., S. J. Radford, S. McMahan, H. M. Kearney, J. G. Ibrahim, *et al.*, 2005 REC, drosophila MCM8, drives formation of meiotic crossovers. PLoS Genet. 1: 343–354. https://doi.org/10.1371/jourral.pgen.0010040

Bochman M. L., S. P. Bell, and A. Schwacha, 2008 Subunit Organization of Mcm2-7 and the Unequal Role of Active Sites in ATP Hydrolysis and Viability. Mol. Cell. Biol. https://doi.org/10.1128/MCB.00161-08

Boddy M. N., P. H. L. Gaillard, W. H. McDonald, P. Shanahan, J. R. Yates, *et al.*, 2001 Mus81-Eme1 are essential components of a Holliday junction resolvase. Cell. https://doi.org/10.1016/S0092-8674(01)00536-0

Bolen H., 1931 A mutual translocation involving the fourth and the X-chromosomes of drosophila. Amer Natur 65: 417–422.

Brachner a., J. Braun, M. Ghodgaonkar, D. Castor, L. Zlopasa, *et al.*, 2012 The endonuclease Ankle1 requires its LEM and GIY-YIG motifs for DNA cleavage in vivo. J. Cell Sci. 125: 1048–1057. https://doi.org/10.1242/jcs.098392

Brady M. M., S. McMahan, and J. Sekelsky, 2018 Loss of drosophila Mei-41/ATR alters meiotic crossover patterning. Genetics 208: 579–588. https://doi.org/10.1534/genetics.117.300634

Brand C. L., M. V. Cattani, S. B. Kingan, E. L. Landeen, and D. C. Presgraves, 2018 Molecular Evolution at a Meiosis Gene Mediates Species Differences in the Rate and Patterning of Recombination. Curr. Biol. 28: 1289-1295.e4. https://doi.org/10.1016/j.cub.2018.02.056

Braun J., A. Meixner, A. Brachner, and R. Foisner, 2016 The GIY-YIG Type Endonuclease Ankyrin Repeat and LEM Domain-Containing Protein 1 (ANKLE1) Is Dispensable for Mouse Hematopoiesis. PLoS One 11: e0152278. https://doi.org/10.1371/journal.pone.0152278

Buonomo S. B., R. K. Clyne, J. Fuchs, J. Loidl, F. Uhlmann, *et al.*, 2000 Disjunction of Homologous Chromosomes in Meiosis I Depends on Proteolytic Cleavage of the Meiotic Cohesin Rec8 by Separin combination (or cross over) of the DNA strands and axes of homologous chromatids. Another is the monoorienta-tion of sister kinetocho. Cell 103: 387–398.

Burnham K. P., D. R. Anderson, and K. P. Huyvaert, 2011 AIC model selection and multimodel inference in behavioral ecology: Some background, observations, and comparisons. Behav. Ecol. Sociobiol. 65: 23–35. https://doi.org/10.1007/s00265-010-1029-6

Bushnell B., 2014 BBMap

Carmena M., and C. González, 1995 Transposable elements map in a conserved pattern of distribution extending from beta-heterochromatin to centromeres in Drosophila melanogaster. Chromosoma 103: 676–684. https://doi.org/10.1007/BF00344228

Carpenter A. T. C., 1975 Electron Microscopy of Meiosis in Drosophila melanogaster Females I. Structure, Arrangement, and Temporal Change of the Synaptonemal Complex in Wild-type. 51: 157–182.

Castor D., N. Nair, A. C. Déclais, C. Lachaud, R. Toth, *et al.*, 2013 Cooperative control of holliday junction resolution and DNA Repair by the SLX1 and MUS81-EME1 nucleases. Mol. Cell 52: 221–233. https://doi.org/10.1016/j.molcel.2013.08.036

Chang C., and A. M. Larracuente, 2019 Heterochromatin-Enriched Assemblies Reveal the Sequence and Organization of the Drosophila. Genetics 211: 333–348.

Charles D. R., 1938 The spatial distribution of cross-overs in X-chromosome tetrads of Drosophila Melanogaster. J. Genet. https://doi.org/10.1007/BF02982376

Chino M., 1929 Genetic studies on the japanese stock of Drosophila virilis. Jpn J Genet 4: 117–131.

Chino M., and H. Kikkawa, 1932 Mutants and crossing over in the dot-like chromosome of Drosophila virilis. Genetics 18: 111–116.

Collins K. A., J. G. Callicoat, C. M. Lake, C. M. McClurken, K. P. Kohl, *et al.*, 2012 A Germline Clone Screen on the X Chromosome Reveals Novel Meiotic Mutants in Drosophila melanogaster. Genes|Genomes|Genetics. https://doi.org/10.1534/g3.112.003723

Comeron J. M., R. Ratnappan, and S. Bailin, 2012 The Many Landscapes of Recombination in Drosophila melanogaster. PLoS Genet. 8: 33–35. https://doi.org/10.1371/journal.pgen.1002905

Copenhaver G. P., E. A. Housworth, and F. W. Stahl, 2002 Crossover interference in arabidopsis. Genetics.

Coulon S., P. L. Gaillard, C. Chahwan, W. H. Mcdonald, J. R. Y. Iii, *et al.*, 2004 Slx1-Slx4 Are Subunits of a Structure-specific Endonuclease That Maintains Ribosomal DNA in. 15: 71–80. https://doi.org/10.1091/mbc.E03

Danecek P., A. Auton, G. Abecasis, C. A. Albers, E. Banks, *et al.*, 2011 The variant call format and VCFtools. Bioinformatics 27: 2156–2158. https://doi.org/10.1093/bioinformatics/btr330

Danzer J. R., and L. L. Wallrath, 2004 Mechanisms of HP1-mediated gene silencing in Drosophila. 3571–3580. https://doi.org/10.1242/dev.01223

Darlington C. D., and S. O. S. Dark, 1932 The Origin and Behaviour of Chiasmata, II Stenobothrus parallelus. Cytologia (Tokyo). 169–185.

Dernburg A. F., K. W. Broman, J. C. Fung, W. F. Marshall, J. Philips, *et al.*, 1996 Perturbation of nuclear architecture by long-distance chromosome interactions. Cell 85: 745–759. https://doi.org/10.1016/S0092-8674(00)81240-4

Dittrich C. M., K. Kratz, A. Sendoel, Y. Gruenbaum, J. Jiricny, *et al.*, 2012 Lem-3 - a lem domain containing nuclease involved in the dna damage response in c. elegans. PLoS One 7. https://doi.org/10.1371/journal.pone.0024555

Dolgin E., and B. Charlesworth, 2008 The effects of recombination rate on the distribution and abundance of transposable elements. Genetics 178: 2169–2177.

Dreesen T. D., S. Henikoff, and K. Loughney, 1991 A pairing-sensitive element that mediates trans-inactivation is associated with the Drosophila brown gene. Genes Dev. 5: 331–340.

Duffy J. B., 2002 GAL4 system indrosophila: A fly geneticist's swiss army knife. genesis. https://doi.org/10.1002/gene.10150

Dunin-Horkawicz S., M. Feder, and J. M. Bujnicki, 2006 Phylogenomic analysis of the GIY-YIG nuclease superfamily. BMC Genomics 7: 98. https://doi.org/10.1186/1471-2164-7-98

Fedorova S. A., S. Nokkala, and L. V. Omel'yanchuk, 2001 Genetic Screening for Meiotic Mutations of the Female Germline Mosaic Clones in Drosophila melanogaster. Russ. J. Genet. https://doi.org/10.1023/A:1013287611004

Fekairi S., S. Scaglione, C. Chahwan, E. R. Taylor, A. Tissier, *et al.*, 2009 Human SLX4 Is a Holliday Junction Resolvase Subunit that Binds Multiple DNA Repair/Recombination Endonucleases. Cell 138: 78–89. https://doi.org/10.1016/j.cell.2009.06.029

Filion G. J., J. G. van Bemmel, U. Braunschweig, W. Talhout, J. Kind, *et al.*, 2010 Systematic Protein Location Mapping Reveals Five Principal Chromatin Types in Drosophila Cells. Cell 143: 212–224. https://doi.org/10.1016/j.cell.2010.09.009

Forsburg S. L., 2004 Eukaryotic MCM Proteins: Beyond Replication Initiation. Microbiol. Mol. Biol. Rev. https://doi.org/10.1128/mmbr.68.1.109-131.2004

Gaillard P. H. L., E. Noguchi, P. Shanahan, and P. Russell, 2003 The endogenous Mus81-Eme1 complex resolves Holliday junctions by a nick and counternick mechanism. Mol. Cell 12: 747–759. https://doi.org/10.1016/S1097-2765(03)00342-3

Gall J. G., 1973 Repetitive DNA in Drosophila. Mol. Cytogenet. 59–60.

Gaskell L. J., F. Osman, R. J. C. Gilbert, and M. C. Whitby, 2007 Mus81 cleavage of Holliday junctions: A failsafe for processing meiotic recombination intermediates?

EMBO J. 26: 1891–1901. https://doi.org/10.1038/sj.emboj.7601645

Giraut L., M. Falque, J. Drouaud, L. Pereira, O. C. Martin, *et al.*, 2011 Genome-wide crossover distribution in Arabidopsis thaliana meiosis reveals sex-specific patterns along chromosomes. PLoS Genet. 7. https://doi.org/10.1371/journal.pgen.1002354

Gramates L., S. Marygold, G. Santos, J. Urbano, G. Antonazzo, *et al.*, 2017 FlyBase at 25: looking to the future. Nucleic Acids Res. 45: D663–D671.

Gratz S. J., A. M. Cummings, J. N. Nguyen, D. C. Hamm, L. K. Donohue, *et al.*, 2013 Genome engineering of Drosophila with the CRISPR RNA-guided Cas9 nuclease. Genetics 194: 1029–1035. https://doi.org/10.1534/genetics.113.152710

Grell R. F., 1971 Heat-induced exchange in the fourth chromosome of diploid females of Drosophila melanogaster. Genetics 69: 523–527.

Grell R. F., 1978 Time of recombination in the Drosophila melanogaster oocyte: evidence from a temperature-sensitive recombination-deficient mutant. Proc. Natl. Acad. Sci. https://doi.org/10.1073/pnas.75.7.3351

Hartmann M. A., and J. Sekelsky, 2017 The absence of crossovers on chromosome 4 in Drosophila melanogaster : Imperfection or interesting exception? Fly (Austin). 6934: 4–11. https://doi.org/10.1080/19336934.2017.1321181

Hartmann M., K. P. Kohl, J. Sekelsky, and T. Hatkevich, 2019 Meiotic MCM Proteins Promote and Inhibit Crossovers During Meiotic Recombination. Genetics. https://doi.org/10.1534/genetics.119.302221

Hassold T., and P. Hunt, 2001 To err (meiotically) is human: the genesis of human aneuploidy. Nat. Rev. Genet. 2: 280–291. https://doi.org/10.1038/35066065

Hatkevich T., K. P. Kohl, S. Mcmahan, M. A. Hartmann, A. M. Williams, *et al.*, 2017 Bloom Syndrome Helicase Promotes Meiotic Crossover Patterning and Homolog Disjunction. Curr. Biol. 27: 96–102.

Hatkevich T., and J. Sekelsky, 2017 Bloom syndrome helicase in meiosis: Pro-crossover functions of an anti-crossover protein. BioEssays 39: 1–11. https://doi.org/10.1002/bies.201700073

Hawley R., H. Irick, A. Zitron, D. Haddox, A. Lohe, *et al.*, 1992 There are two mechanisms of achiasmate segregation in Drosophila females, one of which requires heterocrhomatic

homology. Dev. Genet. 13: 440–467.

Hawley R., K. S. McKim, and T. Arbel, 1993 Meiotic Segregation in Drosophila melanogaster Females: Molecules, Mechanisms, and Myths. Annu. Rev. Genet. 27: 281–317. https://doi.org/10.1146/annurev.genet.27.1.281

Henikoff S., and T. D. Dreesen, 1989 Trans-inactivation of the Drosophila brown gene: evidence for transcriptional repression and somatic pairing dependence. Proc. Natl. Acad. Sci. U. S. A. 86: 6704–8. https://doi.org/10.1073/pnas.86.17.6704

Henikoff S., J. M. Jackson, and P. B. Talbert, 1995 Distance and Pairing Effects on the brown Dominant Heterochromatic Element in Drosophila. Genetics 140: 1007–1017.

Hilliker A. J., S. H. Clark, and A. Chovnick, 1991 The effect of DNA sequence polymorphisms on intragenic recombination in the rosy locus of drosophila melanogaster. Genetics 129: 779–781.

Holliday R., 1964 A mechanism for gene conversion in fungi. Genet. Res. https://doi.org/10.1017/S0016672300001233

Hollingsworth N. M., L. Ponte, and C. Halsey, 1995 MSH5, a novel MutS homolog, facilitates meiotic reciprocal recombination between homologs in Saccharomyces cerevisiae but not mismatch repair. Genes Dev. https://doi.org/10.1101/gad.9.14.1728

Hollingsworth N. M., and S. J. Brill, 2004 The Mus81 solution to resolution: Generating meiotic crossovers without Holliday junctions. Genes Dev.

Hoskins R. A., C. D. Smith, J. W. Carlson, a B. Carvalho, A. Halpern, *et al.*, 2002 Heterochromatic sequences in a Drosophila whole-genome shotgun assembly. Genome Biol. 3. https://doi.org/10.1186/gb-2002-3-12-research0085

Hoskins R. A., J. W. Carlson, K. H. Wan, S. Park, I. Mendez, *et al.*, 2015 The Release 6 reference sequence of the Drosophila melanogaster genome. Genome Res. 25: 445–458. https://doi.org/10.1101/gr.185579.114

Hughes S. E., D. E. Miller, A. L. Miller, and R. S. Hawley, 2018 *Female Meiosis : Synapsis , Recombination , and Segregation in Drosophila melanogaster*.

Iyer L. M., D. D. Leipe, E. V. Koonin, and L. Aravind, 2004 Evolutionary history and higher order classification of AAA+ ATPases, in *Journal of Structural Biology*,.

James P., J. Halladay, and E. A. Craig, 1996 Genomic Libraries and a Host Strain Designed for Highly Efficient Two-Hybrid Selection in Yeast. Genetics 1425–1436.

Jones G. H., and F. C. H. Franklin, 2006 Meiotic Crossing-over: Obligation and Interference. Cell 126: 246–248. https://doi.org/10.1016/j.cell.2006.07.010

Keeney S., C. N. Giroux, and N. Kleckner, 1997 Meiosis-Specific DNA Double-Strand Breaks Are Catalyzed by Spo11 , a Member of a Widely Conserved Protein Family. Cell 88: 375–384.

Kent T. V., J. Uzunović, and S. I. Wright, 2017 Coevolution between transposable elements and recombination. Philos. Trans. R. Soc. B Biol. Sci. 372. https://doi.org/10.1098/rstb.2016.0458

Kerrebrock A. W., D. P. Moore, J. S. Wu, and T. L. Orr-Weaver, 1995 Mei-S332, a drosophila protein required for sister-chromatid cohesion, can localize to meiotic centromere regions. Cell 83: 247–256. https://doi.org/10.1016/0092-8674(95)90166-3

Khost D., D. Eickbush, and A. Larracuente, 2017 Single molecule long read sequencing resolves the detailed structure of complex satellite DNA loci in Drosophila melanogaster. 2Genome Res. 27: 709–721. https://doi.org/10.1101/gr.213512.116.Freely

Kim Y., G. S. Spitz, U. Veturi, F. P. Lach, A. D. Auerbach, *et al.*, 2013 Regulation of multiple DNA repair pathways by the Fanconi anemia protein SLX4. Blood 121: 54–63. https://doi.org/10.1182/blood-2012-07-441212

King J. S., and R. K. Mortimer, 1990 A polymerization model of chiasma interference and corresponding computer simulation. Genetics 126: 1127–1138.

Koehler K. E., C. L. Boulton, H. E. Collins, R. L. French, K. C. Herman, *et al.*, 1996a Spontaneous X chromosome MI and MII nondisjunction events in Drosophila melanogaster oocytes have different recombinational histories. Nat. Genet. 14: 406–414. https://doi.org/10.1038/ng1296-406

Koehler K. E., R. S. Hawley, S. Sherman, and T. Hassold, 1996b Recombination and nondisjunction in humans and flies. Hum. Mol. Genet. 5 Spec No: 1495–1504. https://doi.org/10.1093/hmg/5.Supplement_1.1495

Kohl K. P., C. D. Jones, and J. Sekelsky, 2012 Evolution of an MCM Complex in Flies That Promotes Meiotic Crossovers by Blocking BLM Helicase. Science (80-.). 338.

Kohl K. P., and J. Sekelsky, 2013 Meiotic and Mitotic Recombination in Meiosis. Genetics 194: 327–334. https://doi.org/10.1534/genetics.113.150581

Kuo H. K., S. McMahan, C. M. Rota, K. P. Kohl, and J. Sekelsky, 2014 Drosophila FANCM Helicase Prevents Spontaneous Mitotic Crossovers Generated by the MUS81 and SLX1 Nucleases. Genetics 198: 935–945. https://doi.org/10.1534/genetics.114.168096

Laird C., M. Hammond, and M. Lamb, 1987 Polytene chromosomes of Drosophila. In, pp. 40–47 in *Chromosomes Today, Vol 9*,.

Lake C. M., and R. S. Hawley, 2012 The molecular control of meiotic chromosomal behavior: events in early meiotic prophase in Drosophila oocytes. Annu. Rev. Physiol. 74: 425–51. https://doi.org/10.1146/annurev-physiol-020911-153342

Lake C. M., and R. S. Hawley, 2016 Becoming a crossover-competent DSB. Semin. Cell Dev. Biol. 54: 117–125. https://doi.org/10.1016/j.semcdb.2016.01.008

Lamb N. E., S. B. Freeman, a Savage-Austin, D. Pettay, L. Taft, *et al.*, 1996 Susceptible chiasmate configurations of chromosome 21 predispose to non-disjunction in both maternal meiosis I and meiosis II. Nat. Genet. 14: 400–405. https://doi.org/10.1038/ng1296-400

Li H., B. Handsaker, A. Wysoker, T. Fennell, J. Ruan, *et al.*, 2009 The Sequence Alignment/Map format and SAMtools. Bioinformatics 25: 2078–2079. https://doi.org/10.1093/bioinformatics/btp352

Li H., 2011 A statistical framework for SNP calling, mutation discovery, association mapping and population genetical parameter estimation from sequencing data. Bioinformatics 27: 2987–2993. https://doi.org/10.1093/bioinformatics/btr509

Lindsley D., and G. Zimm, 1992 The Genome of Drosophila melanogaster, in Academic Press, Inc., San Diego, CA.

Liu H., J. K. Jang, J. Graham, K. Nycz, and K. S. McKim, 2000 Two genes required for meiotic recombination in Drosophila are expressed from a dicistronic message. Genetics.

Locke J., and H. E. McDermid, 1993 Analysis of Drosophila chromosome 4 using pulsed field gel electrophoresis. Chromosoma 102: 718–723. https://doi.org/10.1007/BF00650898

Los Santos T. De, J. Loidl, B. Larkin, and N. M. Hollingsworth, 2001 A role for MMS4 in the processing of recombination intermediates during meiosis in Saccharomyces cerevisiae. Genetics.

Los Santos T. De, N. Hunter, C. Lee, B. Larkin, J. Loidl, *et al.*, 2003 Junction Resolution to Promote a Distinct Subset of Crossovers During Meiosis in Budding Yeast. Genetics.

Lu X., X. Liu, L. An, W. Zhang, J. Sun, *et al.*, 2008 The Arabidopsis MutS homolog AtMSH5 is required for normal meiosis. Cell Res. https://doi.org/10.1038/cr.2008.44

Lundin C., M. North, K. Erixon, K. Walters, D. Jenssen, *et al.*, 2005 Methyl methanesulfonate (MMS) produces heat-labile DNA damage but no detectable in vivo DNA double-strand breaks. Nucleic Acids Res. 33: 3799–3811. https://doi.org/10.1093/nar/gki681

Mather K., 1937 The Determination of Position in Crossing-over. II. The chromosome length-chiasma frequency relation. Cytologia (Tokyo). 514–526.

Mather K., 1939 Crossing over and heterochromatin in the X chromosome of Drosophila melanogaster. Genetics 24: 413–435.

Matsubayashi H., and M.-T. Yamamoto, 2003 REC, a new member of the MCM-related protein family, is required for meiotic recombination in Drosophila. Genes Genet. Syst. https://doi.org/10.1266/ggs.78.363

McKim K. S., J. B. Dahmus, and R. S. Hawley, 1996 Cloning of the Drosophila melanogaster meiotic recombination gene mei- 218: A genetic and molecular analysis of interval 15E. Genetics.

McKim K. S., and A. Hayashi-Hagihara, 1998 mei-W68 in Drosophila melanogaster encodes a Spo11 homolog: Evidence that the mechanism for initiating meiotic recombination is conserved. Genes Dev. 12: 2932–2942. https://doi.org/10.1101/gad.12.18.2932

McVey M., J. R. LaRocque, M. D. Adams, and J. J. Sekelsky, 2004 Formation of deletions during double-strand break repair in Drosophila DmBlm mutants occurs after strand invasion. Proc. Natl. Acad. Sci. 101: 15694–15699. https://doi.org/10.1073/pnas.0406157101

McVey M., S. L. Andersen, Y. Broze, and J. Sekelsky, 2007 Multiple functions of drosophila BLM helicase in maintenance of genome stability. Genetics 176: 1979–1992. https://doi.org/10.1534/genetics.106.070052

Mehrotra S., and K. S. McKim, 2006 Temporal analysis of meiotic DNA double-strand break formation and repair in Drosophila females. PLoS Genet. 2: 1883–1897. https://doi.org/10.1371/journal.pgen.0020200

Miklos G. L. G., and J. N. Cotsell, 1990 Chromosome Structure at Interfaces between Major Chromatin Types: alpha- and beta-Heterochromatin. BioEssays 12: 1–6.

Miller D. E., C. B. Smith, N. Yeganeh Kazemi, A. J. Cockrell, and A. V Arvanitakas, 2016 Whole-genome analysis of individual meiotic events in Drosophila melan- ogaster reveals that noncrossover gene conversions are insensitive to inter- ference and the centromere effect. Genetics 203: 159–171. https://doi.org/10.1534/genetics.115.186486

Morgan T., A. H. Sturtevant, and C. B. Bridges, 1926 Constitution of the gernaml material in relation to heredity. Yrbk Carn Inst Wash 25: 308–312.

Morgan T., 1928 The Theory of the Gene, pp. 1–25 in Yale University Press, New Haven, CT.

Morgan T. H., A. H. Sturtevant, and L. V. Morgan, 1945 Special Projects: Biological Sciences. Carnegie Inst. Washingt. Yearb. 55: 157–160.

Muñoz I. M., K. Hain, A. C. Déclais, M. Gardiner, G. W. Toh, *et al.*, 2009 Coordination of Structure-Specific Nucleases by Human SLX4/BTBD12 Is Required for DNA Repair. Mol. Cell 35: 116–127. https://doi.org/10.1016/j.molcel.2009.06.020

Muyt A. De, L. Jessop, E. Kolar, A. Sourirajan, J. Chen, *et al.*, 2012 BLM Helicase Ortholog Sgs1 Is a Central Regulator of Meiotic Recombination Intermediate Metabolism. Mol. Cell 46: 43–53. https://doi.org/10.1016/j.molcel.2012.02.020

Nambiar M., and G. R. Smith, 2016 Repression of harmful meiotic recombination in centromeric regions. Semin. Cell Dev. Biol. 1–10. https://doi.org/10.1016/j.semcdb.2016.01.042

Novak J. E., P. B. Ross-Macdonald, and G. Shirleen Roeder, 2001 The budding yeast Msh4 protein functions in chromosome synapsis and the regulation of crossover distribution. Genetics 158: 1013–1025.

Osborne J., 1999 Crossing over in a T(1;4) Translocation in Drosophila melanogaster

Owen A., 1949 A possible interpretation of the apparent interference across the centromere

found by callan and montalenti in Culex pipiens. Hered. 357–567.

Page S. L., R. J. Nielsen, K. Teeter, C. M. Lake, S. Ong, *et al.*, 2007 A germline clone screen for meiotic mutants in Drosophila melanogaster. Fly (Austin). 1: 172–181. https://doi.org/10.4161/fly.4720

Patterson J. T., and H. J. Muller, 1930 Are “Progressive” Mutations Produced by X-rays? Genetics 15: 495–578.

Pochart P., D. Woltering, and N. M. Hollingsworth, 1997 Conserved properties between functionally distinct MutS homologs in yeast. J. Biol. Chem. 272: 30345–30349. https://doi.org/10.1074/jbc.272.48.30345

R Core Team, 2019 R: A language and environment for statistical computing. R Found. Stat. Comput. Vienna, Austria.

Radford I. R., 1985 The level of induced DNA double-Strand breakage correlates with cell killing after x-irradiation. Int. J. Radiat. Biol. 48: 45–54. https://doi.org/10.1080/09553008514551051

Radford S. J., E. Goley, K. Baxter, S. McMahan, and J. Sekelsky, 2005 Drosophila ERCC1 is required for a subset of MEI-9-dependent meiotic crossovers. Genetics 170: 1737–1745. https://doi.org/10.1534/genetics.104.036178

Radford S. J., S. McMahan, H. L. Blanton, and J. Sekelsky, 2007 Heteroduplex DNA in meiotic recombination in Drosophila mei-9 mutants. Genetics 176: 63–72. https://doi.org/10.1534/genetics.107.070557

Rahman R., G. W. Chirn, A. Kanodia, Y. A. Sytnikova, B. Brembs, *et al.*, 2015 Unique transposon landscapes are pervasive across Drosophila melanogaster genomes. Nucleic Acids Res. 43: 10655–10672. https://doi.org/10.1093/nar/gkv1193

Redfield H., 1930 Crossing over in the third chromosomes of triploids of drosophila melanogaster. Genetics 15: 205–252.

Redfield H., 1932 A comparison of triploid and diploid crossing over for chromosome II of Drosophila melanogaster. 137–152.

Resnick T. D., D. L. Satinover, F. MacIsaac, P. T. Stukenberg, W. C. Earnshaw, *et al.*, 2006 INCENP and Aurora B Promote Meiotic Sister Chromatid Cohesion through Localization of the Shugoshin MEI-S332 in Drosophila. Dev. Cell 11: 57–68.

https://doi.org/10.1016/j.devcel.2006.04.021

Richards S. A., M. J. Whittingham, and P. A. Stephens, 2011 Model selection and model averaging in behavioural ecology: The utility of the IT-AIC framework. Behav. Ecol. Sociobiol. 65: 77–89. https://doi.org/10.1007/s00265-010-1035-8

Riddle N. C., W. Leung, K. A. Haynes, H. Granok, J. Wuller, *et al.*, 2008 An investigation of heterochromatin domains on the fourth chromosome of Drosophila melanogaster. Genetics 178: 1177–1191. https://doi.org/10.1534/genetics.107.081828

Riddle N. C., A. Minoda, P. V. Kharchenko, A. A. Alekseyenko, Y. B. Schwartz, *et al.*, 2011 Plasticity in patterns of histone modifications and chromosomal proteins in Drosophila heterochromatin. Genome Res. 21: 147–163. https://doi.org/10.1101/gr.110098.110

Romero N. E., S. W. Matson, and J. Sekelsky, 2016 Biochemical activities and genetic functions of the Drosophila melanogaster fancm helicase in DNA repair. Genetics 204: 531–541. https://doi.org/10.1534/genetics.116.192534

Ross-Macdonald P., and G. S. Roeder, 1994 Mutation of a meiosis-specific MutS homolog decreases crossing over but not mismatch correction. Cell. https://doi.org/10.1016/0092-8674(94)90037-X

Roy S., J. Ernst, P. Kharchenko, P. Kheradpour, N. Negre, *et al.*, 2010 Identification of functional elements and regulatory circuits by Drosophila modENCODE. Science (80-.). 330: 1787–1797.

Sandler L., D. L. Lindsley, B. Nicoletti, and G. Trippa, 1968 Mutants affecting meiosis in natural populations of Drosophila melanogaster. Genetics.

Sandler L., and P. Szauter, 1978 The effect of recombination-defective meiotic mutants on fourth-chromosome crossing over in Drosophila melanogaster. Genetics 90: 699–712.

Sawant A., A. M. Floyd, M. Dangeti, W. Lei, R. W. Sobol, *et al.*, 2017 Differential role of base excision repair proteins in mediating cisplatin cytotoxicity. DNA Repair (Amst). 51: 46–59. https://doi.org/10.1016/j.dnarep.2017.01.002

Sekelsky J. J., and R. S. Hawley, 1995 The bond between sisters. Cell 83: 157–160. https://doi.org/10.1016/0092-8674(95)90156-6

Sekelsky J. J., K. S. McKim, G. M. Chin, and R. S. Hawley, 1995 The Drosophila meiotic recombination gene mei-9 encodes a homologue of the yeast excision repair protein

Rad1. Genetics.

Sekelsky J. J., K. S. McKim, L. Messina, R. L. French, W. D. Hurley, *et al.*, 1999 Identification of novel Drosophila meiotic genes recovered in a P- element screen. Genetics.

Slatis H. M., 1955 A Reconsideration of the Brown-Dominant Position Effect. Genetics 40: 246–51.

Slawson E., C. Shaffer, C. Malone, W. Leung, E. Kellmann, *et al.*, 2006 Comparison of dot chromosome sequences from D. melanogaster and D. virilis reveals an enrichment of DNA transposon sequences in heterochromatic domains. Genome Biol. 7–15.

Smith G. R., M. N. Boddy, P. Shanahan, and P. Russell, 2003 Fission Yeast Mus81·Eme1 Holliday Junction Resolvase Is Required for Meiotic Crossing over but Not for Gene Conversion. Genetics.

Strom A. R., V. Alexander, M. Mir, D. V. Fyodorov, X. Darzacq, *et al.*, 2017 Phase separation drives heterochromatin domain formation. Nature 547: 241–245. https://doi.org/10.1038/nature22989

Sturtevant A. H., 1913a The linear arrangement of six sex-linked factors in Drosophila, as shown by their mode of association. J. Exp. Zool. https://doi.org/10.1002/jez.1400140104

Sturtevant A. H., 1913b A third group of linked genes in Drosophila ampelophila. Science (80-.). XXXVII: 990–992.

Sturtevant B. A. H., 1915 The Behavior of the Chromosomes as Studied through Linkage. Z. Indukt. Abstamm. Vererbungsl. 13: 234–287.

Sturtevant A. H., and G. W. Beadle, 1936 The Relations of inversions in the X chromosome of Drosophila melanogaster to crossing over and disjunction. Genetics 21: 554–604.

Sturtevant A. H., 1951 A map of the fourth chromosome of Drosophila melanogaster, based on crossing over in triploid females. Proc. Natl. Acad. Sci. U. S. A. 37: 405–7.

Sun F. L., M. H. Cuaycong, C. A. Craig, L. L. Wallrath, J. Locke, *et al.*, 2000 The fourth chromosome of Drosophila melanogaster: interspersed euchromatic and heterochromatic domains. Proc. Natl. Acad. Sci. U. S. A. 97: 5340–5. https://doi.org/10.1073/pnas.090530797

Svendsen J. M., A. Smogorzewska, M. E. Sowa, B. C. O'Connell, S. P. Gygi, *et al.*, 2009 Mammalian BTBD12/SLX4 Assembles A Holliday Junction Resolvase and Is Required for DNA Repair. Cell 138: 63–77. https://doi.org/10.1016/j.cell.2009.06.030

Szostak J. W., T. L. Orr-Weaver, R. J. Rothstein, and F. W. Stahl, 1983 The double-strand-break repair model for recombination. Cell.

Thurmond J., J. Goodman, V. Strelets, H. Attrill, L. Gramates, *et al.*, 2019 FlyBase 2.0: the next generation. Nucleic Acids Res. 47: D759–D765.

Venables W. N., and B. D. Ripley, 2002 *Modern Applied Statistics with S*. Springer.

Villeneuve A. M., and K. J. Hillers, 2001 Whence Meiosis ? Cell 106: 647–650.

Walker J. E., M. Saraste, M. J. Runswick, and N. J. Gay, 1982 Distantly related sequences in the alpha- and beta-subunits of ATP synthase, myosin, kinases and other ATP-requiring enzymes and a common nucleotide binding fold. EMBO J.

Wang S., D. Zickler, N. Kleckner, and L. Zhang, 2015 Meiotic crossover patterns: Obligatory crossover, interference and homeostasis in a single process. Cell Cycle 14: 305–314. https://doi.org/10.4161/15384101.2014.991185

Westphal T., and G. Reuter, 2002 Recombinogenic effects of suppressors of position-effect variegation in Drosophila. Genetics 160: 609–621.

Wiese C., J. M. Hinz, R. S. Tebbs, P. B. Nham, S. S. Urbin, *et al.*, 2006 Disparate requirements for the Walker A and B ATPase motifs of human RAD51D in homologous recombination. Nucleic Acids Res. https://doi.org/10.1093/nar/gkl366

Wu Y., Y. He, I. A. Moya, X. Qian, and Y. Luo, 2004 Crystal structure of archaeal recombinase RadA: A snapshot of its extended conformation. Mol. Cell. https://doi.org/10.1016/j.molcel.2004.07.014

Wu Y., X. Qian, Y. He, I. A. Moya, and Y. Luo, 2005 Crystal structure of an ATPase-active form of Rad51 homolog from Methanococcus voltae: Insights into potassium dependence. J. Biol. Chem. https://doi.org/10.1074/jbc.M411093200

Wyatt H. D. M., S. Sarbajna, J. Matos, and S. C. West, 2013 Coordinated actions of SLX1-SLX4 and MUS81-EME1 for holliday junction resolution in human cells. Mol. Cell 52: 234–247. https://doi.org/10.1016/j.molcel.2013.08.035

Yamamoto M., and G. L. G. Miklos, 1978 Genetic Studies on Heterochromatin in Drosophila melanogaster and Their Implications for the Functions of Satellite DNA. Chromosoma 98: 71–98.

Yamamoto M. T., A. Mitchelson, M. Tudor, K. O'Hare, J. A. Davies, *et al.*, 1990 Molecular and cytogenetic analysis of the heterochromatin-euchromatin junction region of the Drosophila melanogaster X chromosome using cloned DNA sequences. Genetics 125: 821–832.

Yildiz O., S. Majumder, B. Kramer, and J. J. Sekelsky, 2002 Drosophila MUS312 Interacts with the Short Article MEI-9 to Generate Meiotic Crossovers. Mol. Cell 10: 1503–1509.

Yildiz Ö., H. Kearney, B. C. Kramer, and J. J. Sekelsky, 2004 Mutational analysis of the Drosophila DNA repair and recombination gene mei-9. Genetics 167: 263–273. https://doi.org/10.1534/genetics.167.1.263

Zakharyevich K., S. Tang, Y. Ma, and N. Hunter, 2012 Delineation of joint molecule resolution pathways in meiosis identifies a crossover-specific resolvase. Cell 149: 334–347. https://doi.org/10.1016/j.cell.2012.03.023

Zalevsky J., A. J. MacQueen, J. B. Duffy, K. J. Kemphues, and A. M. Villeneuve, 1999 Crossing over during Caenorhabditis elegans meiosis requires a conserved MutS-based pathway that is partially dispensable in budding yeast. Genetics 153: 1271–1283.

Zhang L., Z. Liang, J. Hutchinson, and N. Kleckner, 2014 Crossover Patterning by the Beam-Film Model: Analysis and Implications. PLoS Genet. 10. https://doi.org/10.1371/journal.pgen.1004042

Zlopasa L., A. Brachner, and R. Foisner, 2016 Nucleo-cytoplasmic shuttling of the endonuclease ankyrin repeats and LEM domain-containing protein 1 (Ankle1) is mediated by canonical nuclear export- and nuclear import signals. BMC Cell Biol. 1–12. https://doi.org/10.1186/s12860-016-0102-z